8427-6005-RU000
Total Pages: 111

TRW SPACE TECHNOLOGY LABORATORIES, INC.
One Space Park
Redondo Beach, California

PRELIMINARY DESIGN CONSIDERATIONS FOR A GYRO-DAMPED GRAVITY GRADIENT SATELLITE (U)

8427-6005-RU000 28 May 1965

Prepared By: R. G. Nishinaga

Approved By: A. E. Sabroff
Project Engineer

Approved By: R. K. Whitford, Director
Inertial Guidance and
Control Laboratory

Contract No. NAS5-3304

Prepared for

NATIONAL AERONAUTICS AND SPACE ADMINISTRATION
Goddard Space Flight Center
Greenbelt, Maryland

ABSTRACT

This report presents an investigation of preliminary design considerations for a gravity gradient stabilized satellite which utilizes control moment gyros for damping and control. The study is limited to considering small angle performance of a rigid single body satellite about the desired earth-pointing orientation. Provision is made to include the effect of a spinning wheel which provides a constant angular momentum normal to the orbit plane. The gyroscopic effect of the wheel increases the stiffness of the satellite about the earth-pointing axis.

Linearized equations of motion for arbitrary gyro orientations are derived and then reduced for several specific gyro configurations. For generality the equations are normalized. The Routh-Hurwitz criterion is utilized to establish the range of parameter values for which the system is stable. A design study is made to select parameters on the basis of minimizing pointing errors due to disturbance torques. For this preliminary analysis disturbances are assumed to occur at harmonics of orbit rate. Finally, an analysis is developed to evaluate the effects of gyro imperfections. The results of these studies provide general guidelines in selecting parameters for a gyro-damped satellite.

ACKNOWLEDGEMENTS

The author wishes to extend his appreciation to Dr. A. E. Sabroff and Mr. K. J. McKenna for their numerous technical discussions and helpful suggestions in the preparation of this report.

TABLE OF CONTENTS

LIST OF FIGURES

LIST OF FIGURES (continued)

LIST OF TABLES

1.0 INTRODUCTION

This report is concerned with the small angle performance of a gravity gradient stabilized satellite which utilizes control moment gyros and a pitch angular momentum wheel for damping and control. In this study it is assumed that the configuration of the satellite is that of a single body whose inertias are to be specified by design considerations. The configuration of the control moment gyros is restricted to the class of systems where two gyros provide three axis damping or where a single gyro provides two axis damping. The objective of the report is to present preliminary considerations for designing a gyro-damped satellite. For this study the primary design criterion is that attitude errors be minimized during the normal or Earth pointing mode. Design considerations for the initial acquisition phase are not analyzed.

The small angle design of a gravity gradient stabilized satellite is generally based on minimizing the attitude errors at frequencies where the disturbance torques on the satellite are most significant. However, a difficulty arises because the disturbance torques are functions of system parameters whose values are not known a priori. To resolve this difficulty, it can be assumed that the major sources of disturbances occur at the harmonics of orbit rate frequency. Moreover, by assuming that the disturbances are of equal magnitude at these frequencies, a measure of the system's pointing capability is obtained by summing the attitude error per unit disturbance torque at orbital harmonics[1]*. In this way, a preliminary gyro control system and satellite configuration can be designed on the basis of minimizing the summed gains.

Thus the approach of this study was to obtain a set of curves which depict the attitude error/torque gains as a function of the system parameters. The gains were determined at zero, one, two, and three times orbit rate frequency. Preliminary studies were made to assess the effect of system parameters at the individual frequencies. By this method a suitable range of parameters was selected for further study. The summed gain curves and frequency response curves were then obtained. From this data a set of parameter values was selected on the basis of minimizing attitude errors. Finally, steady state errors due to gyro imperfections were determined.

---

* Note: Numbers in brackets correspond to List of References.

2.0 SYSTEM DESCRIPTION

The system under study involves a satellite which travels nominally about the Earth in a circular orbit. As a rigid body the satellite will tend to be oriented by the combined gravity gradient and centrifugal effects such that the following alignment is met:

1. The axis of maximum moment of inertia is normal to the orbit plane (pitch axis).

2. The axis of minimum moment of inertia lies along the local vertical (yaw axis).

3. The intermediate principal axis lies along the velocity vector (roll axis).

The above alignment is depicted in Figure 1 for an arbitrary rigid body satellite. It is noted that ϕ, θ, and ψ represent attitude errors in the roll, pitch, and yaw axis, respectively. In the study it is assumed that the satellite's principal axes of inertia (x_a, y_a, z_a) coincide with the body axes.

Added to the above rigid body satellite are control moment gyros for attitude stabilization and control. The control moment gyro is a single-degree-of-freedom, rate integrating gyro. The gyro contains a rotor which is placed within a gimbal can, mounted on bearings and immersed in a viscous fluid. Energy dissipation, or damping, occurs when there is fluid shear due to the relative motion between the gimbal can and the satellite. In general, the gimbal can motion is restrained by a spring or a torque generator which provides the torques necessary to maintain a proper orientation of the gyro with respect to the satellite.

In this study, the investigation is limited to the following two classes of gyro systems: the so-called "Roll-Vee" and "Yaw-Vee" systems which employ two control moment gyros; the so-called "Roll" and "Yaw" systems which employ a single control moment gyro.[2,3,4] Each of these systems is defined by the orientation of the gyro with respect to the satellite, as shown in Figures 2 and 3.

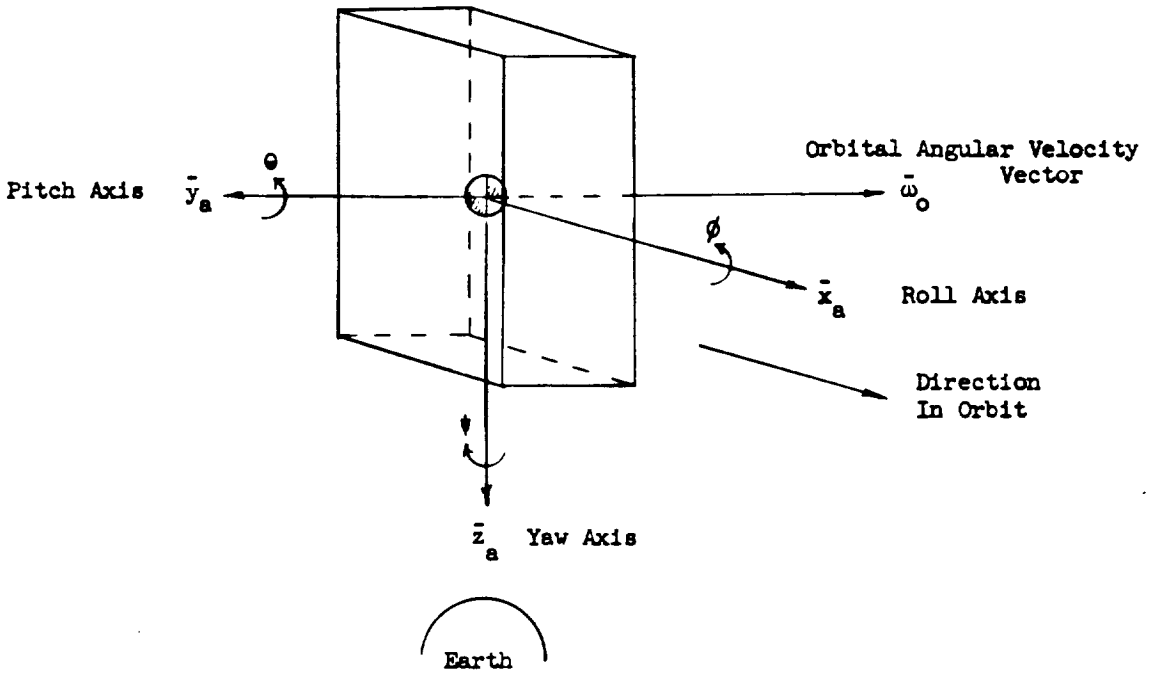

Figure 1. Body Fixed Coordinates in a Rigid Body Satellite

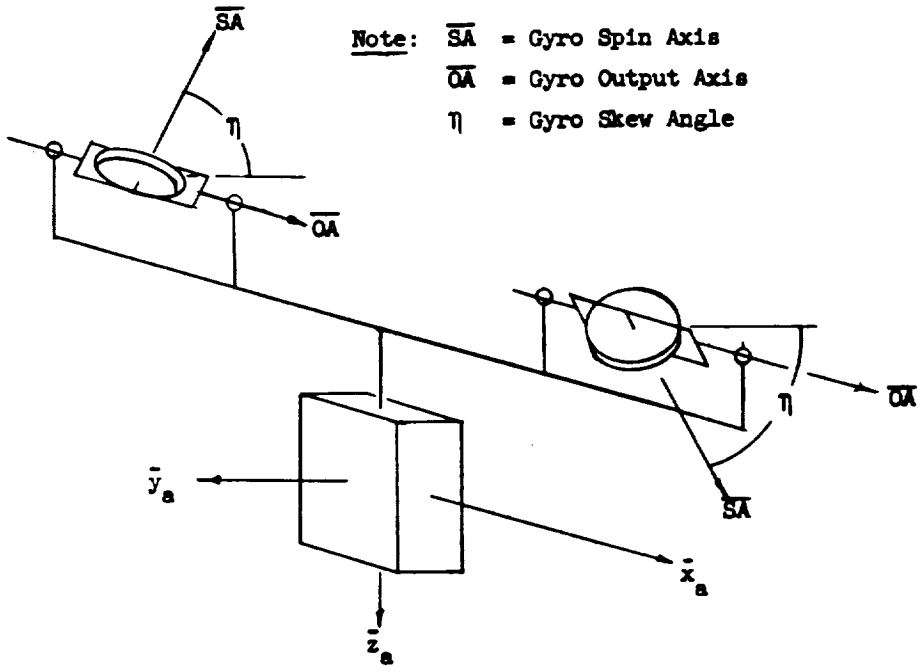

Figure 2a. Roll-Vee Gyro Configuration

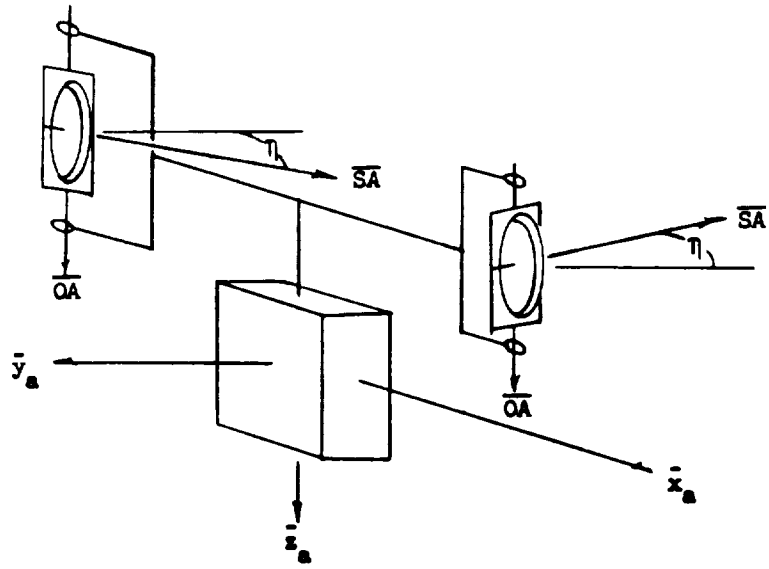

Figure 2b. Yaw-Vee Gyro Configuration

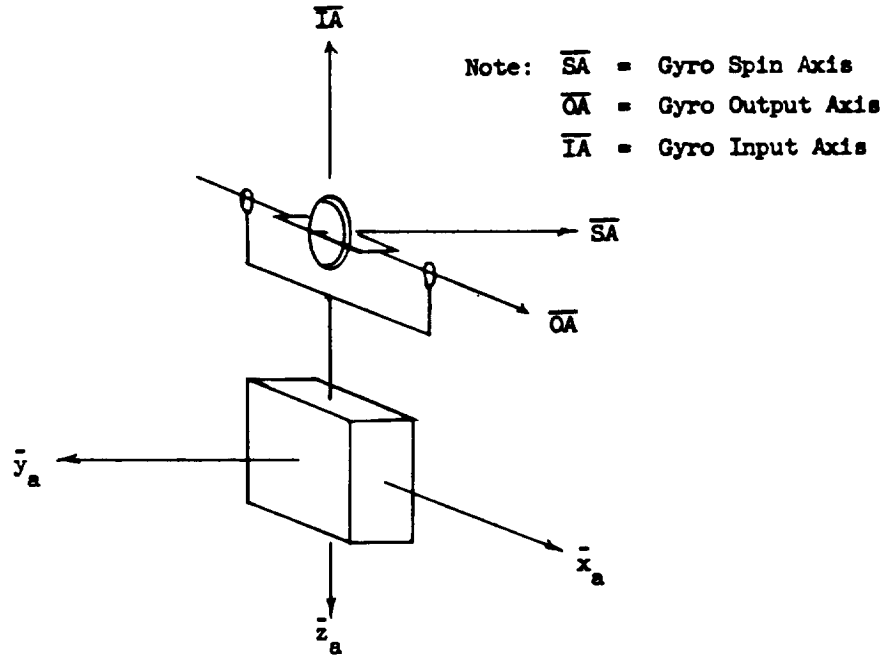

Figure 3a. Roll Gyro Configuration

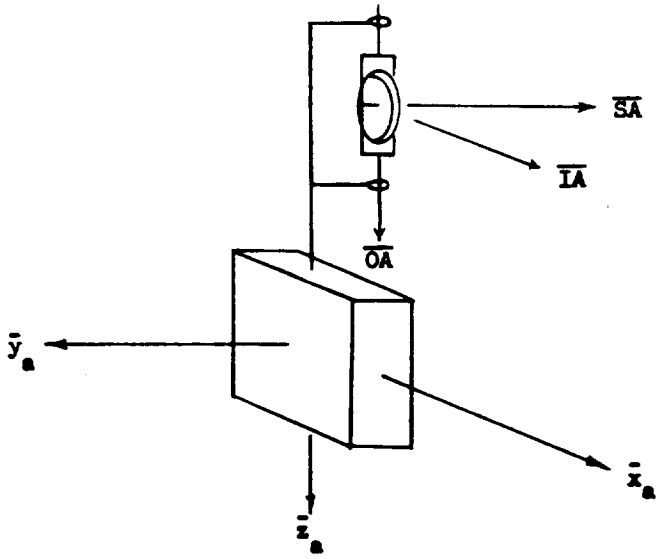

Figure 3b. Yaw Gyro Configuration

(In these figures, the position of the gyro coordinate axes relative to the satellite's principal axes is exaggerated for the purposes of illustration.) It is noted that in the two gyro system the spin axis of each gyro forms a "V" which is bisected by the pitch axis. In the single gyro system, the spin axis is nominally along the negative pitch axis. Moreover, it is noted that in the Roll-Vee or Roll system the output axis of the gyro is along the roll axis. In the Yaw-Vee or Yaw system, the gyro output axis coincides with the yaw axis.

The way in which control moment gyros damp out an arbitrary motion can be explained in terms of the rate or torque-seeking property of gyros. When a torque is applied to a gyro, the gimbal will precess such that the gyro's angular momentum vector lines up with the applied torque. Thus in the case of a Roll-Vee or Yaw-Vee system, a pitch disturbance torque will be sought by the two control moment gyros, resulting in a scissoring motion of the gimbals relative to the satellite, thus damping out the disturbance. An in-phase motion of the gimbals will be the result of a yaw disturbance when applied to a Roll-Vee system or a roll disturbance when applied to a Yaw-Vee system. In either of these systems, coupling of the motion about the roll and yaw axes permit the two control moment gyros to provide three axis damping.

In the case of the single gyro system, a disturbance about the gyro input axis causes the gimbals to precess and thereby produces damping torques about that axis. In the Roll or Yaw systems, gyroscopic coupling between the roll and yaw axes provides damping along both the roll and yaw axes. However, the single gyro systems do not provide damping of the small angle motion about the pitch axis. In this case some other device such as a reaction wheel must be used to provide pitch damping.

In addition to damping satellite librations, the control moment gyro serves to stiffen the satellite's control about the roll and yaw axes. In effect, the control moment gyros increases the angular momentum about the pitch axis and thereby improves the dynamic properties of the system to reduce steady state errors about the roll-yaw axes. In case the "stiffness" in the roll-yaw axes is not sufficient, a spinning wheel (pitch wheel) which provides a constant angular momentum about the pitch axis is added to the control system.

In this study, the Roll-Vee and Yaw-Vee gyro systems are assumed to contain a torque generator to provide a bias torque which is necessary to maintain the spin axis skewed away from the negative pitch axis. However, in the case of a Roll or Yaw system, a torque generator is not employed.

3.0 STEADY STATE ANALYSIS

In this section, the steady state characteristics of a gyro-damped satellite are investigated. Specifically, the small angle equations of motion are presented and the stability criteria for a gyro system are investigated. Expressions of the gain between the attitude error and the disturbance torques are developed and discussed. The aim of the analysis is to limit the selection of system parameters for a preliminary design.

In the Appendix, it is shown that the roll-yaw equations of motion for a Roll-Vee or Yaw-Vee system can be reduced to those of Roll or Yaw system, respectively, by appropriately defining the system parameters. Consequently, the steady state analysis will only be concerned with Roll-Vee and Yaw-Vee systems and the single gyro systems will be treated as special cases.

3.1 Equations of Motion

In Appendix A a set of small angle linearized equations of motion are derived for the Roll-Vee and Yaw-Vee gyro systems. To generalize the study these equations are expressed in terms of the following normalized parameters:

$$p = \frac{1}{\omega_o} \frac{d}{dt}$$

$$b = \frac{I_x}{I_y}$$

$$c = \frac{I_z}{I_y}$$

$$h = \begin{cases} \dfrac{HC\mu}{\omega_o I_y}, & \text{Roll-Vee System} \\ \dfrac{HC\alpha}{\omega_o I_y}, & \text{Yaw-Vee System} \end{cases}$$

$$\gamma = \begin{cases} 2\,\dfrac{HC\mu}{D}, & \text{Roll-Vee System} \\ 2\,\dfrac{HC\alpha}{D}, & \text{Yaw-Vee System} \end{cases}$$

$$\lambda = \begin{cases} \dfrac{K}{\omega_o D} - \dfrac{HC\mu}{D}, & \text{Roll-Vee System} \\ \dfrac{K}{\omega_o D} - \dfrac{HC\alpha}{D}, & \text{Yaw-Vee System} \end{cases}$$

$$m = \frac{H_m}{\omega_o I_y}$$

where t is time; I_x, I_y, I_z represent the satellite's roll, pitch, and yaw inertias, respectively; H, K, D are the control moment gyro's angular momentum, spring constant, and viscous damping coefficient, respectively; μ, α represent the angles to which the gyro's spin axis is skewed from the satellite's pitch axis; H_m is the constant angular momentum of the pitch wheel; ω_o is the orbital angular velocity of the satellite; and S and C denote the sine and cosine of an angle, respectively. The resulting equations of motion relate the disturbance torques (T_{dx}, T_{dy}, T_{dz}) to the attitude errors (θ, ϕ, ψ) and gimbal angles (A_1, A_2) in terms of the operator p as follows:

Roll-Vee System

$$\text{Pitch:}\quad \begin{bmatrix} p^2 + 3(b-c) & \frac{-HS\mu}{\omega_o I_y} \cdot p \\ \frac{2\,HS\mu}{D} \cdot p & p + \lambda \end{bmatrix} \begin{bmatrix} \theta \\ A_2 - A_1 \end{bmatrix} = \begin{bmatrix} \frac{T_{dy}}{\omega_o^2 I_y} \\ 0 \end{bmatrix} \tag{1}$$

$$\text{Roll-Yaw:}\quad \begin{bmatrix} b\,p^2 + 4(1-c) - m - 2h & (1-b-c-m-2h)\,p & -h \\ -(1-b-c-m-2h)\,p & cp^2 + 1 - b - m - 2h & hp \\ -\gamma & -\gamma\,p & p+\lambda \end{bmatrix} \begin{bmatrix} \phi \\ \psi \\ A_1+A_2 \end{bmatrix} = \begin{bmatrix} \frac{T_{dx}}{\omega_o^2 I_y} \\ \frac{T_{dz}}{\omega_o^2 I_y} \\ 0 \end{bmatrix} \tag{2}$$

Yaw-Vee System

$$\text{Pitch:}\quad \begin{bmatrix} p^2 + 3(b-c) & \frac{-HS\alpha}{\omega_o I_y} \cdot p \\ \frac{2\,HS\alpha}{D} \cdot p & p + \lambda \end{bmatrix} \begin{bmatrix} \theta \\ A_1 - A_2 \end{bmatrix} = \begin{bmatrix} \frac{T_{dy}}{\omega_o^2 I_y} \\ 0 \end{bmatrix} \tag{3}$$

$$\text{Roll-Yaw:}\quad \begin{bmatrix} bp^2+4(1-c)-m-2h & (1-b-c-m-2h)\,p & -hp \\ -(1-b-c-m-2h)\,p & cp^2+1-b-m-2h & -h \\ \gamma p & -\gamma & p+\lambda \end{bmatrix} \begin{bmatrix} \phi \\ \psi \\ A_1+A_2 \end{bmatrix} = \begin{bmatrix} \frac{T_{dx}}{\omega_o^2 I_y} \\ \frac{T_{dz}}{\omega_o^2 I_y} \\ 0 \end{bmatrix} \tag{4}$$

The above equations indicate that the pitch motion is independent of roll-yaw motion. In fact, pitch motion of the Roll-Vee and Yaw-Vee systems are identical provided that the skew angle of the gimbals are equal ($\mu = \alpha$). This fact becomes evident when the symmetry of the two gyro orientation about the pitch axis is noted. Thus differences between the Roll-Vee and Yaw-Vee systems lie in the motion about the roll and yaw axis.

As indicated in Appendix A, Equations (2) and (4) reduce to the roll-yaw equations of the single gyro Roll and Yaw systems, respectively, when the following definitions of the system parameters are incorporated:

$$h = -\frac{1}{2}\frac{H}{\omega_o I_y}$$

$$\gamma = -\frac{H}{D}$$

$$\lambda = \frac{K}{\omega_o D} + \frac{H}{D}$$

$$\mu = \alpha = 180^\circ$$

In this case the form of the resulting equations of motion remain exactly the same as the roll-yaw equations of the two gyro systems.

Implied in Equations (1) through (4) is the fact that the torque generator provides the following bias torques for the two gyro configurations:

$$M_{gl} = \begin{cases} \omega_o HS\mu \text{ , Roll-Vee System} \\ -\omega_o HS\alpha \text{, Yaw-Vee System} \end{cases}$$

$$M_{g2} = \begin{cases} -\omega_o \, HS\mu \, , & \text{Roll-Vee System} \\ \\ \omega_o \, HS\alpha \, , & \text{Yaw-Vee System} \end{cases}$$

In this way, the torque generator maintains a finite skew angle between the gyro spin axis and the negative pitch axis. Of course, in the case of the Roll and Yaw systems, a bias torque from the torque generator is not required.

3.2 Stability Analysis

The characteristic equation of the two systems is obtained by evaluating the determinant of the square matrices of Equation (1) through (4). The results are summarized as follows for the Roll-Vee and Yaw-Vee systems:

$$\text{Pitch:} \quad \Delta_3(p) = r_o p^3 + r_1 p^2 + r_2 p + r_3 = 0 \tag{5}$$

where

$$r_o = 1$$

$$r_1 = \lambda + 2 \frac{H^2 S^2 \mu}{\omega_o I_y D}$$

$$r_2 = 3(b-c)$$

$$r_3 = 3(b-c)\,\lambda$$

$$\text{Roll-Yaw:} \quad \Delta_5(p) = a_o p^5 + a_1 p^4 + a_2 p^3 + a_3 p^2 + a_4 p + a_5 = 0 \tag{6}$$

where

$$a_o = b\,c$$

$$a_1 = b\,c\,\lambda + h\,\gamma\,(b\,\delta_1 + c\,\delta_2)$$

$$a_2 = c\,[b+4(1-c)-m-2h] + [1-b-c-m-2h]\,[1-c-m-2h]$$

$$a_3 = \lambda a_2 - 2h\gamma\,[1-b-c-m-2h] - h\gamma\,[c-4(1-c)+m+2h]\,\delta_1 - h\gamma\,[2b-1+m+2h]\,\delta_2$$

$$a_4 = [4(1-c)-m-2h]\,[1-b-m-2h]$$

$$a_5 = \lambda a_4 - h\gamma\,[1-b-m-2h]\,\delta_1 - h\gamma\,[4(1-c)-m-2h]\,\delta_2$$

and

$$\delta_1 = \begin{cases} 1\,, & \text{Roll-Vee System} \\ 0\,, & \text{Yaw-Vee System} \end{cases}$$

$$\delta_2 = \begin{cases} 0\,, & \text{Roll-Vee System} \\ 1\,, & \text{Yaw-Vee System} \end{cases}$$

Applying the Routh Hurwitz criteria to the above characteristic equations yields the following necessary conditions for stability:

Pitch: $b - c > 0$ (7)

$\lambda > 0$ (8)

Roll-Yaw: $m + 2h < 1 - b$ (9)

$$\lambda > \begin{cases} \dfrac{h\gamma}{4(1-c) - (m+2h)}\,, & \text{Roll-Vee System} \\ \dfrac{h\gamma}{1 - b - (m+2h)}\,, & \text{Yaw-Vee System} \end{cases} \qquad (10)$$

The above inequalities will define the range of parameters which comprise a stable system. Inequality (7) requires that satellite's roll inertia be greater than the yaw inertia, a condition which is readily met. In many satellites the roll inertia in the same order of magnitude as the pitch inertia. Thus inequality (9) requires in a practical sense that the pitch wheel momentum vector and the sum of the gyro momentum vectors be directed along the negative pitch axis. In terms of the sign convention used in deriving the equations, the above conditions can be met by imposing the following range of values for the pitch wheel momentum (H_m) and gyro skew angle (α, μ):

$$H_m \leq 0$$

$$180 \leq \mu < 270, \quad \text{Roll-Vee System}$$

$$180 \leq \alpha < 270, \quad \text{Yaw-Vee System}$$

Finally inequalities (8) and (10) impose a lower limit on the values of spring constants (K) required for stability. When there is no spring restraint, these inequalities reduce to the following expressions (K = 0):

$$\gamma < 0$$

$$4(1-c) - m > 0, \quad \text{Roll-Vee System}$$

$$1 - b - m > 0, \quad \text{Yaw-Vee System}$$

However, these conditions are automatically satisfied by the requirements on pitch wheel momentum and skew angle which were imposed previously. Thus in this case, positive values of spring constant will not make the system unstable.

3.3 Error/Torque Gains at Orbital Harmonics

The steady state response to periodic disturbance torques at frequency $N\omega_o$ can be determined by setting $p = i N$ and solving the set of linear equations for the attitude errors. At zero and orbit rate frequency, the gain between attitude

error and disturbance torque are summarized in Table I for the Roll-Vee and Yaw-Vee systems. In particular, it is noted that the static pitch gain and the orbit roll gain are independent of gyro parameters in both gyro systems.

The error torque gains of Table I provides some indication of how to minimize the steady state errors at zero and orbit rate frequency. It is clear that the static pitch gain and the orbit rate roll gain are minimized for large roll inertia and small yaw inertias relative to pitch inertia. For a dumbbell-shaped satellite (b = 1, c ≅ 0), these gains become

$$\frac{|\theta_{yo}|}{T_{dy}/(\omega_o^2 I_y)} = \frac{|\phi_{xl}|}{T_{dx}/(\omega_o^2 I_y)} = \frac{1}{3}$$

where θ_{yo} is the pitch error due to a pitch disturbance at zero frequency, hence, the subscripts y, o.

In general, the remaining gain expressions of Table I are minimized for large values of pitch wheel momentum and gyro angular momentum. The effects of spring constant is not clear. However, when the gyro has no spring restraint, the static roll gain of the Roll-Vee system and the static yaw gain of the Yaw-Vee system are reduced to the following expressions which are not dependent on gyro parameters:

Roll-Vee (K=0):

$$\frac{|\phi_{xo}|}{T_{dx}/(\omega_o^2 I_y)} = \frac{1}{4(1-c) - m} \qquad (11)$$

Yaw-Vee (K=0):

$$\frac{|\psi_{zo}|}{T_{dz}/\omega_o^2 I_y} = \frac{1}{1 - b - m} \qquad (12)$$

In this case, a dumbbell-shaped satellite with a Yaw-Vee gyro configuration will require a finite pitch wheel momentum for stability and control in the yaw axis.

TABLE I

Summary of Amplitude Response Equations at Zero and Orbit Rate Frequencies

Amplitude Ratios (Gain)	Roll-Vee System Equation	Yaw-Vee System Eq.
N=0:		
$\frac{\lvert\theta_{yo}\rvert}{T_{dy}/(\omega_o^2 I_y)}$	$\frac{1}{3(b-c)}$	$\frac{1}{3(b-c)}$
$\frac{\lvert\phi_{xo}\rvert}{T_{dx}/(\omega_o^2 I_y)}$	$\frac{\lambda}{\lambda[4(1-c)-m-2h]-h\gamma}$	$\frac{1}{4(1-c)-m-2h}$
$\frac{\lvert\phi_{zo}\rvert}{T_{dz}(\omega_o^2 I_y)} = \frac{\lvert\psi_{xo}\rvert}{T_{dx}/(\omega_o^2 I_y)}$	0	0
$\frac{\lvert\psi_{zo}\rvert}{T_{dz}/(\omega_o^2 I_y)}$	$\frac{1}{1-b-m-2h}$	$\frac{\lambda}{\lambda(1-b-m-2h)-h\gamma}$
N=1:		
$\frac{\lvert\theta_{y1}\rvert}{T_{dy}/(\omega_o^2 I_y)}$	$\sqrt{\frac{1+\lambda^2}{\left\{\lambda\,[3(b-c)-1]-\frac{2H^2S^2\mu}{\omega_o I_y D}\right\}^2+[3(b-c)-1]^2}}$	same as Roll-Vee equation
$\frac{\lvert\phi_{x1}\rvert}{T_{dx}/(\omega_o^2 I_y)}$	$\frac{1}{3(1-c)}$	$\frac{1}{3(1-c)}$
$\frac{\lvert\phi_{z1}\rvert}{T_{dz}/(\omega_o^2 I_y)} = \frac{\lvert\psi_{x1}\rvert}{T_{dx}/(\omega_o^2 I_y)}$	$\frac{1}{3(1-c)}$	$\frac{1}{3(1-c)}$
$\frac{\lvert\psi_{z1}\rvert}{T_{dz}/(\omega_o^2 I_y)}$	$\frac{1}{3(1-c)}\sqrt{\frac{[4(1-c)-m-2h-b]^2+\{\lambda[4(1-c)-m-2h-b]-h\gamma\}^2}{[1-b-c-m-2h]^2+\{\lambda[1-b-c-m-2h]-h\gamma\}^2}}$	same as Roll-Vee equation

At frequencies greater than orbit rate frequency, the gain expressions become extremely lengthy and complex. However, it can be shown that the expression of the roll gain due to yaw disturbance torques is the same as the expression of the yaw gain due to roll disturbance torques, or

$$\frac{|\phi_z(p)|}{T_{dz}/(\omega_o^2 I_y)} = \frac{|\psi_x(p)|}{T_{dx}/(\omega_o^2 I_y)}$$

In this study a measure of the attitude errors due to disturbance torques is obtained by summing the error/torque gain expressions at specific multiples of orbit rate frequency. This approach is justified by the fact that the major sources of disturbances occur at the harmonics of orbit rate frequency. In the case of gyro systems, the magnitude of the error/torque gains become well attenuated beyond three times orbit rate frequency. Thus a set of normalized error coefficients (weighted attitude errors) can be defined as follows:

$$\text{Weighted Pitch Error} = \sum_{N=0}^{3} \frac{|\theta_y(N)|\, W_{yN}}{T_{dy}/(\omega_o^2 I_y)} \tag{13}$$

$$\text{Weighted Roll Error} = \sum_{N=0}^{3} \frac{|\phi_x(N)|\, W_{xN}}{T_{dx}/(\omega_o^2 I_y)} + \sum_{N=0}^{3} \frac{|\phi_z(N)|\, W_{zN}}{T_{dz}/(\omega_o^2 I_y)} \tag{14}$$

$$\text{Weighted Yaw Error} = \sum_{N=0}^{3} \frac{|\psi_z(N)|\, W_{zN}}{T_{dz}/(\omega_o^2 I_y)} + \sum_{N=0}^{3} \frac{|\psi_x(N)|\, W_{xN}}{T_{dx}/(\omega_o^2 I_y)} \tag{15}$$

where W_{yN}, W_{xN}, W_{zN} are weighting coefficients of the disturbance torques in pitch, roll and yaw, respectively. The values of the weighting coefficients depend upon the relative magnitudes of the disturbance torques at each frequency. For this study the weighting coefficients are set to unity ($W_{yN} = W_{xN} = W_{zN} = 1$) and the magnitude of the disturbance torques is set arbitrarily to $\omega_o^2 I_y$.

The summed weighted error functions then become simply

$$\sum \theta_\epsilon = \sum_{N=0}^{3} \theta_y(N)$$

$$\sum \phi_\epsilon = \sum_{N=0}^{3} [\phi_x(N) + \phi_z(N)] \qquad (16)$$

$$\sum \psi_\epsilon = \sum_{N=0}^{3} [\psi_z(N) + \psi_x(N)]$$

In this way, the resulting weighted errors can be easily evaluated to provide a measure of the satellite's pointing capability. It is emphasized that the simplified weighted error functions are normalized with respect to $T_d/\omega_o^2 I_y$ which has been arbitrarily set to unity. To obtain a measure of the actual pointing accuracy, the magnitude of the disturbance torques must be incorporated in the above expressions as follows:

$$\text{Pitch Error} = \frac{T_{dy}}{\omega_o^2 I_y} \sum \theta_\epsilon$$

$$\text{Roll Error} = \frac{T_{dx}}{\omega_o^2 I_y} \sum \phi_\epsilon$$

$$\text{Yaw Error} = \frac{T_{dz}}{\omega_o^2 I_y} \sum \psi_\epsilon$$

4.0 PARAMETER STUDY

In this section parameter sensitivity curves are presented for the Roll-Vee and Yaw-Vee systems. The parameter study is divided into three parts. In the first part, frequency response curves are obtained for several sets of system

parameter values. The aim is to limit the range of the system parameters to values which will be acceptable in a design in which the attitude errors are minimized. Moreover, the frequency response curves will permit a more meaningful evaluation of the attitude errors when an actual model of the disturbance torques becomes available.

In the second part of the study the weighted attitude errors of Equation (16) are evaluated as a function of the system parameters.

In the third part of the study the weighted error results are used as a basis to compare the design of a gyro control system with that of a reaction wheel control system.

To rapidly assess the effects of parameter changes on the error/torque gains or weighted attitude errors, the STL On-Line Computer was employed. Specifically, the gain and weighted error expressions of the previous section were programmed on the On-Line Computer which permits any one of the system parameters to be treated as a variable. In this way, the gain or weighted error can be calculated and displayed on the computer's cathode ray tube as a function of any one system parameter. Finally, to check that a given set of parameters comprise a stable system, the Routh-Hurwitz coefficients also were programmed on the On-Line Computer.

The On-Line Computer results are collected in Appendix B. Roll and yaw attitude errors are plotted separately to discriminate between the components of disturbance torques from which the attitude errors arise. For example, a "Roll-Yaw" error refers to a roll error due to a yaw disturbance torque. Also it will be noted that the decimal range of the "X" and "Y" scales are denoted in terms of a binary scale. For instance, if the figure is denoted by an X scale of two, the abscissa of the graph ranges from zero to 2^2, or 4. Unless specified otherwise, the units of the X and Y scales are dimensionless. Curves in a given figure are all plotted to the same X and Y scales.

4.1 Preliminary Parameter Selection

In this study the error/torque gains are evaluated in terms of the following normalized parameters:

$\frac{I_x}{I_y}$ = normalized roll inertia

$\frac{I_z}{I_y}$ = normalized yaw inertia

$\frac{H}{\omega_o I_y}$ = normalized gyro momentum

$\frac{H}{D}$ = gyro gain

$\mu = \alpha$ = gyro case (skew) angle

$\frac{K}{\omega_o D}$ = normalized spring constant

$\frac{H_m}{\omega_o I_y}$ = normalized pitch wheel momentum

It is obvious that unless the above parameters are restricted to a small range of values, the number of possible combinations of a given set of parameters is very large and the parameter study becomes unweildy.

In order to limit the number of combinations for the parameter study, a range of parameters was selected initially on the basis of hardware considerations and the stability results of the previous section. The On-Line Computer was then utilized to display the error/torque gains at zero, one, two and three times orbit rate frequency as a function of the system parameters. These curves enabled selecting a range of parameters which not only produced reasonably

small gains but also constituted a stable system. Based on these results, the parameter study was limited to the following values of system parameters:

$$\frac{I_x}{I_y} = \underline{1.0}, .8, .6$$

$$\frac{I_z}{I_y} = \underline{.05}, .2, .4$$

$$\frac{H}{\omega_o I_y} = \underline{1}, 2, 4$$

$$\frac{H}{D} = .5, \underline{1}, 5$$

$$\mu = \alpha = 210^\circ, \underline{220^\circ}, 240^\circ$$

$$\frac{K}{\omega_o D} = \underline{0}, .5, 1, 2, 10$$

$$\frac{H_m}{\omega_o I_y} = \underline{0}, -2, -4$$

A base-line system was chosen which is represented by the set of parameters underscored in the above list. These parameters were selected on the basis of minimizing the error/torque gains at the harmonics of orbital frequency. In the subsequent sections, the parameters are varied about the base-line system to evaluate their effects on the system's frequency response and weighted attitude errors. From this data the system's transient response and pointing accuracy can be evaluated.

4.2 Frequency Response

The first set of parameters which are investigated involves a system where the roll and pitch inertias of the satellite are equal and where there is no pitch wheel. Figure B-1 is the frequency response of a Roll-Vee system with and with a light spring

restraint. It is clear that a spring restraint degrades the error/torque gains especially at the resonance frequency and thus provides a lightly damped transient response. As a result, a large spring restraint for a Roll-Vee system is undesirable.

On the other hand, analysis of Section 3.3 indicates that the above satellite with a Yaw-Vee gyro configuration is unstable in yaw without a spring restraint. Figure B-2 indicates the frequency response of a Yaw-Vee system for several values of spring constant. For decreasing values of spring constant the pitch response is improved but the yaw response at low frequencies is degraded. A spring constant near the value of $\omega_o D$ provides a reasonable frequency response for the Yaw-Vee system.

In Figures B-3 and B-4 the frequency response of a Roll-Vee and Yaw-Vee system is depicted for several roll-pitch inertia ratios of the satellite. When the pitch inertia is fixed, the roll and yaw gains are relatively insensitive to the satellite's roll inertia. The pitch gains, however, are significantly amplified at low frequencies by a reduction of the satellite's roll inertia relative to its pitch inertia. Thus for the values considered, an inertia ratio of unity ($I_x/I_y = 1$) provides the best pitch response for the two gyro configurations.

The effect of the satellite's yaw and pitch inertias on a Roll-Vee and Yaw-Vee frequency response are presented in Figures B-5 and B-6. For both systems a small yaw inertia relative to the pitch inertia is preferable in order to minimize low frequency pitch errors. The Roll-Vee roll and yaw response are found to be relatively insensitive to yaw inertia. In the Yaw-Vee system the effect of increasing the yaw inertia shifts the roll-yaw resonance frequency towards orbit rate frequency where major disturbance sources exist. Thus, a satellite which has a small yaw inertia relative to its pitch inertia is preferred.

The case angle refers to the nominal direction which the gyro's spin axis assumes with respect to the satellite's pitch axis. In Section 3.2, the analysis indicates that a case angle between 180° and 270° is necessary to

insure system stability. At a case angle of 180°, the gyro spin axis is along the negative pitch axis and there will be no damping of motion along the pitch axis. On the other hand, as the case angle approaches 270° there is less damping of the motion along the roll or yaw axis, depending on the gyro configuration.

Figure B-7 and B-8 depict the frequency response of Roll-Vee and Yaw-Vee gyro system for several values of case angles. A case angle of 220° provides relatively small roll and yaw gains and does not amplify pitch gain at the resonance frequency (1.5 ω_o). Case angles much above 220° significantly increase the roll-yaw gains and those below 220° degrade pitch damping in either of the two gyro systems.

The effect of gyro gain on the Roll-Vee and Yaw-Vee systems is shown in Figures B-9 and B-10. Gyro gains much greater than unity tend to increase the pitch and yaw gains near orbit rate frequency and roll gains near twice orbit rate frequency for the Roll-Vee system. On the other hand, gyro gains below unity tend to amplify the gains at resonant frequency and thereby degrades the system's transient response. Gyro gains affect Yaw-Vee pitch gains in the same manner as in the Roll-Vee system. Unlike the Roll-Vee system, the roll-yaw response of the Yaw-Vee system is relatively insensitive to gyro gains except for the low frequency yaw gains which increase with gyro gain. Therefore, within the values considered, a gyro gain of unity provides the best frequency response for both configurations.

In the previous section, it was noted that large values of gyro angular momentum tend to reduce the magnitude of the error/torque gains. This result is verified in Figures B-11 and B-12 where the frequency response of the Roll-Vee and Yaw-Vee systems are shown for several normalized values of gyro momentum. However, besides reducing the gains, an increase in the gyro momentum from $\omega_o I_y$ to $4\omega_o I_y$ shifts the resonance frequency from 1.5 ω_o to 1.2 ω_o. This effect is especially critical in the Yaw-Vee system where the roll and yaw resonance amplitude increase significantly with the corresponding shift in the resonance frequency. This is an undesirable trend because disturbance effects are prominent at and near orbit rate frequencies. This gyro momentum values much beyond $4\omega_o I_y$ should be avoided.

The last set of frequency response curves pertains to a satellite system which employs a pitch wheel. As indicated by the equations of motion, a pitch wheel does not affect small angle pitch response but does increase the angular momentum of satellite's pitch axis to stiffen the control about the roll and yaw axes. The latter effect is shown in Figures B-13 and B-14 for the Roll-Vee and Yaw-Vee systems. Pitch wheel momentum significantly reduces roll and yaw gains except at the resonance frequency. As in the case with gyro momentum, larger values of pitch wheel momentum shift the resonance point toward orbit rate frequency.

4.3 Weighted Error Results

Based on the frequency response results, some limitations are imposed on the system parameters which will be used to determine the weighted attitude errors. First, the case angle is restricted to a value of 220° in order to provide adequate control in the pitch axis as well as the roll-yaw axes. Secondly, the lower limit of the gyro momentum is restricted to the value of $\omega_o I_y$, the angular momentum of the satellite. For the Roll-Vee configuration, no spring restraint is employed since it was found to be undesirable from the standpoint of frequency response. The Yaw-Vee configuration, however, is given a light spring restraint to stabilize the system and to reduce error/torque gains.

In Figure B-15 the weighted pitch error is plotted against gyro momentum with normalized spring constant as a parameter. When the spring constant is zero as in the case of the Roll-Vee system, it is noted that the pitch error decreases with increasing values of gyro momentum. However, when a light spring restraint is used as in the case of the Yaw-Vee system, the effect of gyro momentum on the weighted pitch error is not the same. As indicated in the frequency response of Figure B-12, large values of gyro momentum reduce pitch gains at twice orbit rate frequency but at the expense of increasing the gain at orbit rate frequency. As a result, the weighted pitch errors of the Yaw-Vee system may either increase with gyro momentum or remain relatively insensitive to gyro momentum, depending on the value of the spring constant.

The effect of gyro gain on the weighted roll and yaw error is shown in Figure B-16. Weighted errors are minimized for small values of gyro gains, however, they are not significantly reduced for gyro gains below unity.

To evaluate the effect of satellite inertias, the weighted errors are presented as a function of normalized roll inertia with normalized yaw inertia as a parameter. For the Roll-Vee system, Figure B-17 indicates that the weighted roll and yaw errors are relatively insensitive to normalized roll inertia. The weighted pitch error, however, is reduced as the roll inertia approaches the value of the pitch inertia. Moreover, the weighted errors are minimized for a small yaw inertia relative to the pitch inertia. In fact, when the yaw inertia is decreased from .4 I_y to .05 I_y, the weighted errors are reduced by about 25%. Thus a satellite with a large roll and pitch inertias relative to the yaw inertia is desirable to minimize the attitude errors. Moreover, since the weighted errors must be multiplied by a factor of $T_d/\omega_o^2 I_y$ to obtain the pointing errors, a large value of pitch inertia is desirable to reduce the effect of the disturbance torques.

Figure B-18 shows the effect of roll and yaw inertias on the weighted errors of a Yaw-Vee system without a spring restraint. The inertia effects on the weighted roll error are the same as that for the Roll-Vee system. However, the weighted yaw error is very sensitive to roll inertia as it approaches the value of pitch inertia. Under these conditions, the yaw gain at zero frequency makes the largest contribution to the weighted yaw error. By employing a gyro spring restraint, the Yaw-Vee system becomes relatively insensitive to the roll-pitch inertia ratios, as shown in Figure B-19. The magnitude of the weighted yaw error is significantly reduced. In fact, the extent of the improvement in yaw overshadows the relatively small increase in the roll and pitch errors which result from the use of a spring restraint. Thus a light spring restraint is recommended for the Yaw-Vee system.

In Figure B-20, the weighted roll and yaw errors are evaluated as a function of gyro momentum with pitch wheel momentum as a parameter. Errors are

significantly reduced by increasing the angular momentum of either the gyro or the pitch wheel above the value of $\omega_o I_y$. However, beyond momentum values of $4\omega_o I_y$, the reduction of the errors is not significant.

4.4 Single Gyro Results

The weighted error results for a Roll and Yaw gyro system are presented in Figures B-21 to B-24 (in these figures, the terms "Roll-Vee" and Yaw-Vee" refer to the Roll and Yaw systems, respectively). In general, the sensitivity of the roll and yaw errors due to system parameter variations is the same as that discussed for the Roll-Vee and Yaw-Vee systems. An exception is the effect of the satellite's roll inertia on the weighted errors. Roll and yaw errors of the Roll system are improved when the satellite has a small roll inertia relative to the pitch inertia. However, as the angular momentum of the gyro increases beyond the angular momentum of the satellite, the improvement in the weighted errors is not significant.

4.5 Summary of Parameter Variation Results

In summary, typical values of weighted attitude errors are compared for particular Roll-Vee and Yaw-Vee gyro configurations. Table II lists the data for a system which employs large gyro angular momentum but no pitch wheel and a system which employs smaller gyros and a large pitch wheel momentum. Weighted roll and yaw errors for each of the systems are comparable in magnitude. However, pitch errors are smaller with larger values of gyro momentum. Thus in terms of minimizing the dynamic errors about all axes, it is more desirable to increase the angular momentum of the gyro than to make use of a pitch wheel.

Typical weighted errors for a satellite with a Roll or Yaw gyro configuration are listed in Table III. Only weighted roll and yaw errors are presented since it is assumed that some device other than control moment gyros is used to damp the pitch axis motion. The Roll system with a large pitch wheel momentum provides the smallest roll and yaw errors. A comparison of the data in Tables II and III shows the magnitude of the weighted roll and yaw errors are comparable between the single gyro and the two gyro systems.

TABLE II

Weighted Attitude Errors of Two Gyro Systems

System*	Weighted Pitch Error ($Rad/T_{dy}/\omega_o^2 I_y$)	Weighted Roll Error ($Rad/T_{dx}/\omega_o^2 I_y$)	Weighted Yaw Error ($Rad/T_{dz}/\omega_o^2 I_y$)
I. Roll-Vee System (No Pitch Wheel)	1.06	1.25	1.26
II. Yaw-Vee System (No Pitch Wheel)	1.70	1.04	1.48
III. Roll-Vee System (Pitch Wheel Added)	1.59**	1.09	1.32
IV. Yaw-Vee System (Pitch Wheel Added)	1.61	1.07	1.35

*System Parameters:

$$\frac{I_x}{I_y} = 1.0$$

$$\frac{I_z}{I_y} = .05$$

$$\frac{|H_m|}{\omega_o I_y} = \begin{cases} 0 \text{ , Systems I and II} \\ 4 \text{ , Systems III and IV} \end{cases}$$

$$\frac{H}{\omega_o I_y} = \begin{cases} 4 \text{ , Systems I and II} \\ 1 \text{ , Systems III and IV} \end{cases}$$

$$\mu \text{ , } \alpha = 220^o$$

$$\frac{H}{D} = 1$$

$$\frac{K}{\omega_o D} = \begin{cases} 0 \text{ , Roll-Vee System} \\ 1 \text{ , Yaw-Vee System} \end{cases}$$

**Note: Gyro momentum values account for the differences in weighted pitch error between Systems I and III.

TABLE III

Weighted Attitude Errors of Single Gyro Systems

System*	Weighted Roll Error ($Rad/T_{dx}/\omega_o^2 I_y$)	Weighted Yaw Error ($Rad/T_{dz}/\omega_o^2 I_y$)
I. Roll System (No Pitch Wheel)	1.4	1.5
II. Yaw System (No Pitch Wheel)	1.2	1.9
III. Roll System (Pitch Wheel Added)	1.1	1.1
IV. Yaw System (Pitch Wheel Added)	1.1	1.4

* System Parameters:

$$\frac{I_x}{I_y} = 1.0$$

$$\frac{I_z}{I_y} = .05$$

$$\frac{|H_m|}{\omega_o I_y} = \begin{cases} 0 \text{ , Systems I and II} \\ 4 \text{ , Systems III and IV} \end{cases}$$

$$\frac{H}{\omega_o I_y} = \begin{cases} 4 \text{ , Systems I and II} \\ 1 \text{ , Systems III and IV} \end{cases}$$

$$\frac{H}{D} = 1$$

$$\frac{K}{\omega_o D} = \begin{cases} 0 \text{ , Roll System} \\ 1 \text{ , Yaw System} \end{cases}$$

The values of the parameters which are listed for the gyro systems in Tables II and III represent a reasonably good selection in view of their effects on the weighted errors. Without a disturbance model it is not clear whether these parameter values are optimum with respect to minimizing the weighted errors for a particular configuration. However, these results can serve as a starting point for a more detailed design of a control moment gyro system.

4.6 System Comparisons

In this section the weighted attitude errors of a reaction wheel system and a control moment gyro system are summarized to compare the pointing capability of the two systems. The specific values of the weighted errors are based on the results of the two reaction wheel configurations described in Appendix C and on the Roll-Vee and Roll gyro configurations of the previous section.

In Figure 4, a bar graph of the weighted attitude errors is plotted for the two types of control systems. Each bar in the figure indicates a range of weighted errors to account for the range of values which the system parameters can assume in a given design. This range between the least and worst errors is represented by the unhatched portion of the bar graph.

The data indicates that when no pitch wheel is employed, a reaction wheel system results in a yaw error which is approximately the same magnitude as that of the gyro system. However, the roll and pitch errors of the reaction wheel system are somewhat smaller than those of the gyro system. On the other hand, the use of a pitch wheel in either of the two systems reduces the magnitude of the roll and yaw errors. In fact, the two systems with a pitch wheel have comparable values of weighted roll and yaw errors. Of course, the pitch wheel has nc effect on the pitch errors.

The results show that a control moment gyro system and a reaction wheel system produce comparable roll and yaw errors. If a small pitch error is required, a single control moment gyro can be used to damp the roll-yaw motions and another device such as a reaction wheel can be used to damp the pitch motion. In this way, a single control moment gyro and a reaction wheel can be combined to minimize the weighted errors.

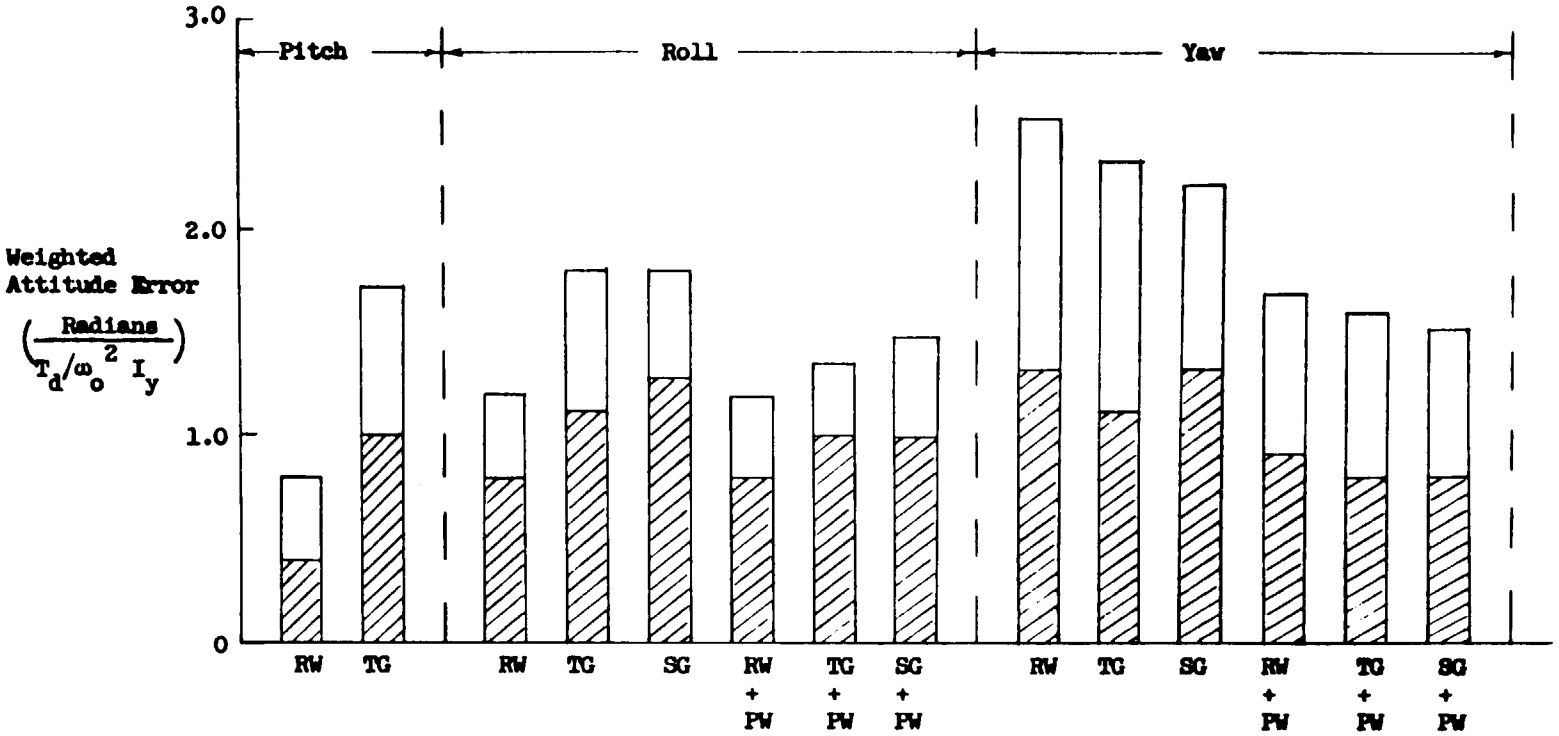

Figure 4

Summary of Weighted Attitude Errors for Reaction Wheel System and Control Moment Gyro System

5.0 GYRO ERROR ANALYSIS

In Section 3.1, the equations of motion were derived for a Roll-Vee and Yaw-Vee system under the assumption that the two control moment gyros were identical and were symmetrically oriented with respect to the satellite. Under this assumption, attitude errors result solely from external disturbances. However, non-identical gyros and/or non-symmetric gyro orientation will add to the system a net non-zero torque which must be overcome by an equal and opposite gravity gradient torque. In this case, additional attitude errors result.

In this section the expressions of the constant attitude errors due to non-idealities of the control moment gyro are derived and discussed. Both Roll-Vee and Yaw-Vee gyro orientations are considered.

5.1 Derivation of Steady State Error Matrix

In terms of the notation used in Appendix A, the gyro parameters are re-defined as follows:

$$H_{Di} = H + \Delta H_i$$

$$D_i = D + \Delta D_i$$

$$K_i = K + \Delta K_i$$

$$M_{g1} = \begin{cases} \omega_o HS\mu + \Delta M_{g1}, & \text{Roll-Vee System} \\ -\omega_o HS\alpha + \Delta M_{g1}, & \text{Yaw-Vee System} \end{cases}$$

$$M_{g2} = \begin{cases} -\omega_o HS\mu + \Delta M_{g2}, & \text{Roll-Vee System} \\ \omega_o HS\alpha + \Delta M_{g2}, & \text{Yaw-Vee System} \end{cases}$$

where ΔH_i, ΔD_i, ΔK_i, ΔM_{gi} represent gyro i's discripancy from the nominal gyro momentum, viscous damping coefficient, spring constant, and torque generator output, respectively. To account for the non-symmetric orientation of gyro i with respect to the satellite, the following angular relations are assumed:

Roll-Vee System:

$$\alpha_i = 90 + \Delta\alpha_i$$

$$\beta_i = 90 + \Delta\beta_i$$

$$\mu_1 = \mu + \Delta\mu_1$$

$$\mu_2 = -(\mu + \Delta\mu_2)$$

Yaw-Vee System:

$$\beta_i = \Delta\beta_i$$

$$\mu_i = \Delta\mu_i$$

$$\alpha_1 = 90 + \alpha + \Delta\alpha_1$$

$$\alpha_2 = 90 - (\alpha + \Delta\alpha_2)$$

where $\Delta\alpha_i$, $\Delta\beta_i$, $\Delta\mu_i$ represent gyro i's angular discrepancy from the nominal displacement in yaw, pitch and roll axis, respectively. The equations of motion can be obtained by substituting the above relationships into Equations (A.18), (A.19), (A.20) and (A.31) of Appendix A. By assuming zero disturbance torques and by neglecting higher order terms, the equations can be reduced to the following steady state matrix:

$$\begin{bmatrix} a_{11} & 0 & 0 & a_{14} & a_{15} \\ a_{21} & a_{22} & a_{23} & 0 & 0 \\ 0 & 0 & a_{33} & a_{34} & a_{35} \\ a_{41} & 0 & a_{43} & a_{44} & 0 \\ a_{51} & 0 & a_{53} & 0 & a_{55} \end{bmatrix} \begin{bmatrix} \phi_{ss} \\ \theta_{ss} \\ \psi_{ss} \\ A_{1ss} \\ A_{2ss} \end{bmatrix} = \begin{bmatrix} T_{r1} \\ T_{r2} \\ T_{r3} \\ T_{r4} \\ T_{r5} \end{bmatrix} \qquad (17)$$

where the ϕ_{ss}, θ_{ss}, ψ_{ss} represent the steady state errors in roll, pitch, yaw, respectively; A_{1ss}, A_{2ss} are the steady state gimbal errors; a_{ij} are normalized elements defined as

$$a_{11} = 4(1-c) - m - 2h - h\left(\frac{\Delta H_1}{H} + \frac{\Delta H_2}{H}\right) + \frac{HS\mu}{\omega_o I_y}(\Delta\mu_1 + \Delta\mu_2)\,\delta_1 + \frac{HS\alpha}{\omega_o I_y}(\Delta\alpha_1+\Delta\alpha_2)\,\delta_2$$

$$a_{14} = -\left[h\left(1 + \frac{\Delta H_1}{H}\right) - \frac{HS\mu}{\omega_o I_y}\Delta\mu_1\right]\delta_1 - \frac{H}{\omega_o I_y}\Delta\beta_1\,\delta_2$$

$$a_{15} = -\left[h\left(1 + \frac{\Delta H_2}{H}\right) - \frac{HS\mu}{\omega_o I_y}\Delta\mu_2\right]\delta_1 - \frac{H}{\omega_o I_y}\Delta\beta_2\,\delta_2$$

$$a_{21} = -h(\Delta\alpha_1 + \Delta\alpha_2)\,\delta_1 - \left[\frac{HS\alpha}{\omega_o I_y}\left(\frac{\Delta H_1}{H} - \frac{\Delta H_2}{H}\right) + h(\Delta\alpha_1 - \Delta\alpha_2)\right]\delta_2$$

$$a_{22} = 3(b-c)$$

$$a_{23} = -\left[\frac{HS\mu}{\omega_o I_y}\left(\frac{\Delta H_1}{H} - \frac{\Delta H_2}{H}\right) + h(\Delta\mu_1 - \Delta\mu_2)\right]\delta_1 - \frac{H}{\omega_o I_y}(\Delta\mu_1 + \Delta\mu_2)\,\delta_2$$

$$a_{33} = 1 - b - m - 2h - h\left(\frac{\Delta H_1}{H} + \frac{\Delta H_2}{H}\right) + \frac{HS\mu}{\omega_o I_y}(\Delta\mu_1 + \Delta\mu_2)\,\delta_1 - \frac{HS\alpha}{\omega_o I_y}(\Delta\alpha_1+\Delta\alpha_2)\,\delta_2$$

$$a_{34} = \left[\frac{H}{\omega_o I_y}\Delta\beta_1 - \frac{HS\mu}{\omega_o I_y}\Delta\alpha_1\right]\delta_1 - \left[h\left(1 + \frac{\Delta H_1}{H}\right) - \frac{HS\alpha}{\omega_o I_y}\Delta\alpha_1\right]\delta_2$$

$$a_{35} = \left[\frac{H}{\omega_o I_y}\Delta\beta_2 + \frac{HS\mu}{\omega_o I_y}\Delta\alpha_2\right]\delta_1 - \left[h\left(1 + \frac{\Delta H_2}{H}\right) - \frac{HS\alpha}{\omega_o I_y}\Delta\alpha_2\right]\delta_2$$

$$a_{41} = -\left[\frac{H}{D}C\mu\left(1 + \frac{\Delta H_1}{H}\right) - \frac{HS\mu}{D}\Delta\mu_1\right]\delta_1 - \left[\frac{H}{D}\Delta\beta_1\right]\delta_2$$

$$a_{43} = \left[\frac{H}{D}\Delta\beta_1 - \frac{HS\mu}{D}\Delta\alpha_1\right]\delta_1 - \left[\frac{HC\alpha}{D}\left(1 + \frac{\Delta H_1}{H}\right) - \frac{HS\alpha}{D}\Delta\alpha_1\right]\delta_2$$

$$a_{44} = \frac{K + \Delta K_1}{\omega_o D} - \left[\frac{HC\mu}{D}\left(1 + \frac{\Delta H_1}{H}\right) - \frac{HS\mu}{D}\Delta\mu_1\right]\delta_1 - \left[\frac{HC\alpha}{D}\left(1 + \frac{\Delta H_1}{H}\right) - \frac{HS\alpha}{D}\Delta\alpha_1\right]\delta_2$$

$$a_{51} = -\left[\frac{HC\mu}{D}\left(1 + \frac{\Delta H_2}{H}\right) - \frac{HS\mu}{D}\Delta\mu_2\right]\delta_1 - \left[\frac{H}{D}\Delta\beta_2\right]\delta_2$$

$$a_{53} = \left[\frac{H}{D}\Delta\beta_2 + \frac{HS\mu}{D}\Delta\alpha_2\right]\delta_1 - \left[\frac{HC\alpha}{D}\left(1 + \frac{\Delta H_2}{H}\right) - \frac{HS\alpha}{D}\Delta\alpha_2\right]\delta_2$$

$$a_{55} = \frac{K + \Delta K_2}{\omega_o D} - \left[\frac{HC\mu}{D}\left(1 + \frac{\Delta H_2}{H}\right) - \frac{HS\mu}{D}\Delta\mu_2\right]\delta_1 - \left[\frac{HC\alpha}{D}\left(1 + \frac{\Delta H_2}{H}\right) - \frac{HS\alpha}{D}\Delta\alpha_2\right]\delta_2$$

and T_{ri} are constant forcing terms which are given as follows:

$$T_{r1} = -\left[\frac{HS\mu}{\omega_o I_y}\left(\frac{\Delta H_1}{H} - \frac{\Delta H_2}{H}\right) + \frac{HC\mu}{\omega_o I_y}(\Delta\mu_1 - \Delta\mu_2)\right]\delta_1 - \frac{H}{\omega_o I_y}(\Delta\mu_1 + \Delta\mu_2)\,\delta_2$$

$$T_{r2} = 0$$

$$T_{r3} = h\,(\Delta\alpha_1 + \Delta\alpha_2)\,\delta_1 + \left[\frac{HS\alpha}{\omega_o I_y}\left(\frac{\Delta H_1}{H} - \frac{\Delta H_2}{H}\right) + h\,(\Delta\alpha_1 - \Delta\alpha_2)\right]\delta_2$$

$$T_{r4} = -\left[\frac{H}{D}S\mu\left(\frac{\Delta M_{g1}}{\omega_o HS\mu} + \frac{\Delta H_1}{H}\right) + \frac{HC\alpha}{D}\Delta\mu_1\right]\delta_1 + \left[\frac{H}{D}S\alpha\left(\frac{\Delta M_{g1}}{\omega_o HS\mu} + \frac{\Delta H_1}{H}\right) + \frac{HC\alpha}{D}\Delta\alpha_1\right]\delta_2$$

$$T_{r5} = \left[\frac{HS\mu}{D}\left(\frac{\Delta M_{g2}}{\omega_o HS\mu} + \frac{\Delta H_2}{H}\right) + \frac{HC\mu}{D}\Delta\mu_2\right]\delta_1 + \left[\frac{H}{D}S\alpha\left(\frac{\Delta M_{g2}}{\omega_o HS\alpha} - \frac{\Delta H_2}{H}\right) - \frac{HC\alpha}{D}\Delta\alpha_2\right]\delta_2$$

From the constant forcing terms T_{ri}, it is evident that the main sources of errors are represented by the following gyro non-idealities:

1. Gyro momentum offsets (ΔH_i)
2. Torque Generator Output Errors (ΔM_{gi})
3. Gyro Roll Misalignment ($\Delta\mu_i$)
4. Gyro Yaw Misalignment ($\Delta\alpha_i$)

The other non-idealities affect the steady state errors indirectly through the elements a_{ij} in Equation (17) and are not considered in this study.

5.2 Evaluation of Steady State Errors

In this section the steady state errors of Equation (17) are evaluated. Unlike attitude errors due to disturbance torques which are normalized with respect to $T_d/\omega_o^2 I_y$, the attitude errors due to gyro non-idealities are expressed directly in radians (or degrees).

A particularly common source of errors occurs when there exists momentum offsets (ΔH_i) in the two control moment gyros. By solving Equation (17) the steady state attitude errors due only to gyro momentum offsets can be expressed as follows:

Roll-Vee System:

$$\phi_{ss} = \frac{T_{r1} - \frac{a_{14}}{a_{44}} T_{r4} - \frac{a_{15}}{a_{55}} T_{r5}}{a_{11} - \left(\frac{a_{14}a_{41}}{a_{44}} + \frac{a_{15}a_{51}}{a_{55}}\right)} \qquad (18)$$

$$\theta_{ss} = 0$$

$$\psi_{ss} = 0$$

Yaw-Vee System:

$$\phi_{ss} = 0$$

$$\theta_{ss} = 0$$

$$\psi_{ss} = \frac{T_{r3} - \frac{a_{34}}{a_{44}} T_{r4} - \frac{a_{35}}{a_{55}} T_{r5}}{a_{33} - \left(\frac{a_{34}a_{43}}{a_{44}} + \frac{a_{35}a_{53}}{a_{55}}\right)} \qquad (19)$$

Gyro momentum offsets affect only the roll axis in the case of the Roll-Vee system or the yaw axis in the case of the Yaw-Vee system. As illustrated in Figure 5, unequal momentum values between the two gyros produce a total gyro momentum vector which is not colinear with the orbit rate axis. As a result, the orbital motion of the satellite couples with the gyro momentum vector to

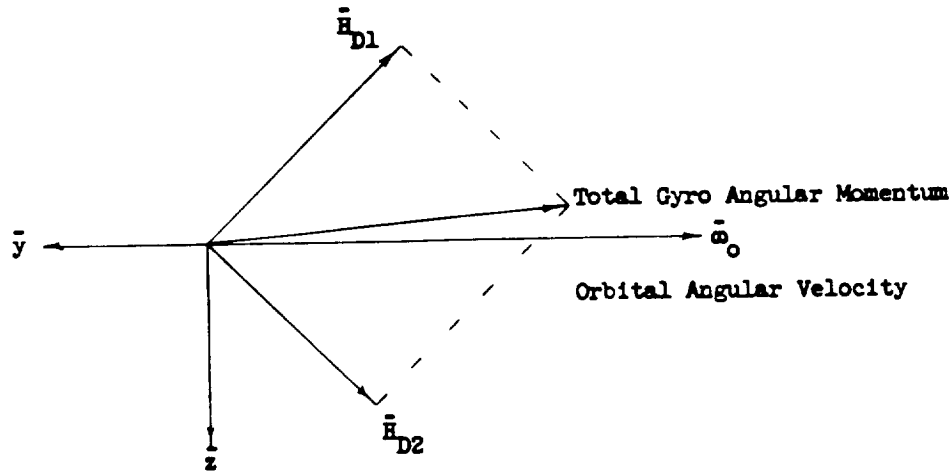

Figure 5

Vector Relationships for a System with Gyro Momentum Offsets
$\left(|\bar{H}_{D1}| \neq |\bar{H}_{D2}|\right)$

produce a torque about the roll axis in the Roll-Vee system or a torque about the yaw axis in the Yaw-Vee system. The magnitude of the resulting attitude errors are obtained by substituting for the terms in Equations (18) and (19). By neglecting second order effects, the steady state attitude errors are reduced to the following expressions:

Roll-Vee System:

$$\phi_{ss} \cong \frac{-\left(\frac{HS\mu}{\omega_o I_y}\right)\left[\frac{\frac{K}{\omega_o D}}{\frac{K}{\omega_o D} - \frac{HC\mu}{D}}\right]\left(\frac{\Delta H_1}{H} - \frac{\Delta H_2}{H}\right)}{4(1-c) - m - h\left(\frac{\Delta H_1}{H} + \frac{\Delta H_2}{H}\right) - 2h\left[\frac{\frac{K}{\omega_o D}}{\frac{K}{\omega_o D} - \frac{HC\mu}{D}}\right]} \qquad (20)$$

Yaw-Vee System:

$$\psi_{ss} \cong \frac{\left(\frac{HS\alpha}{\omega_o I_y}\right)\left[\frac{\frac{K}{\omega_o D}}{\frac{K}{\omega_o D} - \frac{HC\alpha}{D}}\right]\left(\frac{\Delta H_1}{H} - \frac{\Delta H_2}{H}\right)}{1-b-m-h\left(\frac{\Delta H_1}{H} + \frac{\Delta H_2}{H}\right) - 2h\left[\frac{\frac{K}{\omega_o D}}{\frac{K}{\omega_o D} - \frac{HC\alpha}{D}}\right]} \qquad (21)$$

The effect of employing a gyro spring restraint on the system can be noted in the above equations. When there is no spring restraint ($K = 0$), it is evident that gyro momentum offsets do not contribute to the steady state attitude errors. In this case, the gimbals of each gyros are free to rotate until the total gyro angular momentum vector is colinear with the orbit rate axis. On the other hand, a spring restraint couples the motion between the satellite and gyros. As a result, gyro momentum offsets produce a finite attitude error on the satellite.

In Figures 6 and 7 the attitude errors of Equations (20) and (21) are plotted against values of pitch wheel momentum with gyro spring constant as a parameter. A nominal 5% offset is assumed in the angular momentum of each gyro.($|\Delta H_i/H| = .05$). For no pitch wheel bias and a spring constant of $\omega_o D$, the steady state roll error is .45° in the Roll-Vee system and the yaw error is 2.4° in the Yaw-Vee system. For this source of attitude error it is clear that a Roll-Vee is preferred to a Yaw-Vee system. It should be noted that a small spring constant and large pitch wheel momentum are desirable to reduce the above attitude errors.

For the Roll-Vee system, the expressions of the steady state errors due to asymmetric gyro orientations ($\Delta\mu_i$, $\Delta\alpha_i$) and torque generator errors (ΔM_{gi}) are summarized in Table IV. These expressions represent approximations of the errors since the second order effects were neglected in the derivation. The table lists, as two limiting cases, the error expressions for systems with no spring restraint ($K = 0$) and for systems with a large spring restraint ($K \gg \omega_o HC\mu$). It is noted that the most critical of the listed sources of error is misalignment of the gyro about the yaw axis. In fact, for a system with equal roll and pitch inertias ($b = 1$) but no pitch wheel, yaw misalignment ($\Delta\alpha_i$) causes the satellite to precess about the yaw axis until the following yaw error is obtained:

$$\psi_{ss} \cong \frac{\Delta\alpha_1 + \Delta\alpha_2}{2}$$

Thus, in this case the magnitude of steady state error is in the order of the gyro's yaw misalignment.

In Figure 8, the yaw error due to gyro yaw misalignment in a Roll-Vee system is plotted against values of pitch wheel momentum. In the figure a nominal yaw misalignment of 1° is assumed for each gyro. It is clear that a pitch wheel significantly reduces the steady state yaw error. In fact, with a pitch wheel momentum of $4\omega_o I_y$, the resulting yaw error is .28° as compared to a yaw error of 1° when no pitch wheel is employed.

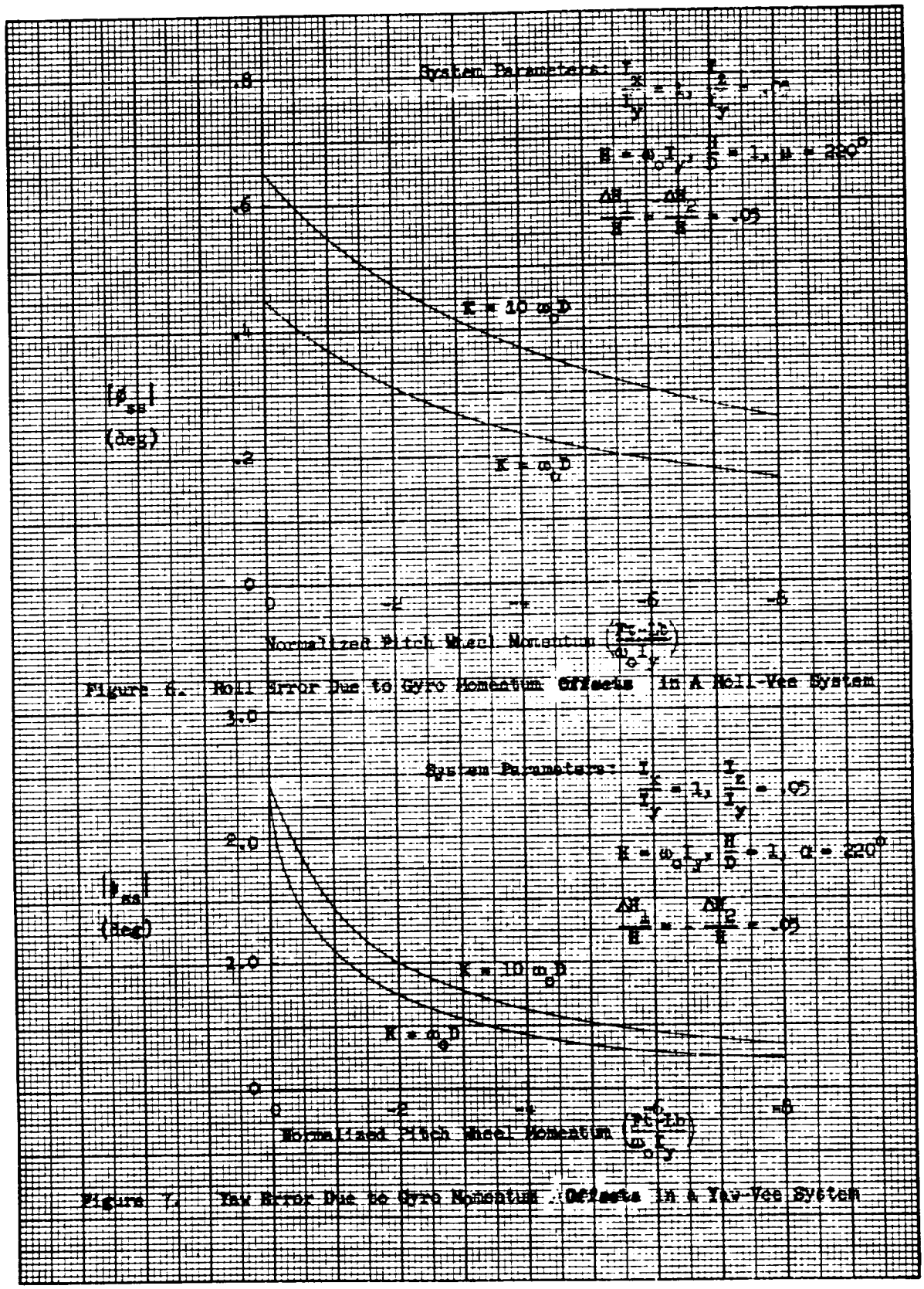

Figure 6. Roll Error Due to Gyro Momentum Offsets in A Roll-Yaw System

Figure 7. Yaw Error Due to Gyro Momentum Offsets in a Yaw-Yaw System

TABLE IV

Summary of Steady State Error Expressions Due to Gyro Non-Idealities

(Roll-Vee System)

Error Source	ϕ_{ss}		θ_{ss}		ψ_{ss}	
	$K = 0$	$K \gg \omega_o HC\mu$	$K = 0$	$K \gg \omega_o HC\mu$	$K = 0$	$K \gg \omega_o HC\mu$
Gyro Momentum Offset (ΔH_i)	0	$-\frac{HS\mu}{\omega_o I_y} \cdot \frac{\left[\frac{\Delta H_1}{H} - \frac{\Delta H_2}{H}\right]}{4(1-c)-m-2h}$	0	0	0	0
Torque Generator Output Error (ΔM_{gi})	$\frac{HS\mu}{\omega_o I_y} \cdot \frac{\left[\frac{\Delta M_{g1}-\Delta M_{g2}}{\omega_o HS\mu}\right]}{4(1-c)-m}$	$-h\left(\frac{\omega_o HS\mu}{K}\right) \cdot \frac{\left[\frac{\Delta M_{g1}-\Delta M_{g2}}{\omega_o HS\mu}\right]}{4-(1-c)-m-2h}$	0	0	0	0
Gyro Roll Misalignment $(\Delta\mu_i)$	0	$\frac{-h(\Delta\mu_1 - \Delta\mu_2}{4(1-c)-m-2h}$	0	0	0	0
Gyro Yaw Misalignment $(\Delta\alpha_i)$	~ 0	~ 0	~ 0	~ 0	$\frac{h(\Delta\alpha_1+\Delta\alpha_2)}{1-b-m-2h}$	$\frac{h(\Delta\alpha_1+\Delta\alpha_2)}{1-b-m-2h}$

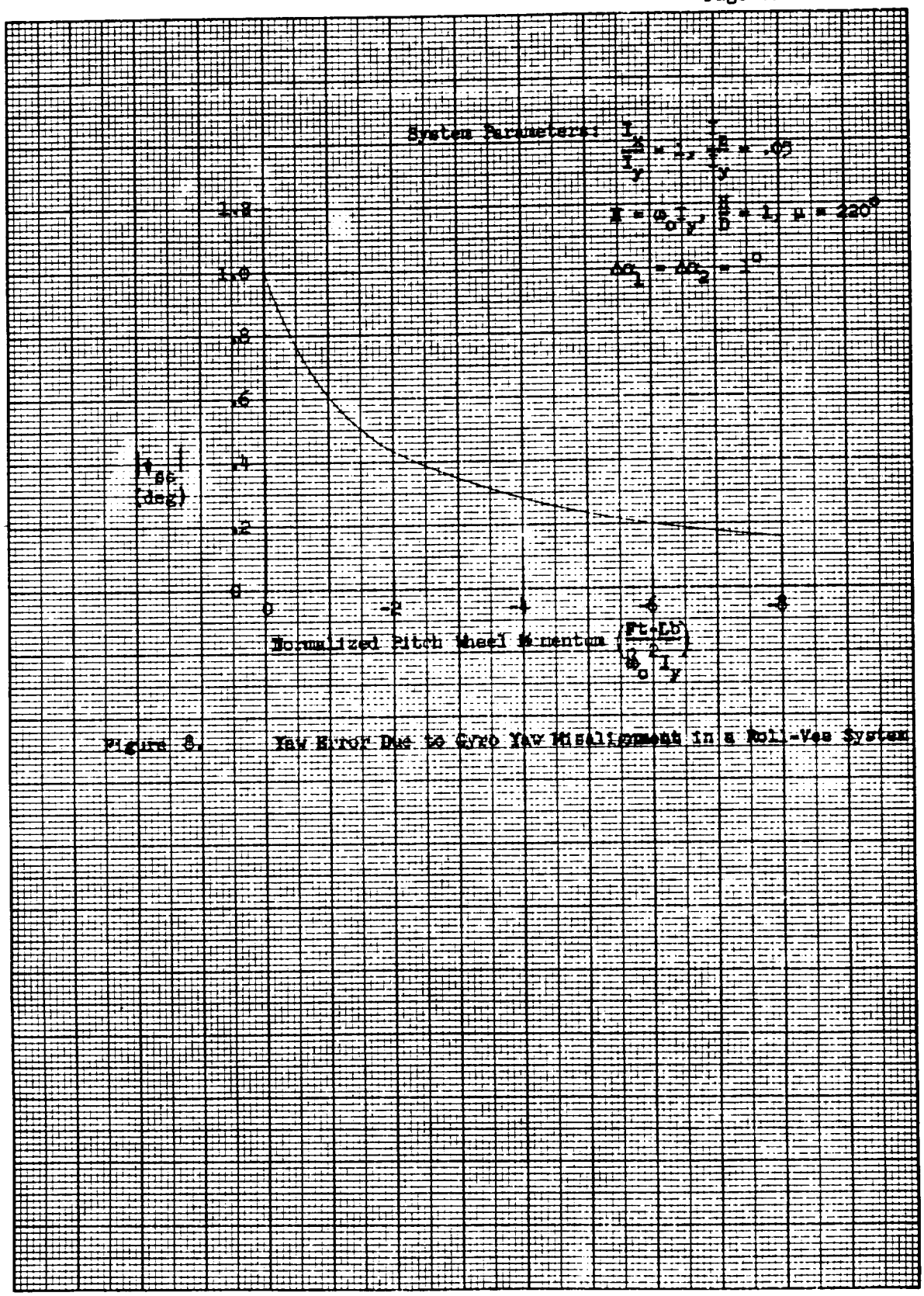

Figure 8. Yaw Error Due to Gyro Yaw Misalignment in a Roll-Yaw System

In a Roll-Vee system, an error in orienting the gyro's spin axis relative to the satellite's pitch axis is referred to as a roll misalignment ($\Delta\mu_1$). Roll misalignment affects the gyro's angular momentum vector in the pitch-yaw plane such that a gyroscopic torque is applied about the satellite's roll axis. As in the case of gyro momentum offsets, a roll error may result depending on whether or not a spring restraint is employed. In fact, Table IV indicates that the roll error due to roll misalignment is very similar in character to the roll error due to gyro momentum offsets.

In Figure 9, the effect of roll misalignment is evaluated for a Roll-Vee system. It is assumed that the system employs relatively stiff springs ($K >> \omega_o HC\mu$) in order to evaluate the worst case roll errors. A nominal roll misalignment of 1^o in each gyro results in a roll error of $.28^o$ when no pitch wheel is employed. In comparing the attitude error resulting from roll and yaw misalignments, the effect of roll misalignment is found to be much less pronounced.

Finally, the effect of torque generator output errors is evaluated. Nominally, the output of a torque generator is used to buck out the gyroscopic torque which results from maintaining a finite skew angle between the gyro spin axis and the pitch axis. If the cancellation of the above torques is not exact, there results a net torque (ΔM_{gi}) about the output axis of the gyro, which is arbitrarily designated as a torque generator error.

In a Roll-Vee system, a torque generator error results in a satellite roll error which can be expressed as follows:

$$\phi_{ss} \cong \frac{-h\left(\frac{HS\mu}{D}\right)\left[\frac{\Delta M_{g1} - \Delta M_{g2}}{\omega_o HS\mu}\right]}{\left[\frac{K}{\omega_o D} - \frac{HC\mu}{D}\right]\left[4(1-c) - m - \frac{\left(2h\frac{K}{\omega_o D}\right)}{\frac{K}{\omega_o D} - \frac{HC\mu}{D}}\right]}$$

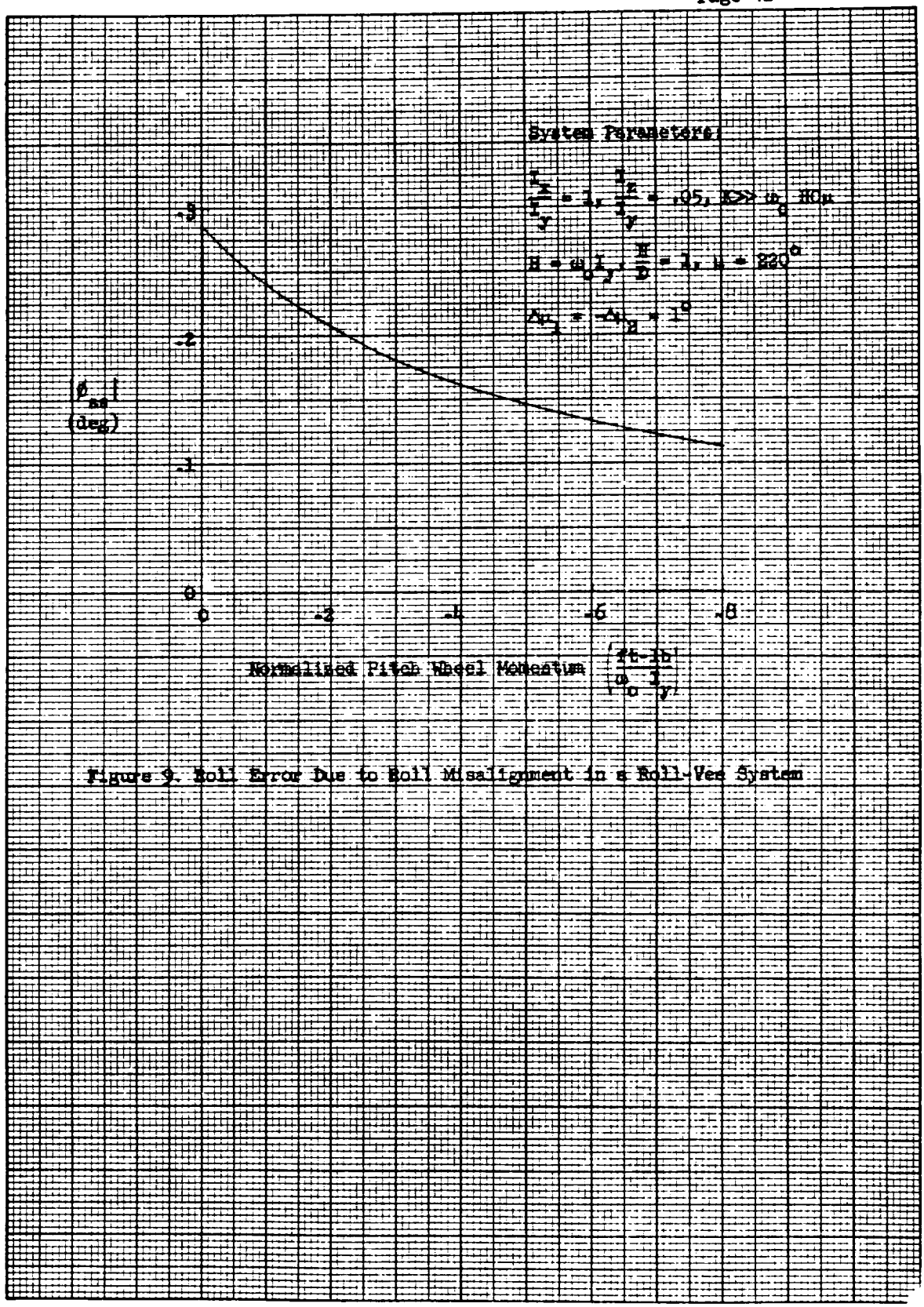

Figure 9. Roll Error Due to Roll Misalignment in a Roll-Vee System

In Figure 10, the above roll error is plotted against values of pitch wheel momentum with spring constant as a parameter. A nominal 5% error is assumed on the torque generator output $\left(|\Delta M_{gi}/\omega_o \, HS\mu| = .05\right)$. It is evident that the resulting roll error is reduced by the use of pitch wheel. The magnitude of the roll error is comparable to the error resulting from gyro momentum offsets when the spring constant has a value of $\omega_o D$. However, unlike gyro momentum offsets, the torque generator errors produce a roll error which decreases with larger values of spring constant.

For the Yaw-Vee system, it can be shown that the steady state errors due to gyro non-idealities are generally larger than those of the Roll-Vee system. The primary reason is that the Yaw-Vee system contains less "dynamic stiffness" between its yaw axis. For instance, Equations (20) and (21) indicates that the errors due to gyro momentum offsets in a Roll-Vee and Yaw-Vee system differ by the terms 4(1-c) and 1-b, respectively. Since the term 4(1-c) is greater than 1-b in most satellites, the resulting errors of the Yaw-Vee system is larger than that of the Roll-Vee system.

6.0 CONCLUSIONS

In this study, parameters for a gyro damped satellite were selected on the basis of minimizing error/torque gains summed at orbital harmonics. Coupled with an error analysis of gyro non-idealities, this approach leads to the following guidelines in selecting the system parameters for gyro-damped satellite:

a. To minimize errors due to disturbance torques, the roll and yaw inertias of the satellite should be in the same order of magnitude while the yaw inertia should be small relative to the pitch inertia.

b. To reduce dynamic errors and to de-sensitize the control system to parameter variations, the angular momentum of the gyros and the satellite should be in the same order of magnitude. Additional angular momentum may be provided by the gyros or by a pitch momentum wheel to increase the stiffness about the roll-yaw axes and thereby reduce the dynamic errors. In particular, the pitch wheel is especially effective

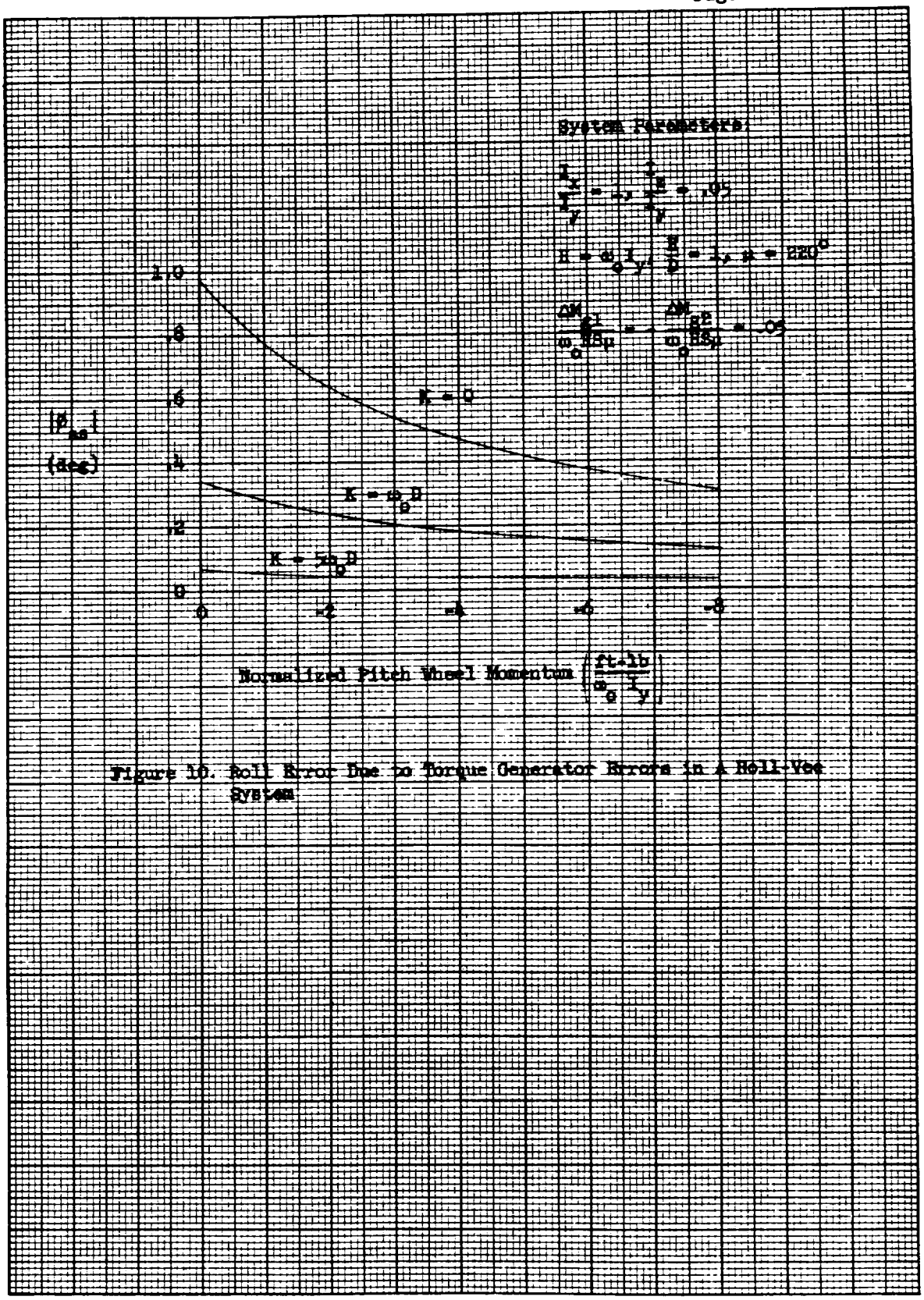

Figure 10. Roll Error Due to Torque Generator Errors in A Roll-Yaw System

in reducing errors due to gyro non-idealities such as gyro yaw misalignment. In either case, momentum values much beyond $4\omega_o I_y$ should be avoided since an increase in the angular momentum shifts the system's resonance frequency toward orbit rate frequency.

c. To provide reasonable damping characteristics, the gyro gain should be in the order of unity $\left(\frac{H}{D} = 1\right)$ and the gyro spring constant should be relatively small ($K \approx \omega_o D$). For the Roll-Vee system, the steady state errors due to gyro momentum offsets and gyro roll misalignments are minimized when the gyro spring constant is zero. For the Yaw-Vee system, a small spring restraint is required to stabilize the system and to reduce dynamic errors.

The results of the study also provide a means for making comparisons between gyro configurations and damping systems. Specifically, the following conclusions are listed:

a. A Roll-Vee gyro configuration is preferred over a Yaw-Vee configuration based on the fact that the former results in smaller errors due to disturbance torques and gyro non-idealities. Larger errors result in the Yaw-Vee system mainly because of its smaller stiffness about the yaw axis.

b. The single gyro Roll and Yaw system results in dynamic roll-yaw errors which are comparable in magnitude to those resulting in the Roll-Vee and Yaw-Vee systems.

c. Based on errors due to disturbance torques, a reaction wheel system and a control moment gyro system produce comparable roll and yaw pointing accuracy. The reaction wheel system achieves better pointing accuracy about the pitch axis. By employing a single gyro to damp the roll-yaw motion and a reaction wheel to damp the pitch motion, the resulting control system provides pointing accuracy comparable to a three reaction wheel system.

LIST OF REFERENCES

1. Moyer, R. C., R. J. Katucki, and L. K. Davis, "A System for Passive Control of Satellites Through the Viscous Coupling of Gravity Gradient and Magnetic Fields," AIAA Guidance and Control Conference Paper, No. 64-659, August 1964.

2. DeLisle, J. E., E. G. Ogletree and B. M. Hildebrant, "Applications of Gyro Stabilizers to Satellite Attitude Control," AIAA Guidance and Control Conference Paper, No. 63-325, August 1963.

3. Scott, E. D., "Control Moment Gyro Gravity Stabilization," AIAA Guidance and Control Conference Paper, No. 63-324, August 1963.

4. Lewis, J. A. and E. E. Zajac, "A Two Gyro, Gravity-Gradient Satellite Attitude Control System," Bell System Technical Journal, November 1964, pp 2705-2765.

5. Sabroff, A. E., "A Summary of Gravity Gradient Stabilization of Earth Satellites," STL Report 9990-6715-RU000, July 1964, pp 4.8.

6. McKenna, K. J., J. C. Fox and A. M. Frew, "Final Report/Nimbus Reaction Wheel Damped Gravity Gradient Stabilization Studies," STL Report 8427-6002-RU000, December 1964.

APPENDIX A

Derivation of Equations of Motion

In this appendix small angle equations of motion are derived for a satellite which includes a pair of control moment gyros for damping. For generality, an arbitrary orientation of the gyros relative to the satellite's body axes is initially considered. These generalized equations of motion are then reduced to specific gyro configurations.

In this derivation, it is assumed that the control moment gyro acts as an ideal rate integrating gyro which contains a torque generator and a spring restraint (inertia for the gyro is neglected). Moreover, it is assumed that the satellite includes a wheel spinning at a constant speed along the pitch axis. For this small angle study, the angular limitation imposed by gimbal stops are not considered. The symbols and notation used in the derivation are listed in Table A-I.

A.1 Coordinate Systems

Consider a right-handed set of geocentric coordinate axes (x_o, y_o, z_o) in which the $\bar{z}_o$ axis points toward the earth center and $\bar{y}_o$ axis is normal to the orbit plane. Consider a corresponding set of body axes (x_a, y_a, z_a) which coincides with above geocentric coordinates when there is no attitude error. As shown in Figure A-1, the body axes can be obtained from the geocentric axes by three successive rotations, ψ, θ, ϕ about yaw, pitch, and roll axes, respectively. Using small angle approximations the transformation matrix (Q_{AO}) between the body and geocentric axes becomes

$$Q_{AO} = \begin{bmatrix} 1 & \psi & -\theta \\ -\psi & 1 & \phi \\ \theta & -\phi & 1 \end{bmatrix} \qquad (A.1)$$

It is assumed that the satellite principal axes of inertia coincide with the body axes.

TABLE A-I

List of Symbols

(x_I, y_I, z_I)	Geocentric, inertial reference set
(x_o, y_o, z_o)	Orbital reference set
(x_a, y_a, z_a)	Body (satellite) reference set
(x_{ic}, y_{ic}, z_{ic})	Gyro case reference set of gyro i
(x_{ig}, y_{ig}, z_{ig})	Gyro gimbal reference set of gyro i
β_i, μ_i, α_i	Transformation angles from "A" set to "C" set
A_i	Gimbal angle of gyro i relative to its equilibrium position
H_m	Angular momentum of pitch wheel
H_{Di}	Angular momentum of gyro i
D_i	Viscous damping coefficient of gyro i
K_i	Spring constant of gyro i
M_{gi}	Torque output of generator in gyro i
ω_o	Orbital angular velocity

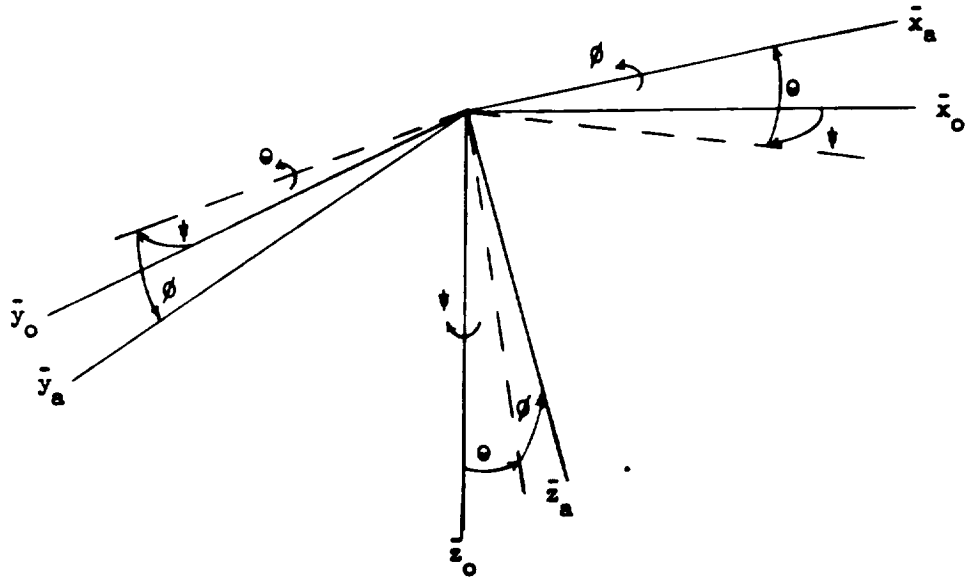

Figure A-1. Orientation of Body Reference Axes
Relative to Geocentric Reference Axes

The orientation of the i-th gyro (i = 1, 2) relative to the satellite's body axes can be described by a transformation matrix, $Q_{iC,A}$, where

$$Q_{iC,A} = \begin{bmatrix} 1 & 0 & 0 \\ 0 & C\beta_i & S\beta_i \\ 0 & -S\beta_i & C\beta_i \end{bmatrix} \begin{bmatrix} C\mu_i & 0 & -S\mu_i \\ 0 & 1 & 0 \\ S\mu_i & 0 & C\mu_i \end{bmatrix} \begin{bmatrix} C\alpha_i & S\alpha_i & 0 \\ -S\alpha_i & C\alpha_i & 0 \\ 0 & 0 & 1 \end{bmatrix} \quad (A.2)$$

where S and C is an abbreviation of sine and cosine.

The angles α_i, μ_i, and β_i which relates the case of gyro i (i = 1, 2) to the body axes are defined in Figure A-2. The gimbal error angle A_i relates the gimbal axes to the case axes of gyro i in the matrix, $Q_{iG,C}$, where

$$Q_{iG,C} = \begin{bmatrix} CA_i & SA_i & 0 \\ -SA_i & CA_i & 0 \\ 0 & 0 & 1 \end{bmatrix} \cong \begin{bmatrix} 1 & A_i & 0 \\ -A_i & 1 & 0 \\ 0 & 0 & 1 \end{bmatrix} \quad (A.3)$$

for small angles A_i.

Combining Equations (A.2) and (A.3) yields the matrix $Q_{iG,A}$, or

$$Q_{iG,A} = Q_{iG,C} \cdot Q_{iC,A} = [g_{ikj}] \quad (A.3)$$

where

$$g_{i11} = C\mu_i C\alpha_i - A_i (C\beta_i S\alpha_i - S\beta_i S\mu_i C\alpha_i)$$

$$g_{i12} = C\mu_i S\alpha_i + A_i (C\beta_i C\alpha_i + S\beta_i S\mu_i S\alpha_i)$$

$$g_{i13} = -S\mu_i + A_i S\beta_i C\mu_i$$

$$g_{i21} = -A_i C\mu_i C\alpha_i - C\beta_i S\alpha_i + S\beta_i S\mu_i C\alpha_i$$

a. Main Body to Gyro Case Coordinates

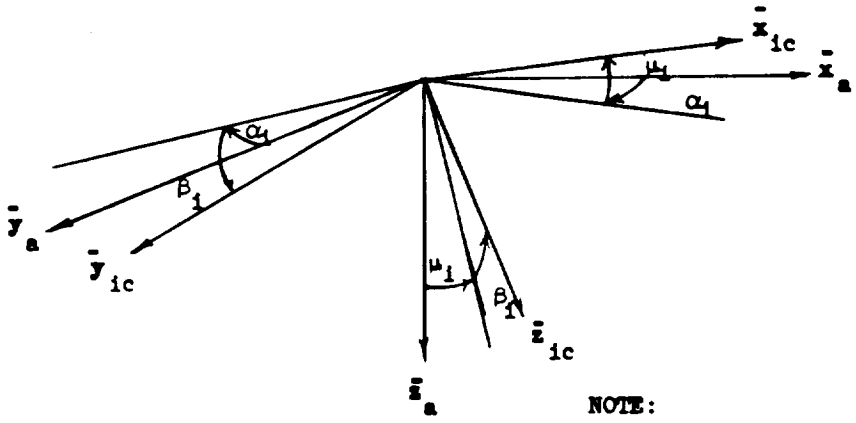

NOTE:

$\bar{x}_{ic}$ = Spin reference axis for case of gyro i

$\bar{y}_{ic}$ = Input reference axis for case of gyro i

$\bar{z}_{ic}$ = Output reference axis for case of gyro i

b. Gyro Case to Gimbal Coordinates

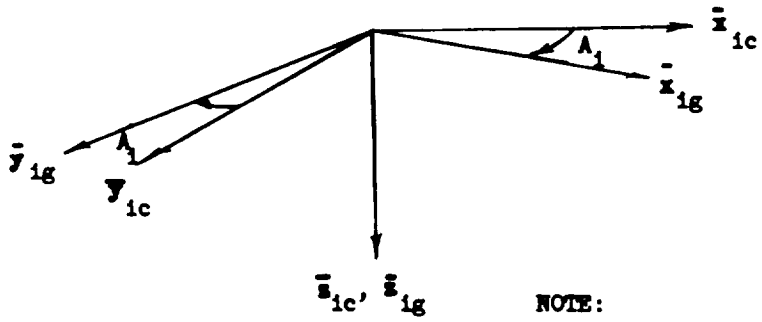

NOTE:

$\bar{x}_{ig}$ = Gimbal spin axis of gyro i

$\bar{y}_{ig}$ = Gimbal input axis of gyro i

$\bar{z}_{ig}$ = Gimbal output axis of gyro i

Figure A-2. Main Body-to-Gyro Transformation Geometry

$$\varepsilon_{i22} = -A_i\, C\mu_i\, S\alpha_i + C\beta_i\, C\alpha_i + S\beta_i\, S\mu_i\, S\alpha_i$$

$$\varepsilon_{i23} = A_i\, S\mu_i + S\beta_i\, C\mu_i$$

$$\varepsilon_{i31} = S\beta_i\, S\alpha_i + C\beta_i\, S\mu_i\, C\alpha_i$$

$$\varepsilon_{i32} = -S\beta_i\, C\alpha_i + C\beta_i\, S\mu_i\, S\alpha_i$$

$$\varepsilon_{i33} = C\beta_i\, C\mu_i$$

A.2 Dynamics

Newton's Second Law applied to the satellite provides the following equation:

$$\left(\frac{d\bar{H}}{dt}\right)_I = (\dot{\bar{H}})_I = (\Sigma\bar{M})_I \qquad (A.5)$$

where

$\bar{H}$ = total angular momentum of the satellite with the gyros and constant momemtum wheel,

$\bar{M}$ = external torques acting on the satellite,

and the derivatives are with respect to inertial space.

But the total angular momentum can be expressed as

$$(\bar{H})_I = Q_{IA} \cdot (\bar{H})_A$$

where

Q_{IA} = transformation matrix from principal body axes (A) into inertial axes (I).

Differentiating the above equation and transforming the result into principal body coordinates yeild

$$Q_{AI}\,(\dot{\bar{H}})_I = Q_{AI} \cdot Q_{IA}\left[(\dot{\bar{H}})_A + \bar{\omega}_{IA} \times (\bar{H})_A\right]$$

$$Q_{AI}(\Sigma\bar{M})_I = (\dot{\bar{H}})_A + \bar{\omega}_{IA} \times (\bar{H})_A$$

or

$$(\Sigma\bar{M})_A = (\dot{\bar{H}})_A + \bar{\omega}_{IA} \times (\bar{H})_A \tag{A.6}$$

where

$\bar{\omega}_{IA}$ = total angular velocity of the satellite with respect to inertial space.

The external torques may be divided into gravitational torque $\bar{T}_G$ and disturbance torques $\bar{T}_d$, or

$$(\Sigma\bar{M})_A = (\bar{T}_G)_A + (\bar{T}_d)_A \tag{A.7}$$

For small attitude errors, gravity gradient torques can be expressed as[5]

$$\left.\begin{aligned} T_{Gx} &= -3\,\omega_o^2\,(I_y - I_z)\,\phi \\ T_{Gy} &= -3\,\omega_o^2\,(I_x - I_z)\,\theta \\ T_{Gz} &= 0 \end{aligned}\right\} \tag{A.8}$$

The total angular momentum $(\bar{H})$ can be expressed in terms of the angular momentum of the satellite body $(\bar{H}_B)$, angular momentum of the gyros $(\bar{H}_{D1})$, and angular momentum component along the pitch axis $(\bar{H}_w)$, as follows:

$$(\bar{H})_A = (\bar{H}_B)_A + (\bar{H}_{D1})_A + (H_{D2})_A + (\bar{H}_w)_A \tag{A.9}$$

But the angular momentum of the satellite body is given by

$$(\bar{H}_B)_A = (\bar{J})_A \cdot \bar{\omega}_{IA} \tag{A.10}$$

where

$(\bar{J})_A$ = moment of inertia matrix about principal body axes.

$$= \begin{bmatrix} I_x & 0 & 0 \\ 0 & I_y & 0 \\ 0 & 0 & I_z \end{bmatrix}$$

The angular velocity $\bar{\omega}_{IA}$ is found as follows:

$$\bar{\omega}_{IA} = Q_{AO} \begin{bmatrix} 0 \\ -\omega_o \\ 0 \end{bmatrix} + \begin{bmatrix} \dot{\phi} \\ \dot{\theta} \\ \dot{\psi} \end{bmatrix}$$

or

$$\bar{\omega}_{IA} = \begin{bmatrix} \dot{\phi} - \omega_o \psi \\ \dot{\theta} - \omega_o \\ \dot{\psi} + \omega_o \phi \end{bmatrix}$$

Substituting the above terms into Equation (A.10) yields

$$(\bar{H}_B)_A = \begin{bmatrix} I_x (\dot{\phi} - \omega_o \psi) \\ I_y (\dot{\theta} - \omega_o) \\ I_z (\dot{\psi} + \omega_o \phi) \end{bmatrix} \qquad (A.11)$$

The angular momentum of gyro i (i = 1, 2) can be expressed as

$$(\bar{H}_{Di})_A = Q_{A,iG} \cdot (\bar{H}_{Di})_G \qquad (A.12)$$

where

$$(\bar{H}_{Di})_G = \begin{bmatrix} H_{Di} \\ 0 \\ 0 \end{bmatrix}$$

and

$$Q_{A,iG} = (Q_{A,iG})^{-1} = \lfloor g_{ikj} \rfloor^T$$

$$= \lfloor g_{ijk} \rfloor$$

Thus Equation (A.12) becomes

$$(\bar{H}_{Di})_A = \begin{bmatrix} g_{i11} & g_{i21} & g_{i31} \\ g_{i12} & g_{i22} & g_{i32} \\ g_{i13} & g_{i23} & g_{i33} \end{bmatrix} \begin{bmatrix} H_{Di} \\ 0 \\ 0 \end{bmatrix}$$

$$= \begin{bmatrix} g_{i11} & H_{Di} \\ g_{i12} & H_{Di} \\ g_{i13} & H_{Di} \end{bmatrix} \quad (i = 1, 2) \qquad \text{(A.13)}$$

where the g's are defined in Equation (A.4) and H_{Di} is the constant angular momentum of the spin axis of gyro i.

The pitch wheel provides a constant angular momentum H_m along the pitch axis of the satellite and can be described as

$$(\bar{H}_\omega)_A = \begin{bmatrix} 0 \\ H_m \\ 0 \end{bmatrix} \tag{A.14}$$

Combining Equations (A.11), (A.13), and (A.14) into Equation (A.9) yields

$$(\bar{H})_A = \begin{bmatrix} I_x (\dot{\phi} - \omega_o \psi) + \Sigma g_{i11} H_{Di} \\ I_y (\dot{\theta} - \omega_o) + \Sigma g_{i12} H_{Di} + H_m \\ I_z (\dot{\psi} + \omega_o \phi) + \Sigma g_{i13} H_{Di} \end{bmatrix}$$

$$= \begin{bmatrix} I_x (\dot{\phi} - \omega_o \psi) + \Sigma C\mu_i C\alpha_i H_{Di} - \Sigma A_i H_{Di} (C\beta_i S\alpha_i - S\beta_i S\mu_i C\alpha_i) \\ I_y (\dot{\theta} - \omega_o) + H_m + \Sigma C\mu_i S\alpha_i H_{Di} + \Sigma A_i H_{Di} (C\beta_i C\alpha_i + S\beta_i S\mu_i S\alpha_i) \\ I_z (\dot{\psi} + \omega_o \phi) - \Sigma S\mu_i H_{Di} + \Sigma A_i H_{Di} S\beta_i C\mu_i \end{bmatrix} \tag{A.15}$$

and

$$(\dot{\bar{H}})_A = \begin{bmatrix} I_x (\ddot{\phi} - \omega_o \dot{\psi}) - \Sigma \dot{A}_i H_{Di} (C\beta_i S\alpha_i - S\beta_i S\mu_i C\alpha_i) \\ I_y (\ddot{\theta}) + \Sigma \dot{A}_i H_{Di} (C\beta_i C\alpha_i + S\beta_i S\mu_i S\alpha_i) \\ I_z (\ddot{\psi} - \omega_o \dot{\phi}) + \Sigma \dot{A}_i H_{Di} S\beta_i C\mu_i \end{bmatrix} \tag{A.16}$$

where

$$\Sigma = \sum_{i=1}^{2}$$

The cross product $\bar{\omega}_{IA} \times (\bar{H})_A$ becomes

$$\bar{\omega}_{IA}x(\bar{H})_A = \begin{bmatrix} -\dot{\theta}\,\Sigma\, S\mu_i\, H_{Di} + \omega_o\,\dot{\psi}\left[-I_z+I_y - \frac{1}{\omega_o} H_m - \frac{1}{\omega_o}\Sigma\, C\mu_i\, S\alpha_i\, H_{Di}\right] \\ + \phi\,\omega_o^{\,2}\left[-I_z + I_y - \frac{1}{\omega_o} H_m - \frac{1}{\omega_o}\Sigma\, C\mu_i\, S\alpha_i\, H_{Di}\right] \\ - \omega_o\,\Sigma A_i\, H_{Di}\, S\beta_i\, C\mu_i + \omega_o\,\Sigma\, S\mu_i\, H_{Di} \\ \hline \dot{\phi}\,\Sigma\, S\mu_i\, H_{Di} + \dot{\psi}\,\Sigma\, C\mu_i\, C\alpha_i\, H_{Di} \\ + \phi\,\omega_o\,\Sigma\, C\mu_i\, C\alpha_i\, H_{Di} - \psi\,\omega_o\,\Sigma\, S\mu_i\, H_{Di} \\ \hline - \dot{\theta}\,\Sigma\, C\mu_i\, C\alpha_i\, H_{Di} + \omega_o\,\dot{\phi}\left[-I_y + I_x + \frac{1}{\omega_o} H_m + \frac{1}{\omega_o}\Sigma\, C\mu_i\, S\alpha_i\, H_{Di}\right] \\ + \psi\,\omega_o^{\,2}\left[I_y - I_x - \frac{H_m}{\omega_o} - \frac{1}{\omega_o}\Sigma\, C\mu_i\, S\alpha_i\, H_{Di}\right] \\ - \omega_o\,\Sigma A_i\,(C\beta_i\, S\alpha_i - S\beta_i\, S\mu_i\, C\alpha_i)\, H_{Di} + \omega_o\,\Sigma\, C\mu_i\, C\alpha_i\, H_{Di} \end{bmatrix} \tag{A.17}$$

Substituting Equations (A.7), (A.8), (A.16), and (A.17) into Equation (A.6) yields the following three component equations along the principal axis:

$\bar{x}_a$ Component

$$\begin{aligned} & I_x\,\ddot{\phi} + \phi\,\omega_o^{\,2}\left[4\,(I_y - I_z) - \frac{H_m}{\omega_o} - \frac{1}{\omega_o}\Sigma\, C\mu_i\, S\alpha_i\, H_{Di}\right] \\ & \quad + \dot{\psi}\,\omega_o\left[(I_y - I_x - I_z) - \frac{H_m}{\omega_o} - \frac{1}{\omega_o}\Sigma\, C\mu_i\, S\alpha_i\, H_{Di}\right] - \dot{\theta}\,\Sigma\, S\mu_i\, H_{Di} \\ & \quad - \Sigma\dot{A}_i\, H_{Di}\,(C\beta_i\, S\alpha_i - S\beta_i\, S\mu_i\, C\alpha_i) - \omega_o\,\Sigma A_i\, H_{Di}\, S\beta_i\, C\mu_i \\ & \quad + \omega_o\,\Sigma\, S\mu_i\, H_{Di} = T_{dx} \end{aligned} \tag{A.18}$$

$\bar{y}_a$ Component

$$I_y \ddot{\theta} + 3\omega_o^2 (I_x - I_z)\theta + \dot{\phi} \Sigma S\mu_i H_{Di} + \phi \omega_o \Sigma C\mu_i C\alpha_i H_{Di} + \dot{\psi} \Sigma C\mu_i C\alpha_i H_{Di} - \psi \omega_o \Sigma S\mu_i H_{Di} + \Sigma \dot{A} H_{Di} \left[C\beta_i C\alpha_i + S\beta_i S\mu_i S\alpha_i\right] = T_{dy} \quad \text{(A.19)}$$

$\bar{z}_a$ Component

$$I_z \ddot{\psi} + \psi \omega_o^2 \left[I_y - I_x - \frac{H_m}{\omega_o} - \frac{1}{\omega_o} \Sigma C\mu_i S\alpha_i H_{Di}\right] - \dot{\theta} \Sigma C\mu_i C\alpha_i H_{Di} + \omega_o \dot{\phi} \left[I_x + I_z - I_y + \frac{H_m}{\omega_o} + \frac{1}{\omega_o} \Sigma C\mu_i S\alpha_i H_{Di}\right] + \Sigma \dot{A}_i H_{Di} S\beta_i C\mu_i \quad \text{(A.20)}$$

$$- \omega_o \Sigma A_i H_{Di} (C\beta_i S\alpha_i - S\beta_i S\mu_i C\alpha_i) + \omega_o \Sigma C\mu_i C\alpha_i H_{Di} = T_{dz}$$

In Equation (A.18) through (A.20), the terms A_i and $\dot{A}_i$ are unknown. Thus expressions for the gyro gimbal angles must be derived to complete the description. Since each gyro obeys the conservation of angular momentum principle, the following relations can be written for the gimbal assembly of gyro i:

$$(\dot{\bar{H}}_{gim})_I = (\Sigma \bar{M}_{gim})_I = Q_{I,G} (\Sigma \bar{M}_{gim})_G \quad \text{(A.21)}$$

$$(\bar{H}_{gim})_I = Q_{I,G} \cdot (\bar{H}_{gim})_G \quad \text{(A.22)}$$

where

$\bar{H}_{gim}$ = angular momentum of the gyro gimbal assembly,

$\bar{M}_{gim}$ = external moments acting on the gyro gimbal assembly,

Q_{IG} = transformation matrix from the gimbal axes of gyro i to the geocentric inertial axes.

Differentiating Equation (A.22) yields

$$(\dot{\bar{H}}_{gim})_I = Q_{I,G}\left[(\dot{\bar{H}}_{gim})_G + \bar{\omega}_{I,G} \times (\bar{H}_{gim})_G\right] \tag{A.23}$$

Combining Equations (A.21) and (A.23) results in the following expression:

$$(\dot{\bar{H}}_{gim})_G + \bar{\omega}_{I,G} \times (\bar{H}_{gim})_G = (\Sigma\bar{M}_{gim})_G \tag{A.24}$$

But the angular velocity of the gyro gimbal assembly is concentrated about its spin axis, or

$$(\bar{H}_{gim})_G = (\bar{H}_{Di})_G = \begin{bmatrix} H_{Di} \\ 0 \\ 0 \end{bmatrix} \tag{A.25}$$

and

$$(\dot{\bar{H}}_{gim})_G = \bar{0}$$

Moreover, the external torques on the gyro can be expressed as

$$(\Sigma\bar{M}_{gim})_G = \begin{bmatrix} (\Sigma M_{gim})_x \\ (\Sigma M_{gim})_y \\ -D_i \dot{A}_i - K_i A_i + M_{gi} \end{bmatrix} \tag{A.26}$$

where

D_i = viscous damping coefficient of gyro i,

K_i = spring constant of gyro i,

M_{gi} = torque generator torque of gyro i exerted about its output axis,

and $(\Sigma M_{gim})_x$ and $(\Sigma M_{gim})_y$ are the sum of the x and y components of the torques

exerted by the satellite on the gimbal assembly of gyro i. Because of the linearizing small angle assumptions, only the torques exerted on the gimbal about the gyro output axis (z_{ig}) are required in the derivation. Equations (A.25) and (A.26) are substituted into Equation (A.24) and the resulting equation about the z_{ig} axis is given as follows:

$$\omega_{Gyi} H_{Di} = - D_i \dot{A}_i - K_i A_i + M_{gi} \tag{A.27}$$

where

ω_{Gyi} = y component of $\bar{\omega}_{I,G}$

The angular velocity of the gimbal assembly can be expressed as:

$$\bar{\omega}_{IG} = Q_{GO} \begin{bmatrix} 0 \\ -\omega_o \\ 0 \end{bmatrix} + Q_{GA} \begin{bmatrix} \dot{\phi} \\ \dot{\theta} \\ \dot{\psi} \end{bmatrix} \begin{bmatrix} 0 \\ 0 \\ \dot{A}_i \end{bmatrix} \tag{A.28}$$

But

$$Q_{GO} = Q_{G,A} \cdot Q_{A,O} \tag{A.29}$$

Substituting Equations (A.1), (A.2), and (A.28) into Equation (A.29) results in the following relation for ω_{Gyi}:

$$\omega_{Gyi} = g_{i21} (\dot{\phi} - \omega_o \psi) + g_{i22} (\dot{\theta} - \omega_o) + g_{i23} (\dot{\psi} + \omega_o \phi) \tag{A.30}$$

The desired differential equation describing the gimbal angle of gyro i can be obtained by substituting Equation (A.30) into (A.27). The results are given as follows:

$$D_i \dot{A}_i + A_i \left[K_i - \omega_o H_{Di} C\mu_i S\alpha_i\right] - H_{Di} \left[- C\beta_i S\alpha_i + S\beta_i S\mu_i C\alpha_i\right] \dot{\phi}$$

$$- \omega_o \left(H_{Di} S\beta_i C\mu_i\right) \phi - H_{Di} \left[C\beta_i C\alpha_i + S\beta_i S\mu_i S\alpha_i\right] \dot{\theta}$$

$$- H_{Di} S\beta_i C\mu_i \dot{\psi} + \omega_o H_{Di} \left[- C\beta_i S\alpha_i + S\beta_i S\mu_i C\alpha_i\right] \psi$$

$$+ \omega_o H_{Di} \left[C\beta_i C\alpha_i + S\beta_i S\mu_i S\alpha_i\right] = M_{gi} \qquad (i = 1, 2) \qquad (A.31)$$

Equations (A.18), (A.19), (A.20), and (A.31) are the linear differential equations that describe the motion of the satellite.

A.3 Reduction to Roll-Vee and Yaw-Vee Gyro Configurations

In the previous section the equations of motion were derived under the assumption that the principal axes coincides with the body reference axes of the satellite. This assumption imposes the condition that the sum of the angular momentum of the gyros must be parallel to the pitch axis. Otherwise, the sum of the angular momentum of the gyros will couple with the orbital angular velocity and cause an unbalanced torque on the satellite. In this case, the unbalanced torque will require a net non-zero gravity gradient torque at equilibrium and thus will result in an undesired attitude error.

Figure A-3 illustrates the angular momentum relationships in an arbitrary configuration of two gyros. It is noted that the angular momentum vectorsof the body ($\bar{H}_B$) and th e gyros ($\bar{H}_{Di}$) are coplanar and satisfy the following relation:

$$|H_{D1} S\eta_1| = |H_{D2} S\eta_2|$$

where

η_i = angle between $\bar{y}_a$ axis and angular momentum vector of gyro i.

In this section the study was limited to two specific gyro configurations: a "Roll-Vee" and a "Yaw-Vee" orientation of the gyro cases. In the Roll-Vee system the yaw-pitch plane contains the angular momentum vectors $\bar{H}_B$, $\bar{H}_{D1}$, $\bar{H}_{D2}$

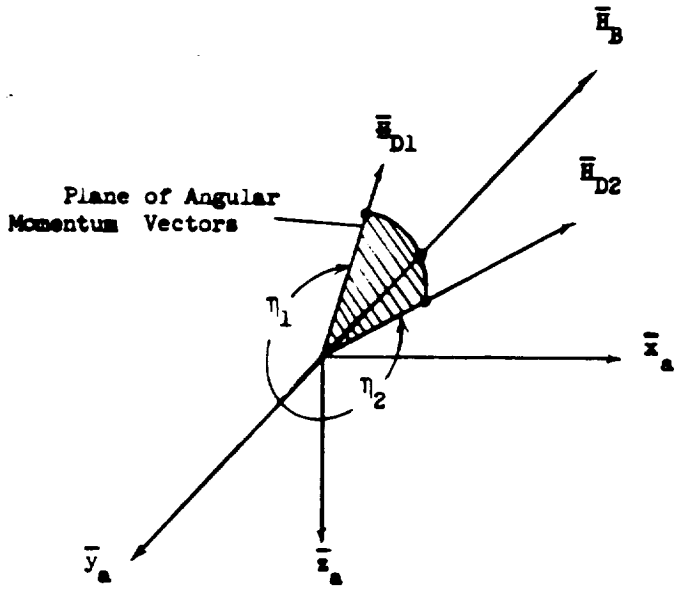

Figure A-3. Arbitrary Configuration of a Two Gyro System

(see Figure A-4). In the Yaw-Vee system, the plane of the angular momentum vectors is in the roll-pitch plane (see Figure A-5). These two configurations may not be optimum; however, their characteristics will provide a starting basis for comparisons with other gyro configurations.

Before reducing the set of equations of motion for the Roll-Vee and Yaw-Vee systems, the following limitations are made to simplify the task:

$$\left.\begin{aligned} H_{D1} &= H_{D2} = H \\ \frac{H_{D1}}{D_1} &= \frac{H_{D2}}{D_2} = \frac{H}{D} \\ K_1 &= K_2 = K \end{aligned}\right\} \qquad (A.32)$$

It is noted from Figure A-3 that the equal angular momentum of the gyros requires that the magnitude of the case angle η_1 be equal, or

$$|\eta_1| = |\eta_2|$$

The above relations are desirable not only from hardware considerations but also from an optimization point of view.

From Figures A-4 and A-5 the following angular relations can be obtained for the two gyro configurations:

Roll-Vee:

$$\left.\begin{aligned} \alpha_1 &= \alpha_2 = 90 \\ \beta_1 &= \beta_2 = 90^\circ \\ \eta_1 &= -\eta_2 = \mu_1 = -\mu_2 = \mu \geq 0 \end{aligned}\right\} \qquad (A.33)$$

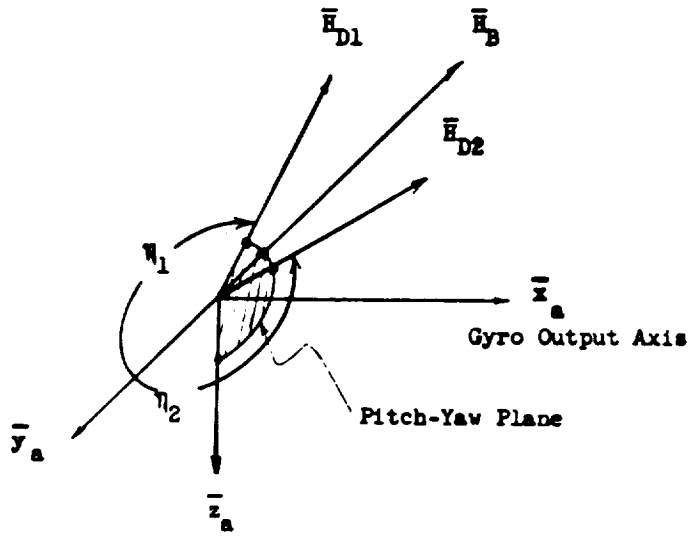

Figure A-4. Roll-Vee Gyro Configuration

$$(|\bar{H}_{D1}| = |\bar{H}_{D2}| \ , \ |\eta_1| = |\eta_2|)$$

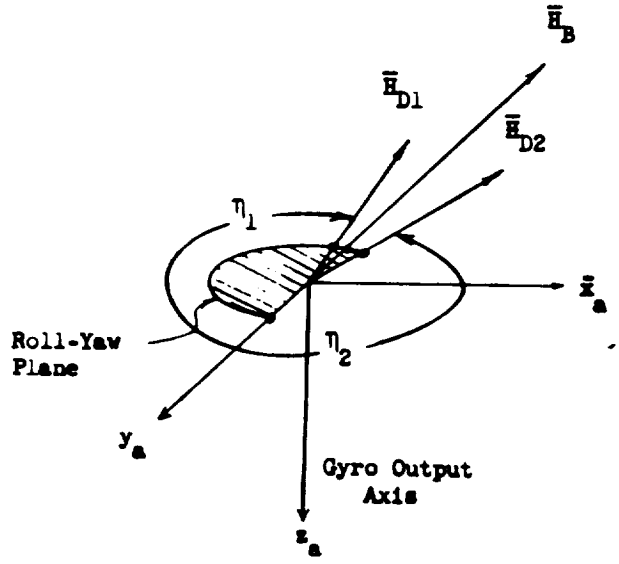

Figure A-5. Yaw-Vee Gyro Configuration

$$(|\bar{H}_{D1}| = |H_{D2}| \ , \ |\eta_1| = |\eta_2|)$$

Yaw-Vee:

$$\left.\begin{aligned} \beta_1 &= \beta_2 = 0 \\ \mu_1 &= \mu_2 = 0 \\ \eta_2 &= -\eta_1 = \alpha \geq 0 \\ \alpha_1 &= 90 + \alpha \\ \alpha_2 &= 90 - \alpha \end{aligned}\right\} \qquad (A.34)$$

The equations of motion of the Roll-Vee and Yaw-Vee systems are obtained by substituting the relations of Equations (A.32), (A.33), and (A.34) into Equations (A.18), (A.19), (A.20), and (A.31). The results are presented as follows:

Roll-Vee:

$$I_x \ddot{\phi} + \omega_o^2 \left[4 (I_y - I_z) - \frac{H_m}{\omega_o} - \frac{2HC\mu}{\omega_o}\right] \phi$$

$$+ \omega_o \left[I_y - I_x - I_z - \frac{H_m}{\omega_o} - \frac{2HC\mu}{\omega_o}\right] \dot{\psi} - \omega_o HC\mu (A_1 + A_2) = T_{dx} \qquad (A.35)$$

$$I_y \ddot{\theta} + 3\omega_o^2 (I_x - I_z) \theta + HS\mu (\dot{A}_2 - \dot{A}_1) = T_{dy} \qquad (A.36)$$

$$I_z \ddot{\psi} + \omega_o^2 \left[I_y - I_x - \frac{H_m}{\omega_o} - \frac{2HC\mu}{\omega_o}\right] \psi$$

$$- \omega_o \left[I_y - I_x - I_z - \frac{H_m}{\omega_o} - \frac{2HC\mu}{\omega_o}\right] \dot{\phi} + HC\mu (\dot{A}_1 + \dot{A}_2) = T_{dz} \qquad (A.37)$$

$$D (\dot{A}_2 - \dot{A}_1) + \left[K - \omega_o HC\mu\right] (A_2 - A_1) = -2HS\mu\dot{\theta} + 2\omega_o HS\mu - M_{g1} + M_{g2} \qquad (A.38)$$

$$D\,(\dot{A}_1 + \dot{A}_2) + \left[K - \omega_o\, HC\mu\right](A_1 + A_2) = 2\omega_o\, HC\mu\phi + 2HC\mu\dot{\psi} + M_{g1} + M_{g2} \quad (A.39)$$

Yaw-Vee:

$$I_x \ddot{\phi} + \omega_o^2 \left[4\,(I_y - I_z) - \frac{H_m}{\omega_o} - \frac{2HC\alpha}{\omega_o}\right]\phi$$

$$+ \omega_o \left[I_y - I_x - I_z - \frac{H_m}{\omega_o} - \frac{2HC\alpha}{\omega_o}\right]\dot{\psi} - HC\alpha\,(\dot{A}_1 + \dot{A}_2) = T_{dx} \quad (A.40)$$

$$I_y \ddot{\theta} + 3\omega_o^2\,(I_x - I_z)\,\theta - HS\alpha\,(\dot{A}_1 - \dot{A}_2) = T_{dy} \quad (A.41)$$

$$I_z \ddot{\psi} + \omega_o^2 \left[I_y - I_x - \frac{H_m}{\omega_o} - \frac{2HC\alpha}{\omega_o}\right]\psi$$

$$- \omega_o \left[I_y - I_x - I_z - \frac{H_m}{\omega_o} - \frac{2HC\alpha}{\omega_o}\right]\dot{\phi} - \omega_o\, HC\alpha\,(A_1 + A_2) = T_{dz} \quad (A.42)$$

$$D\,(\dot{A}_1 - \dot{A}_2) + \left[K - \omega_o\, HC\alpha\right](A_1 - A_2) = -2\,HS\alpha\dot{\theta} + 2\omega_o\, HS\alpha + M_{g1} - M_{g2} \quad (A.43)$$

$$D\,(\dot{A}_1 + A_2) + \left[K - \omega_o\, HC\alpha\right](A_1 + A_2) = -2\,HC\alpha\dot{\phi} + 2\omega_o\, HC\alpha\psi + M_{g1} + M_{g2} \quad (A.44$$

In either configuration, the above set of equations represent a third order system describing motion about the body pitch axis and a fifth order system describing motion about the body roll-yaw axes.

It is evident that the pitch motion depends on the out of phase, or "scissoring", motion of the gyro gimbals, given by the difference angle $(A_1 - A_2)$. On the other hand, the roll-yaw motion depends only on the in-phase gimbal motion, given by the sum angle $(A_1 + A_2)$. The similarity in the equations between the

two configurations merely reflects the fact that a 90° rotation of the Roll-Vee gyro axes about the pitch axis results in a Yaw-Vee system.

At this point it is proper to cite the problem of maintaining the gyro's spin axis at the angle η_1 relative to the pitch axis. During a given orbit, each gyro experiences body torques which can cause its spin vector to precess toward the spin axis of the satellite. Without some compensation, the gyro's spin vector cannot be maintained at the nominal skew angle η_1 which is necessary for three axis damping.

One means of maintaining the nominal skew angle is to provide a constant torque from the torque generator of each gyro. In this case, the torque generator provides a torque whose magnitude is given by $\omega_o H_{D1} S \eta_1$, or

$$M_{g1} = \omega_o H_{D1} S \eta_1$$

$$M_{g2} = \omega_o H_{D2} S \eta_2$$

Substituting the about relations into Equations (A.38), (A.39), (A.43), and (A.44) indicates that the torque generator removes the constant forcing terms in the gimbal equations. As a result, the gimbals of each gyro are nulled at the skewed case axes (x_{ic}, y_{ic}, z_{ic}).

Another means of maintaining the nominal skew angle is to employ relatively stiff springs between the gyro's case and gimbal. In this case a torque generator output is not required, or

$$M_{g1} = M_{g2} = 0$$

Substituting the above relations into Equations (A.38), (A.39), (A.43), and (A.44) indicates that a constant forcing term remains in the gimbal equations. Consequently, the small angle gyro motion is perturbed about the following non-zero angle:

Roll-Vee:

$$A_2 - A_1 = \frac{-2\,\omega_o\,HS\mu}{K - \omega_o\,HC\mu}$$

Yaw-Vee:

$$A_1 - A_2 = \frac{-2\,\omega_o\,HS\alpha}{K - \omega_o\,HC\alpha}$$

In this case a relatively large value of spring constant is required to limit the above angular excursion to small angles. However, a stiff spring restraint restricts the relative motion between the gimbal and satellite body. As a result, the gyro control system will be highly underdamped, a condition which is undesirable in terms of the system's transient response. Thus, a control system with a torque generator is assumed in this study to permit a range of gyro spring constants which provide acceptable damping characteristics.

A.4 Reduction to Roll and Yaw Gyro Configurations

The system under study consists of a satellite with a pitch momentum wheel and a single control moment gyro. The gyro configuration is restricted to class in which the spin axis is nominally along the negative pitch axis, and the gyro output axis is along the roll or yaw axis. In this configuration the single control moment gyro will damp motion only about the roll and yaw axes. It is assumed that motion along the pitch axis is damped by another device. Since roll-yaw motion is uncoupled from pitch motion under small angle behavior, the system's small angle performance in the roll-yaw axes and in the pitch axis can be investigated independently.

The single control moment gyro systems under study are the so-called "Roll" and "Yaw" gyro systems. As shown in Figures A-6 and A-7, the Roll and Yaw systems are analogous to Roll-Vee and Yaw-Vee systems, respectively, in regards to the orientation of the gyro's output axis. In fact, it will be shown that a two gyro Roll-Vee and Yaw-Vee system can be made equivalent to the Roll and Yaw system by setting the gyro skew angle to zero ($\mu = \alpha = 180^o$) and by removing one of the two gyros.

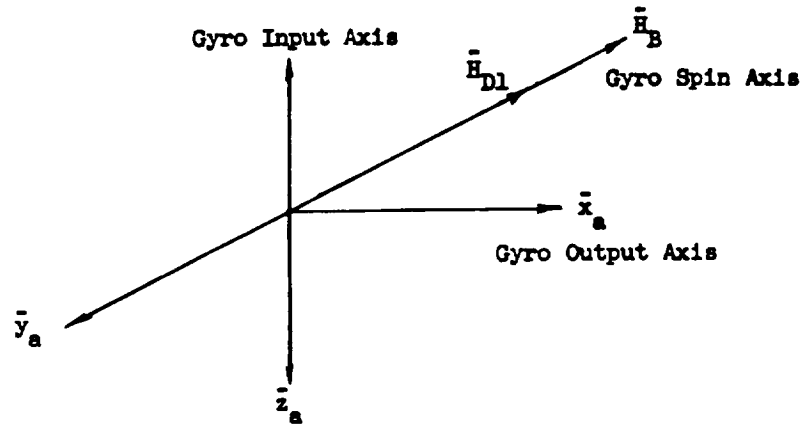

Figure A-6. Gyro Orientation of the Roll System

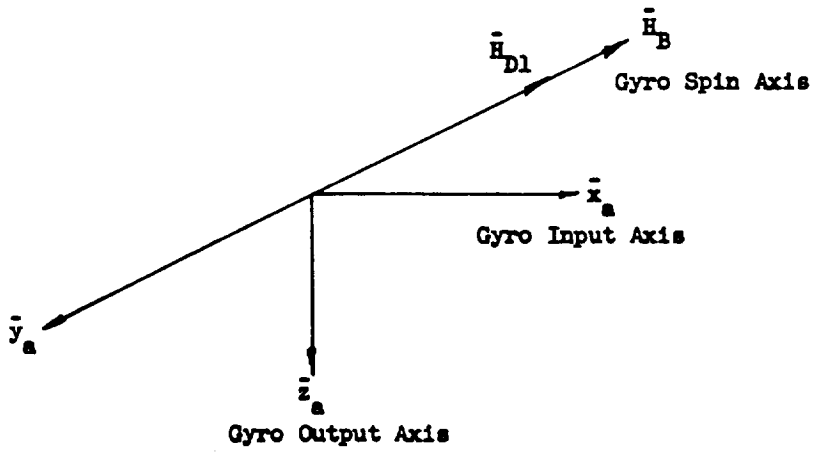

Figure A-7. Gyro Orientation of the Yaw System

In terms of the nomenclature used in the previous section, the following relationship are written for the Roll and Yaw gyro systems:

Roll System:	Yaw System:
$\alpha_1 = \beta_1 = -90^\circ$	$\alpha_1 = -90$
$\mu_1 = 0$	$\mu_1 = \beta_1 = 0$
$H_{D1} = H_o$	$H_{D1} = H_o$
$D_1 = D_o$	$D_1 = D_o$
$K_1 = K_o$	$K_1 = K_o$
$H_{D2} = 0$	$H_{D2} = 0$

Substituting the above relations into the generalized equations of motion for the two gyro system yields the following equations which describes the motion about the roll and yaw axes for the single gyro system:

Roll System:

$$T_{dx} = I_x \ddot{\phi} + \omega_o^2 \left[4 (I_y - I_z) - \frac{H_m}{\omega_o} + \frac{H_o}{\omega_o}\right] \phi$$

$$+ \omega_o \left[I_y - I_x - I_z - \frac{H_m}{\omega_o} + \frac{H_o}{\omega_o}\right] \dot{\psi} + \omega_o H_o A_1 \qquad (A.45)$$

$$T_{dz} = I_z \ddot{\psi} + \omega_o^2 \left[I_y - I_x - \frac{H_m}{\omega_o} + \frac{H_o}{\omega_o}\right] \psi$$

$$- \omega_o \left[I_y - I_x - I_z - \frac{H_m}{\omega_o} + \frac{H_o}{\omega_o}\right] \dot{\phi} - H_o \dot{A}_1 \qquad (A.46)$$

$$D_o \dot{A}_1 + \left[K_o + \omega_o H_o\right] A_1 + \omega_o H_o \phi + H_o \dot{\psi} = 0 \qquad (A.47)$$

Yaw System:

$$T_{dx} = I_x \ddot{\phi} + \omega_o^2 \left[4 (I_y - I_z) + \frac{H_o}{\omega_o} - \frac{H_m}{\omega_o}\right] \phi$$

$$+ \omega_o \left[I_y - I_x - I_z + \frac{H_o}{\omega_o} - \frac{H_m}{\omega_o}\right] \dot{\psi} + H_o \dot{A}_1 \qquad \text{(A.48)}$$

$$T_{dz} = I_z \ddot{\psi} + \omega_o^2 \left[I_y - I_x + \frac{H_o}{H_m} - \frac{H_m}{\omega_o}\right] \psi$$

$$- \omega_o \left[I_y - I_x - I_z + \frac{H_o}{\omega_o} - \frac{H_m}{\omega_o}\right] \dot{\phi} + \omega_o H_o A_1 \qquad \text{(A.49)}$$

$$D_o \dot{A}_1 + \left[K_o + \omega_o H_o\right] A_1 - H_o \dot{\phi} + \omega_o H_o \psi = 0 \qquad \text{(A.50)}$$

To obtain the above equation in terms of a Laplace transform matrix, the following definitions are made:

$$b = \frac{I_x}{I_y}$$

$$c = \frac{I_z}{I_y}$$

$$h_o = \frac{H_o}{\omega_o I_y}$$

$$\lambda_o = \frac{K_o}{\omega_o D_o} + \frac{H_o}{D_o}$$

$$\gamma_o = \frac{H_o}{D_o}$$

$$m = \frac{H_m}{\omega_o I_y}$$

$$p = \frac{1}{\omega_o} \frac{d}{dt}$$

Substituting the above relations into Equations (A.44) to (A.50) yields the following normalized equations:

Roll System:

$$\begin{bmatrix} b\,p^2 + 4(1-c) + h_o - m & (1-b-c+h_o-m)\,p & h_o \\ -(1-b-c+h_o-m)\,p & cp^2+1-b+h_o-m & -h_o p \\ \gamma_o & \gamma_o\,p & p+\lambda_o \end{bmatrix} \begin{bmatrix} \phi \\ \psi \\ A_1 \end{bmatrix} = \begin{bmatrix} \frac{T_{dx}}{\omega_o^2 I_y} \\ \frac{T_{dz}}{\omega_o^2 I_y} \\ 0 \end{bmatrix}$$

Yaw System:

$$\begin{bmatrix} bp^2+4\,(1-c)+h_o-m & (1-b-c+h_o-m)\,p & h_o p \\ -(1-b-c+h_o-m)\,p & cp^2+1-b+h_o-m & h_o \\ -\gamma_o\,p & \gamma_o & p+\lambda_o \end{bmatrix} \begin{bmatrix} \phi \\ \psi \\ A_1 \end{bmatrix} = \begin{bmatrix} \frac{T_{dx}}{\omega_o^2 I_y} \\ \frac{T_{dz}}{\omega_o^2 I_y} \\ 0 \end{bmatrix}$$

The form of the above equations for the single gyro Roll and Yaw systems is exactly the same as that for the two gyro Roll-Vee and Yaw-Vee systems, respectively. In fact, the two gyro system can be made equivalent to the single gyro system when the following relations are observed:

$$h = -\frac{1}{2} h_o$$

$$\gamma = -\gamma_o$$

$$\lambda = \lambda_o$$

$$\mu = \alpha = 180^o$$

With the above relations in mind, all of the roll-yaw stability conditions and gain expressions derived for the two gyro system can be utilized for the single gyro system. Consequently, the behavior of the Roll and Yaw gyro systems can be described as special cases of Roll-Vee and Yaw-Vee systems.

APPENDIX B

List of On-Line Computer Figures

Figure	Title
B-1	Error/Torque Gain Vs. Normalized Frequency (Roll-Vee System: Parameter = Normalized Spring Constant)
B-2	Error/Torque Gain Vs. Normalized Frequency (Yaw-Vee System: Parameter = Normalized Spring Constant)
B-3	Error/Torque Gain Vs. Normalized Frequency (Roll-Vee System: Parameter = Normalized Roll Inertia)
B-4	Error/Torque Gain Vs. Normalized Frequency (Yaw-Vee System: Parameter = Normalized Roll Inertia)
B-5	Error/Torque G in Vs. Normalized Frequency (Roll-Vee System: Parameter = Normalized Yaw Inertia)
B-6	Error/Torque Gain Vs. Normalized Frequency (Yaw-Vee System: Parameter = Normalized Yaw Inertia)
B-7	Error/Torque Gain Vs. Normalized Frequency (Roll-Vee System: Parameter = Case Angle)
B-8	Error/Torque Gain Vs. Normalized Frequency (Yaw-Vee System: Parameter = Case Angle)
B-9	Error/Torque G in Vs. Normalized Frequency (Roll-Vee System: Parameter = Gyro Gain)
B-10	Error/Torque Gain Vs. Normalized Frequency (Yaw-Vee System: Parameter = Gyro Gain)
B-11	Error/Torque Gain Vs. Normalized Frequency (Roll-Vee System: Parameter = Normalized Gyro Momentum)

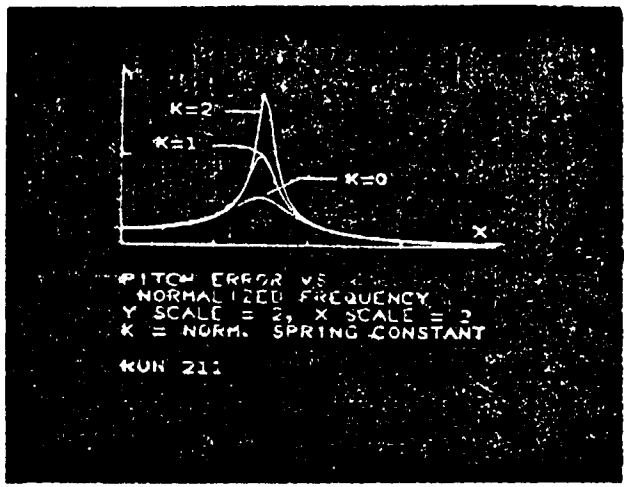

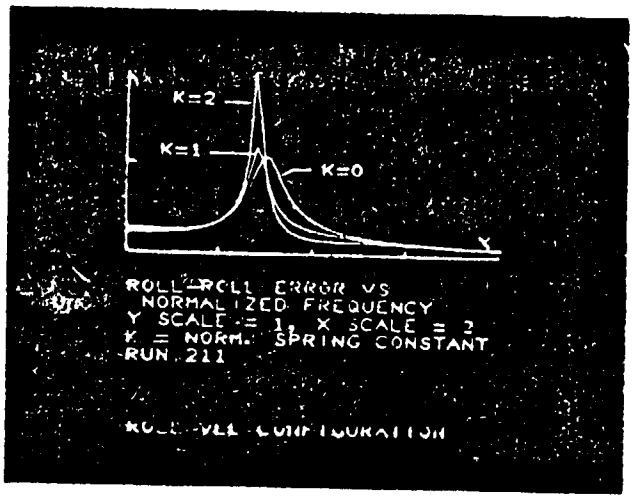

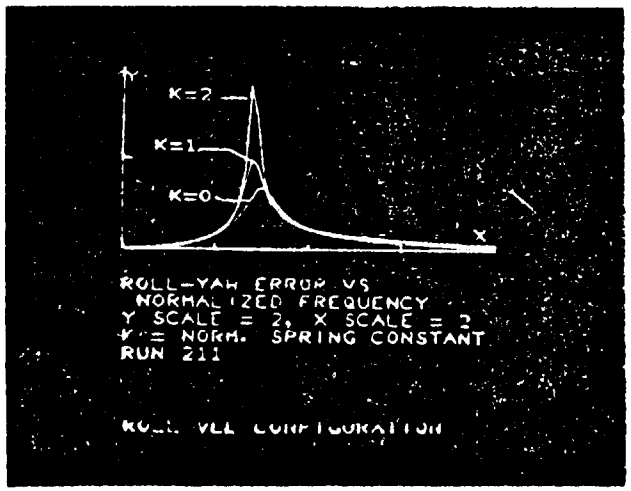

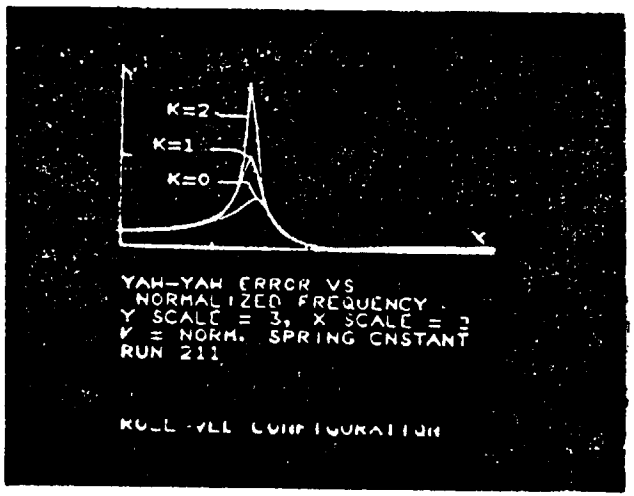

Figure B-1 $\frac{I_x}{I_y} = 1$; $\frac{I_z}{I_y} = .05$; $\frac{H_m}{\omega_o I_y} = 0$; $\frac{K}{\omega_o D} = 0,1,2$; $\frac{H}{\omega_o I_y} = 1$; $\frac{H}{D} = 1$; $\mu = \alpha = 220^o$

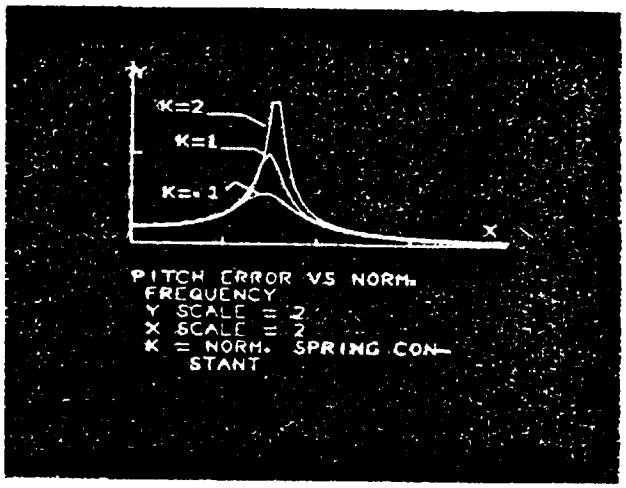

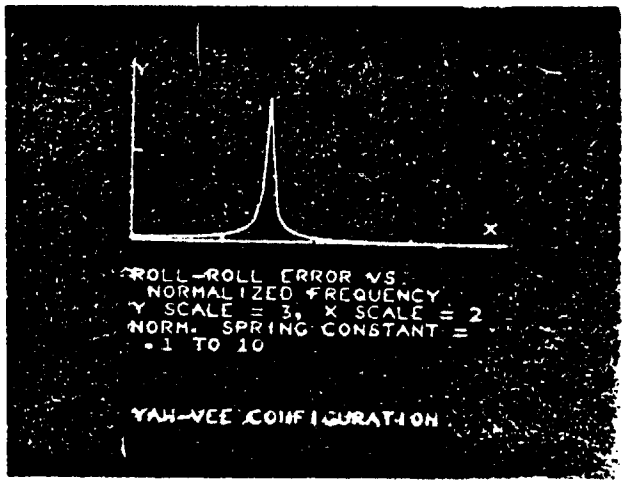

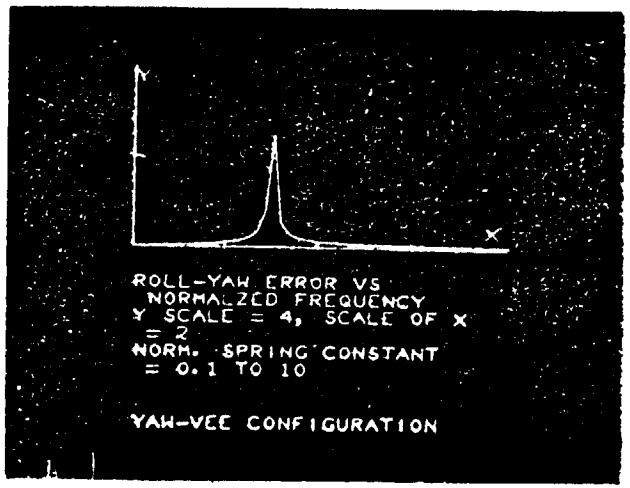

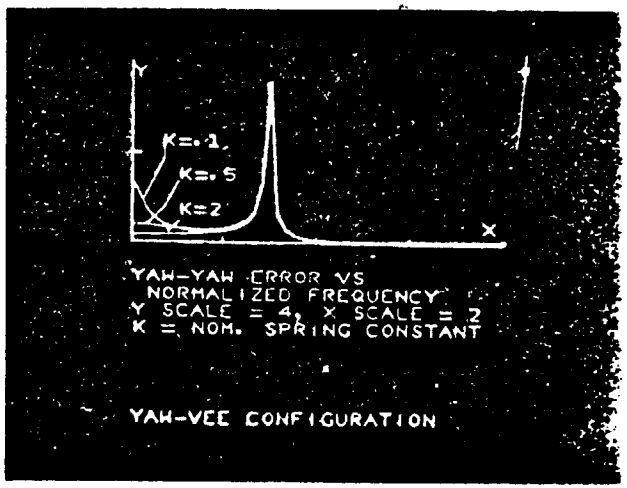

Figure B-2 $\frac{I_x}{I_y} = 1$; $\frac{I_z}{I_y} = .05$; $\frac{\bar{h}_m}{\omega_o I_y} = 0$; $\frac{K}{\omega_o D} = .1,1,10$; $\frac{\bar{h}}{\omega_o I_y} = 1$; $\frac{H}{D} = 1$; $\mu = \alpha = 220^\circ$

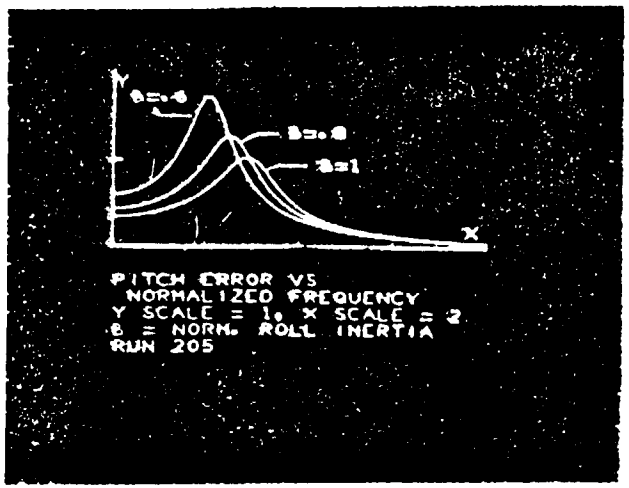

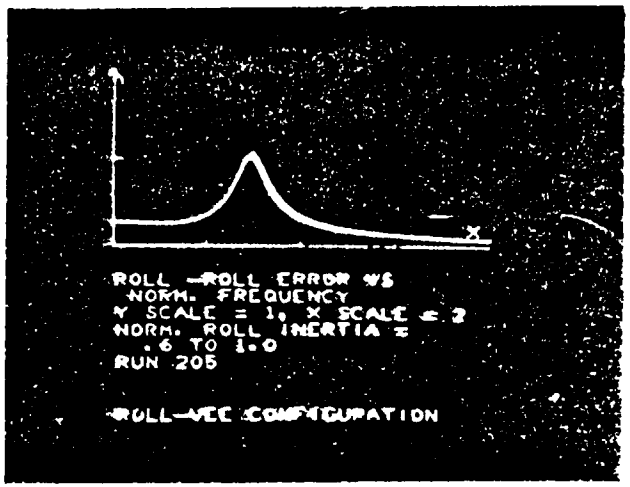

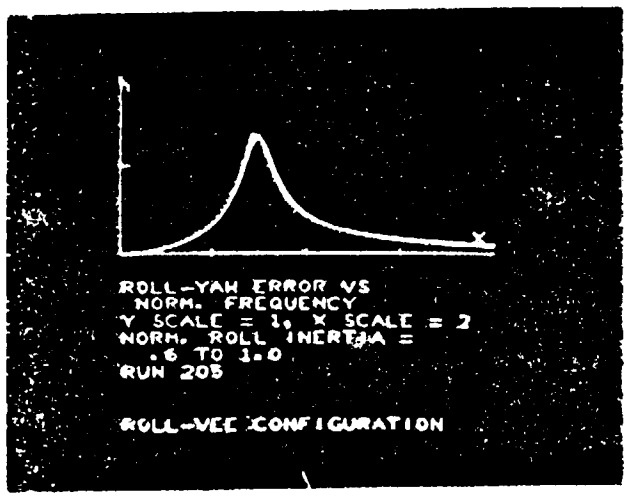

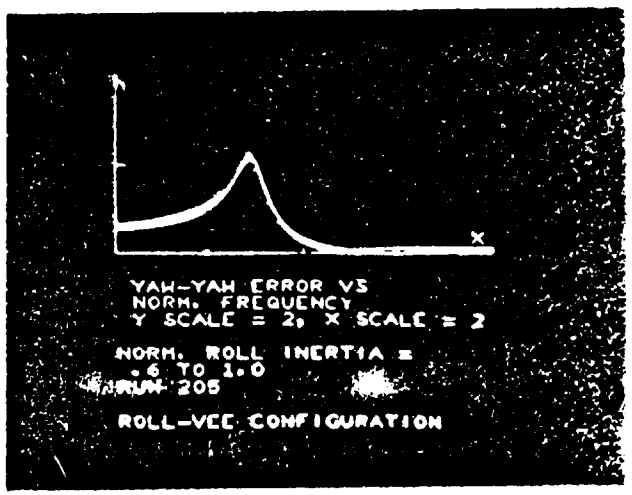

Figure B-3 $\frac{I_x}{I_y} = .6,.8,1$; $\frac{I_z}{I_y} = .05$; $\frac{H_m}{\omega_o I_y} = 0$; $\frac{K}{\omega_o D} = 0$; $\frac{H}{\omega_o I_y} = 1$; $\frac{H}{D} = 1$; $\mu = \gamma = 220^o$

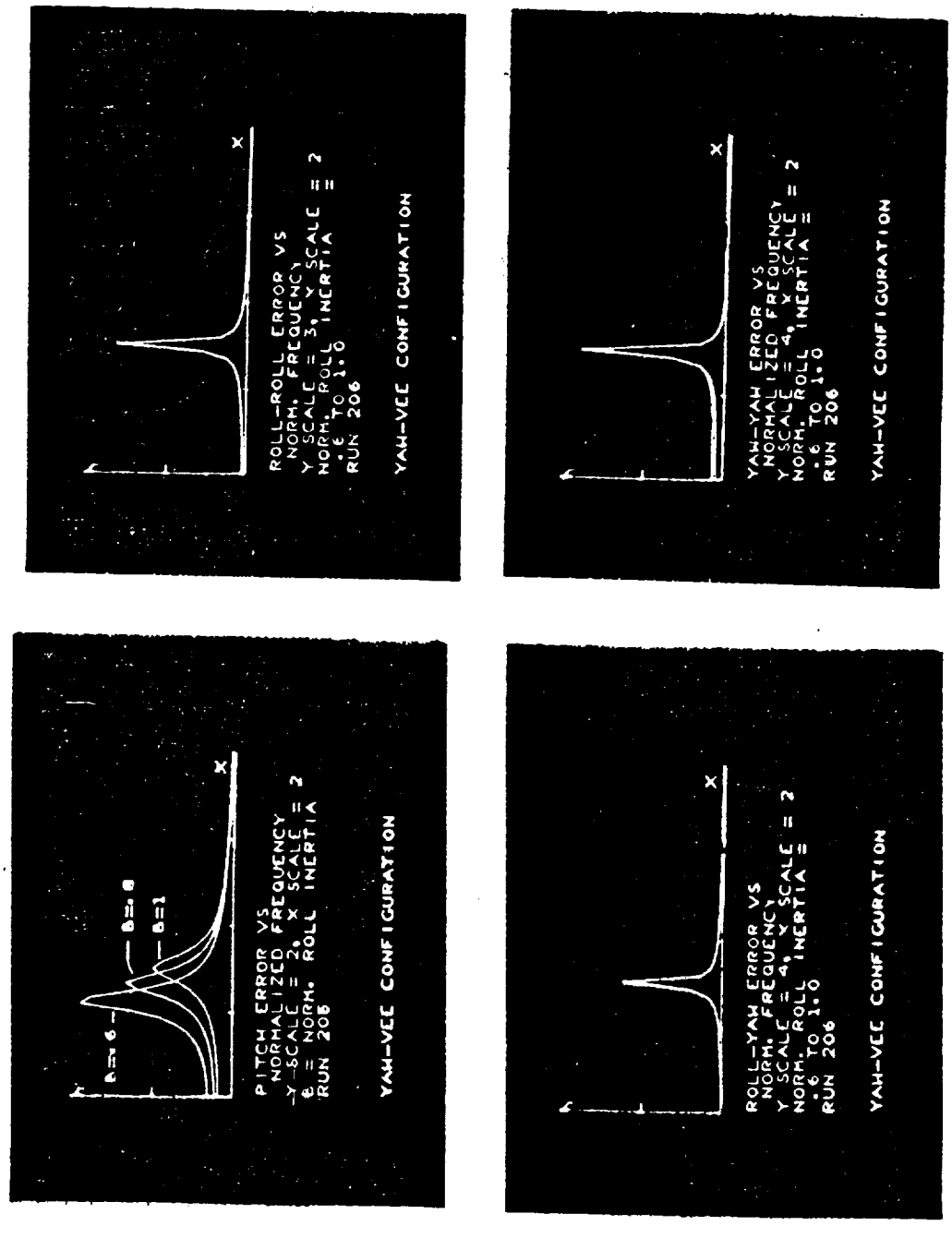

Figure B-4 $\frac{I_x}{I_y} = .6,.8,1;\ \frac{I_z}{I_y} = .05;\ \frac{H_m}{\omega_o I_y} = 0;\ \frac{K}{\omega_o D} = 1;\ \frac{H}{\omega_o I_y} = 1;\ \frac{H}{D} = 1;\ \mu = \alpha = 220^\circ$

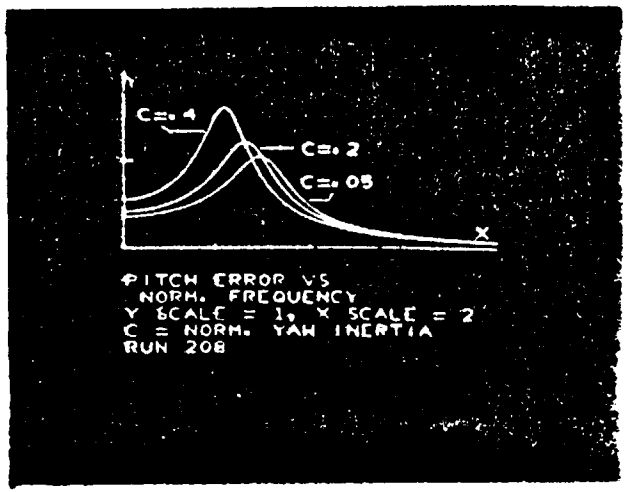

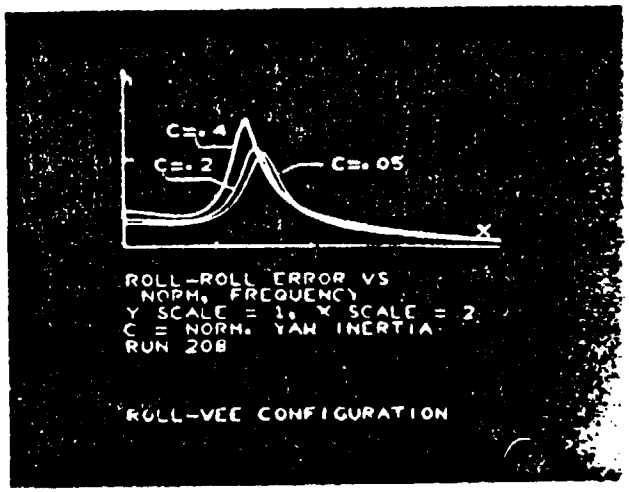

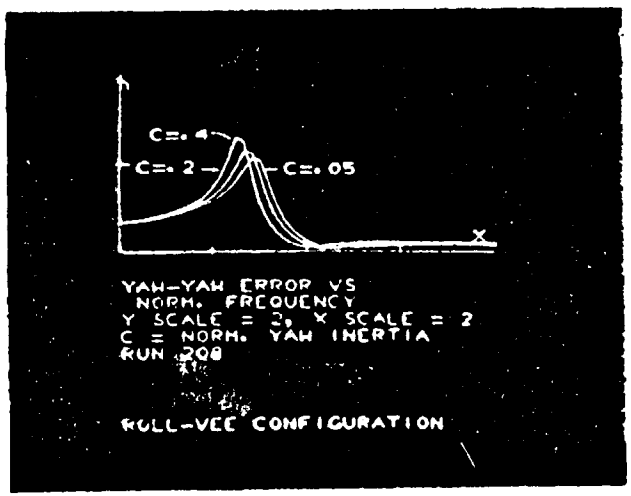

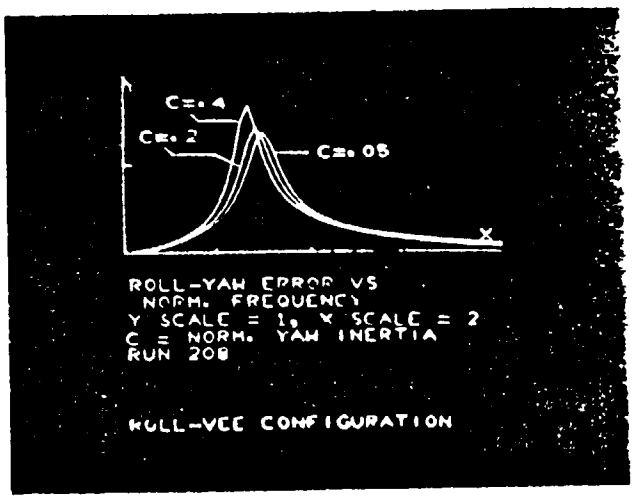

Figure B-5 $\frac{I_x}{I_y} = 1$; $\frac{I_z}{I_y} = .05, .2, .4$; $\frac{H_m}{\omega_o I_y} = 0$; $\frac{\dot{x}}{\omega_o D} = 0$; $\frac{H}{\omega_o I_y} = 1$; $\frac{H}{D} = 1$; $\mu = \alpha = 220^\circ$

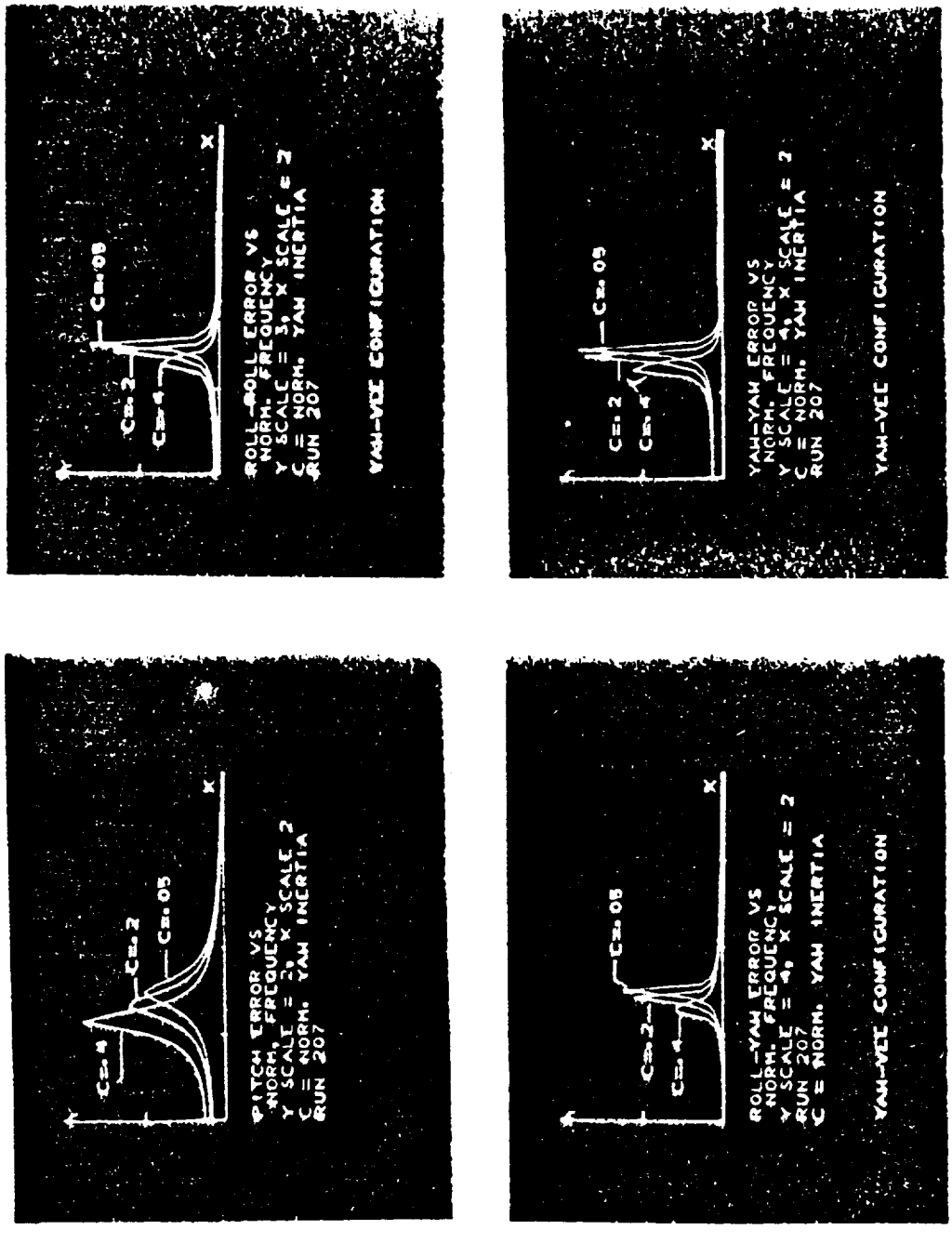

Figure B-6 $\frac{I_x}{I_y} = 1$; $\frac{I_z}{I_y} = .05, .2, .4$; $\frac{h_s}{\omega_o I_y} = 0$; $\frac{\dot{\gamma}}{\omega_o D} = 1$; $\frac{h}{\omega_o I_y} = 1$; $\frac{h}{D} = 1$; $\mu = 1$

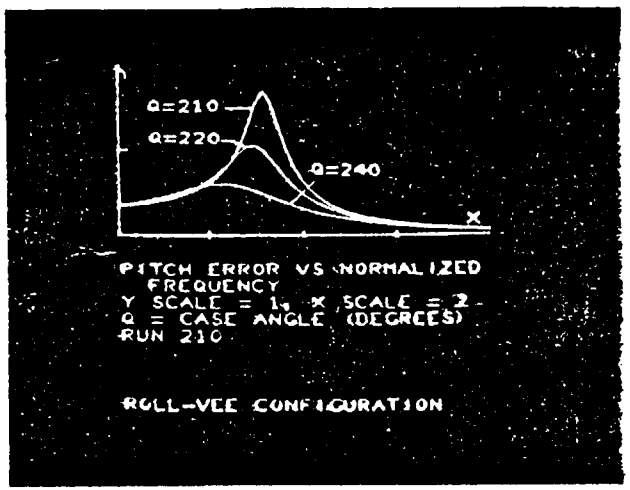

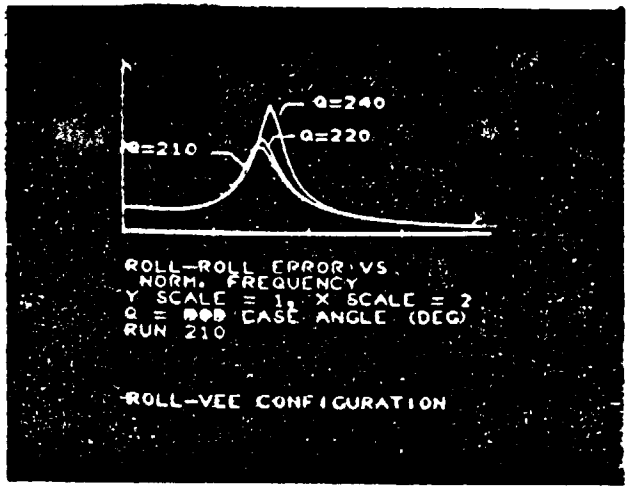

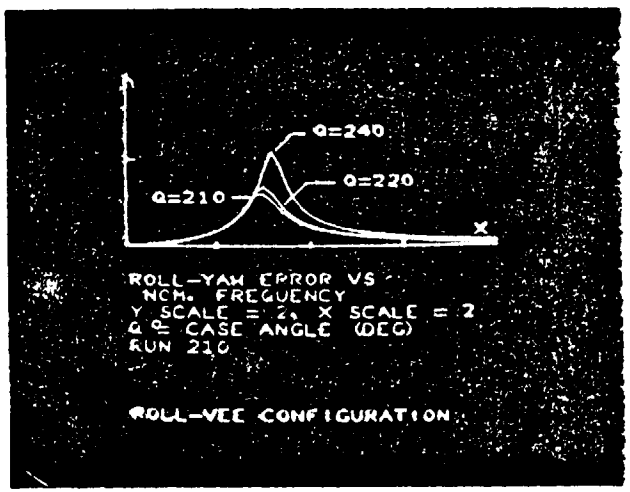

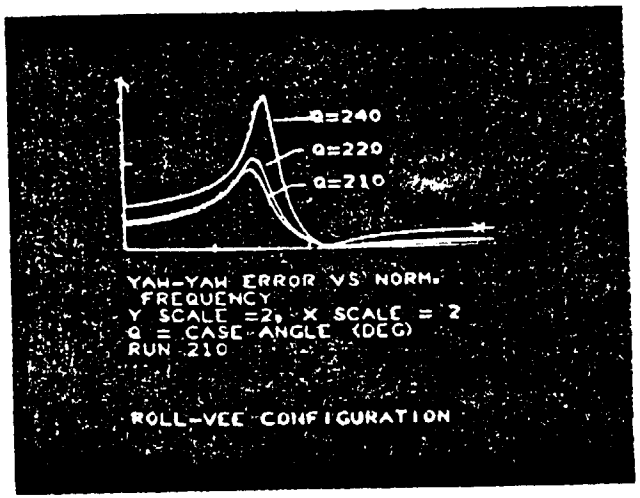

Figure B-7 $\frac{I_x}{I_y} = 1$; $\frac{I_z}{I_y} = .05$; $\frac{H_m}{\omega_o I_y} = 0$; $\frac{K}{\omega_o D} = 0$; $\frac{H}{\omega_o I_y} = 1$; $\frac{H}{D} = 1$; $\mu = \alpha = 210^o, 220^o, 240^o$

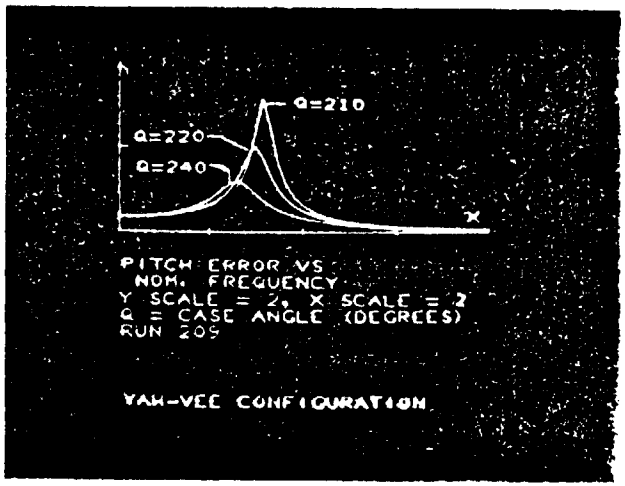
Q=210
Q=220
Q=240
X
PITCH ERROR VS
NOM. FREQUENCY
Y SCALE = 2, X SCALE = 2
Q = CASE ANGLE (DEGREES)
RUN 209
YAW-VEE CONFIGURATION

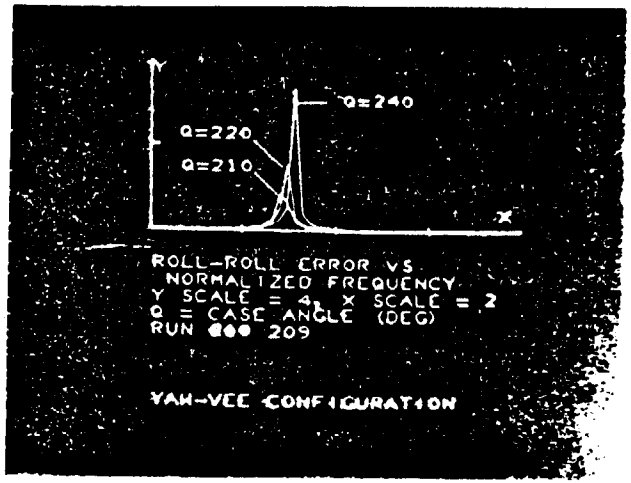
Q=240
Q=220
Q=210
X
ROLL-ROLL ERROR VS
NORMALIZED FREQUENCY
Y SCALE = 4, X SCALE = 2
Q = CASE ANGLE (DEG)
RUN 209
YAW-VEE CONFIGURATION

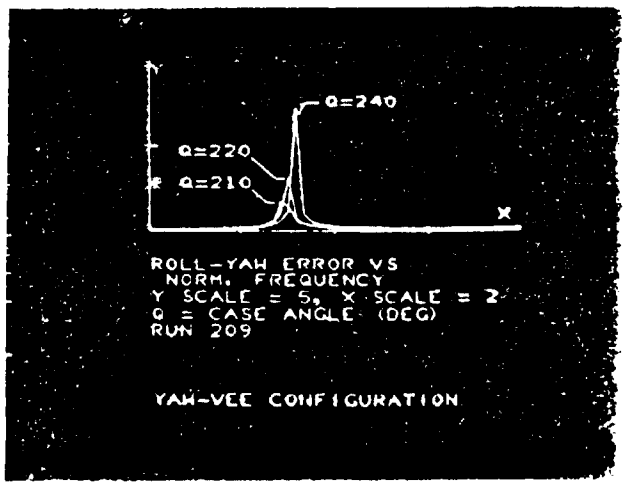
Q=240
Q=220
Q=210
X
ROLL-YAW ERROR VS
NORM. FREQUENCY
Y SCALE = 5, X SCALE = 2
Q = CASE ANGLE (DEG)
RUN 209
YAW-VEE CONFIGURATION

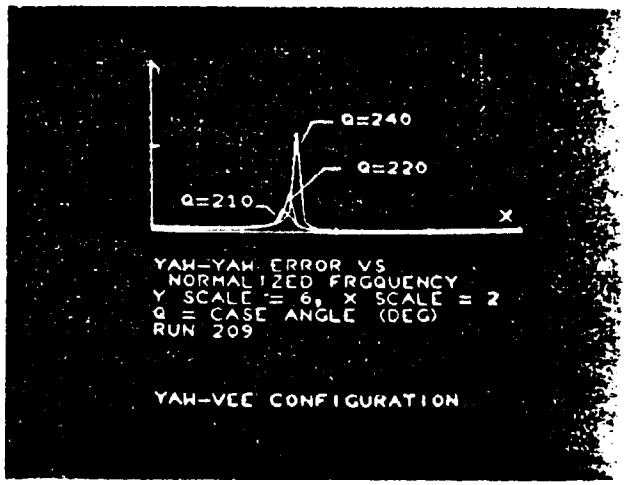
Q=240
Q=220
Q=210
X
YAW-YAW ERROR VS
NORMALIZED FRQUENCY
Y SCALE = 6, X SCALE = 2
Q = CASE ANGLE (DEG)
RUN 209
YAW-VEE CONFIGURATION

Figure B-1 [illegible]

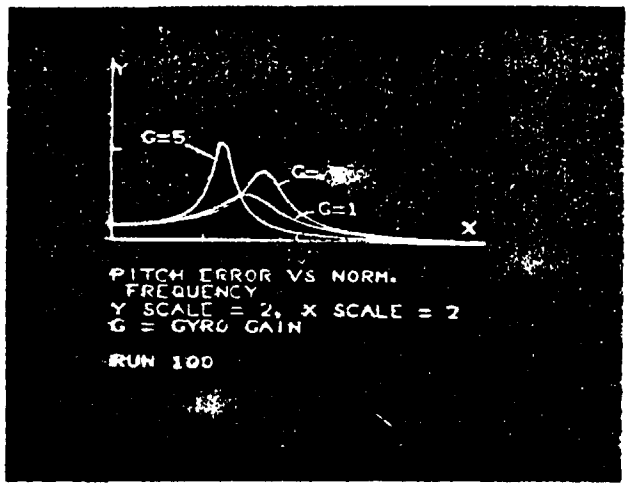

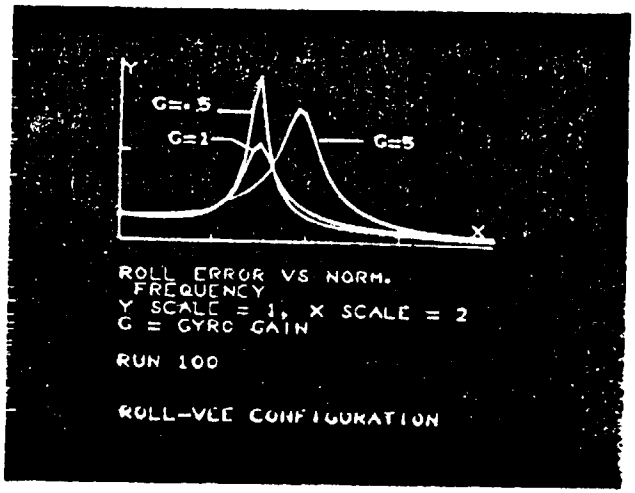

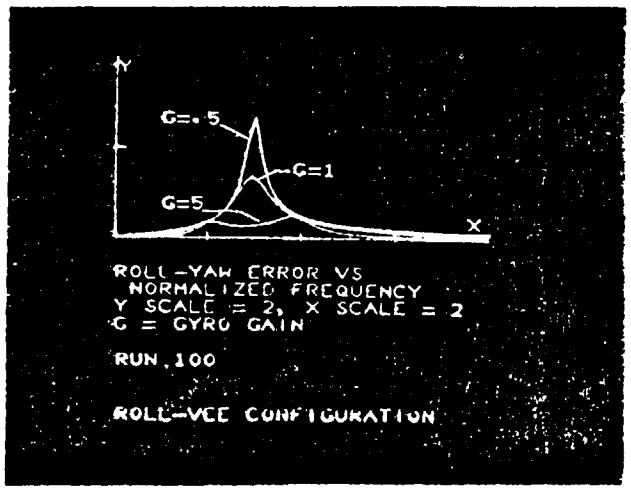

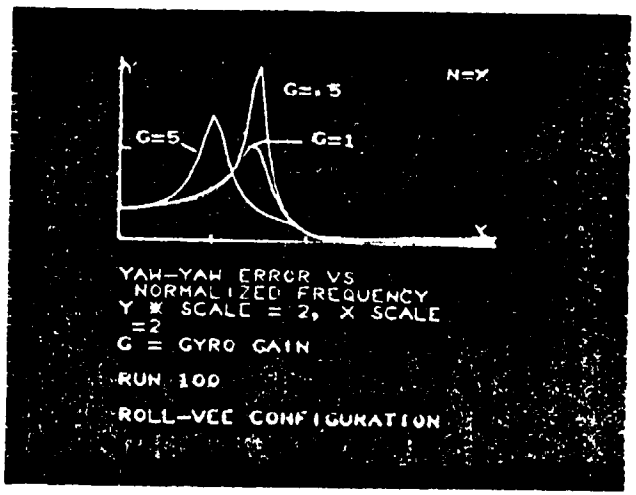

Figure B-9 $\frac{I_x}{I_y} = 1$; $\frac{I_z}{I_y} = .05$; $\frac{H_m}{\omega_o I_y} = 0$; $\frac{K}{\omega_o D} = 0$; $\frac{H}{\omega_o I_y} = 1$; $\frac{H}{D} = .5,2,5$; $\mu = \gamma = 220^\circ$

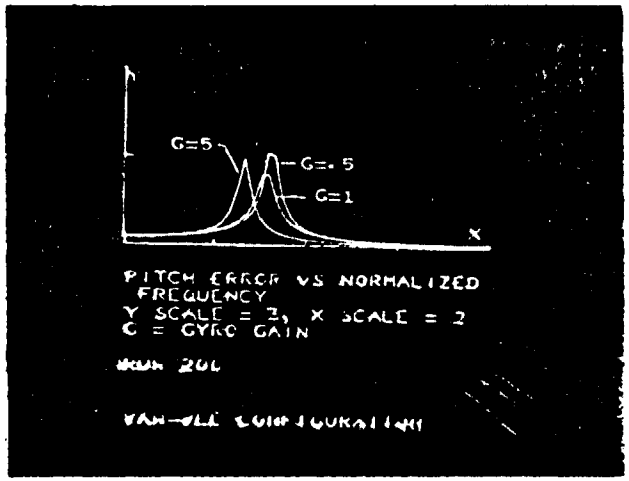

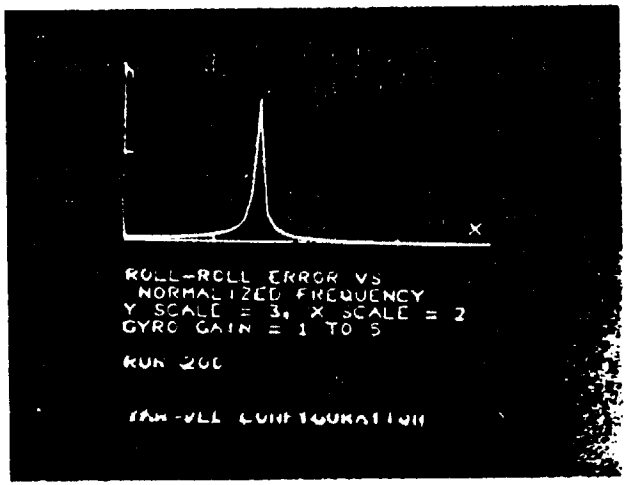

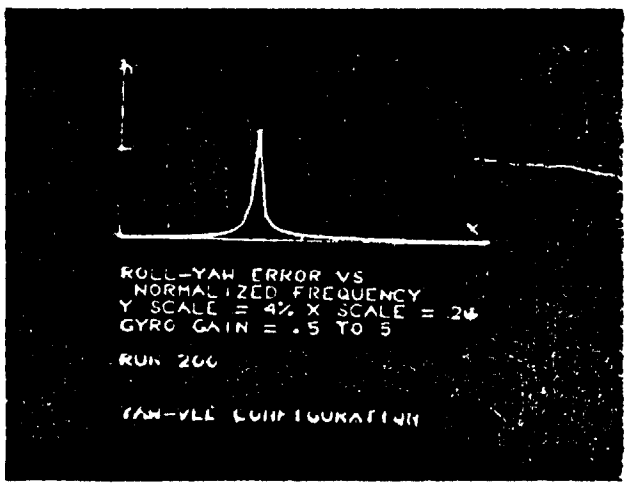

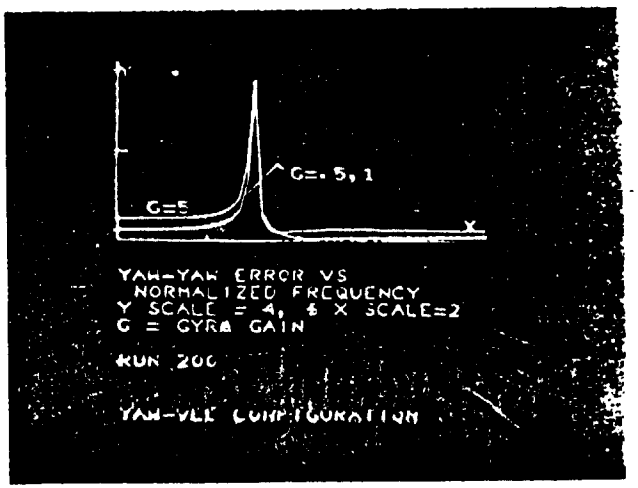

Figure B-10 $\frac{I_x}{I_v} = 1$; $\frac{I_z}{I_y} = .05$; $\frac{H_m}{\omega_o I_y} = 0$; $\frac{K}{\omega_o D} = 2$; $\frac{H}{\omega_o I_y} = 1$; $\frac{H}{D} = .5,1,5$; $\mu = \alpha = 220^o$

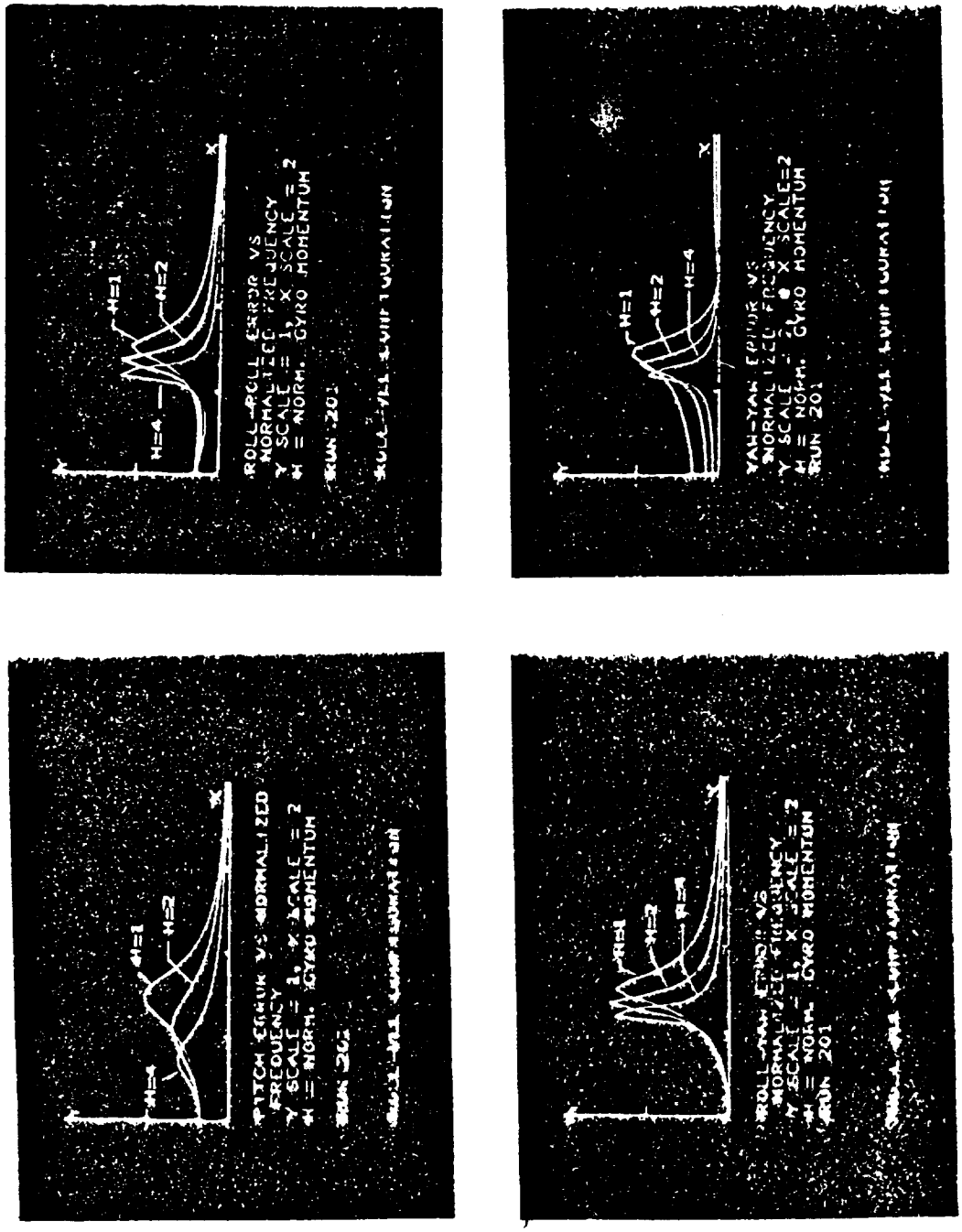

Figure B-11 $\frac{I_x}{I_y} = 1$; $\frac{\dot{H}}{I_y} = .05$; $\frac{H}{\omega_o I_y} = 0$; $\frac{\dot{h}}{\omega_o D} = 0$; $\frac{H}{\omega_o I_y} = 1,2,4$; $\frac{H}{D} = 1$; $\mu = \alpha = 220^0$

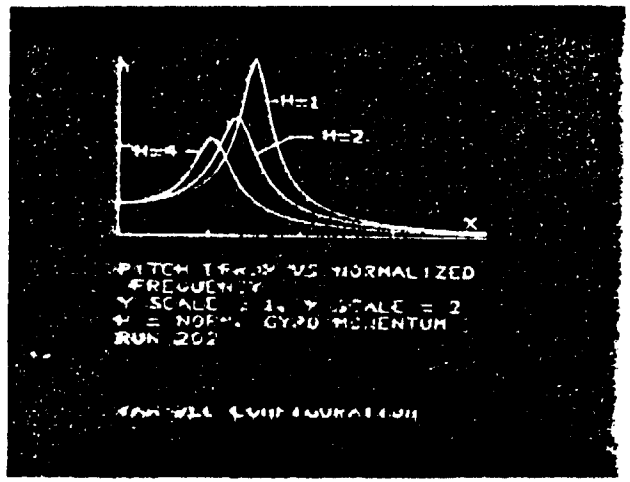

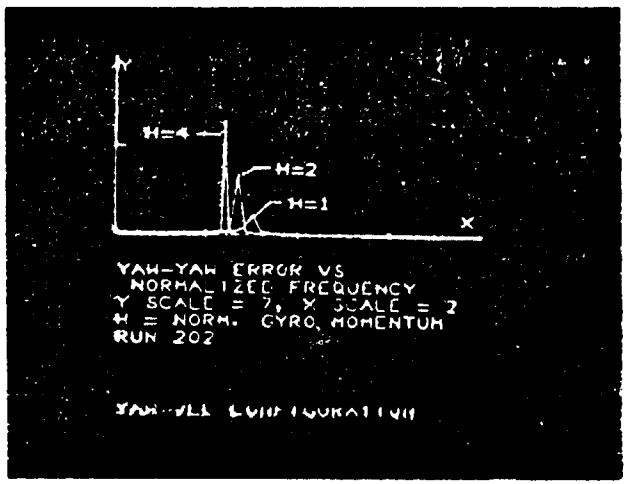

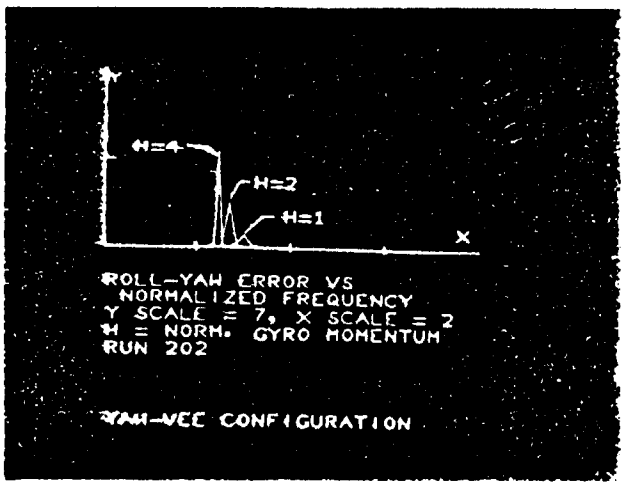

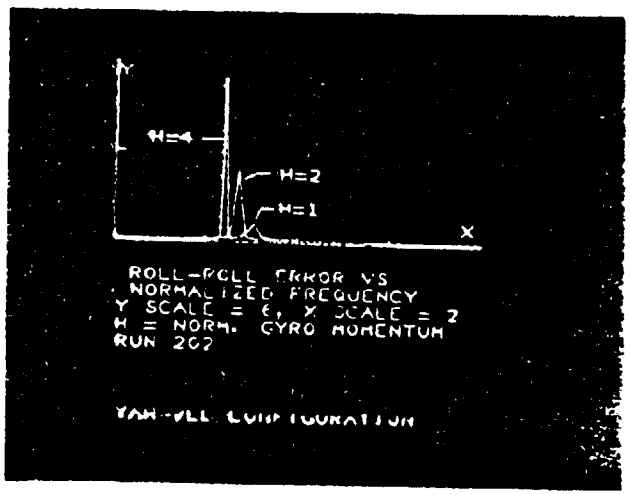

Figure B-12 $\frac{I_x}{I_y} = 1$; $\frac{I_z}{I_y} = .05$; $\frac{H_m}{\omega_o I_y} = 0$; $\frac{K}{\omega_o D} = 1$; $\frac{n}{\omega_o I_y} = 1,2,4$; $\frac{H}{I} = 1$; $\mu = \gamma = 220^o$

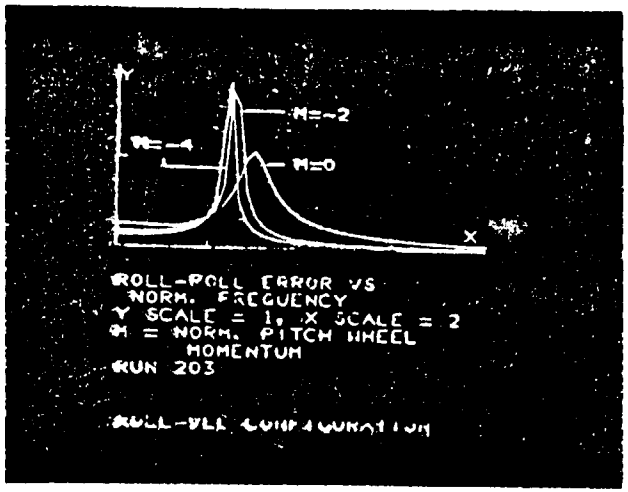

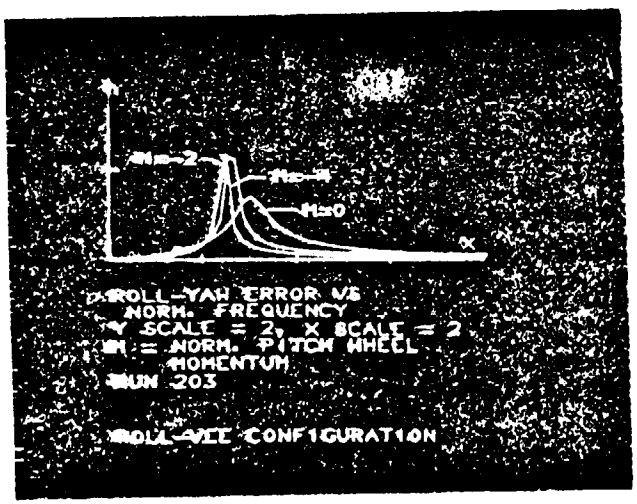

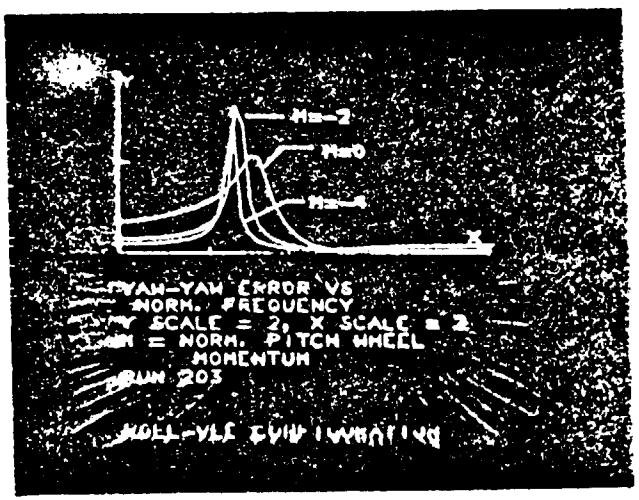

...ure B-13 $\frac{I_x}{I_y} = 1$; $\frac{I_z}{I_y} = .05$; $\frac{H_m}{\omega_o I_y} = 0,-2,-4$; $\frac{K}{\omega_o D} = 0$; $\frac{H}{\omega_o I_y} = 1$; $\frac{H}{D} = 1$; $\mu = 0 = 90^0$

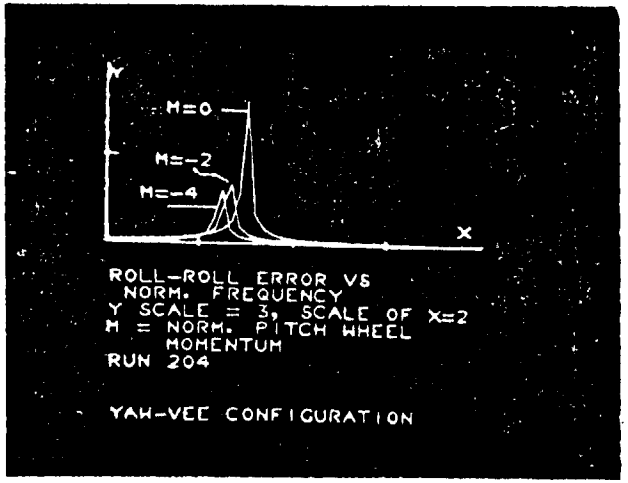

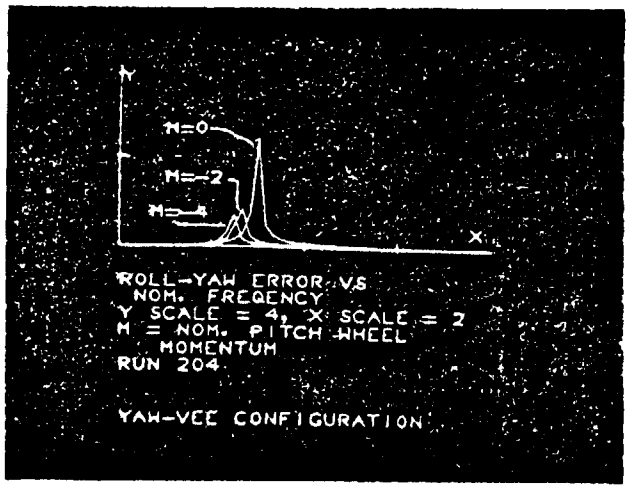

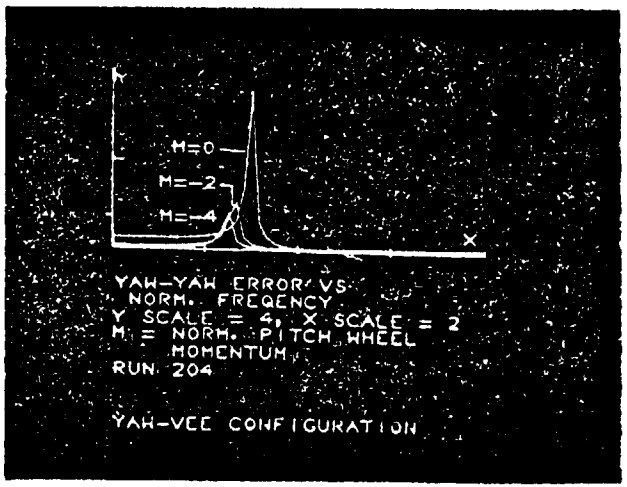

Figure B-14 $\frac{I_x}{I_y} = 1$; $\frac{I_z}{I_y} = .05$; $\frac{H_m}{\omega_o I_y} = 0,-2,-4$; $\frac{K}{\omega_o D} = 1$; $\frac{H}{\omega_o I_y} = 1$; $\frac{H}{D} = 1$; $\mu = \alpha = 220^\circ$

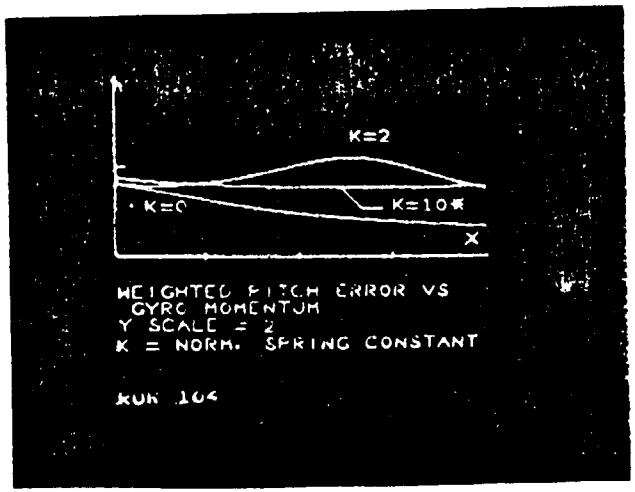

$\frac{I_x}{I_y} = 1.0$; $\frac{I_z}{I_y} = .05$; $\frac{H_m}{\omega_o I_y} = 0$; $\frac{K}{\omega_o D} = 0,2,10$; $\frac{H}{\omega_o I_y} = 1$ to 9 ; $\frac{H}{D} = 1.0$; $\mu = \alpha = 220^o$

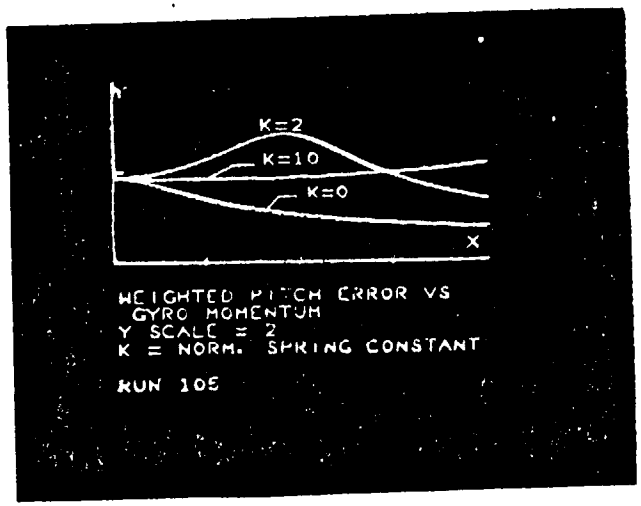

Figure B-15 $\frac{I_x}{I_y} = 1.0$; $\frac{I_z}{I_y} = .2$; $\frac{H_m}{\omega_o I_y} = 0$; $\frac{K}{\omega_o D} = 0,2,10$; $\frac{H}{\omega_o I_y} = 1$ to 9 ; $\frac{H}{D} = 1.0$; $\mu = \alpha = 220^o$

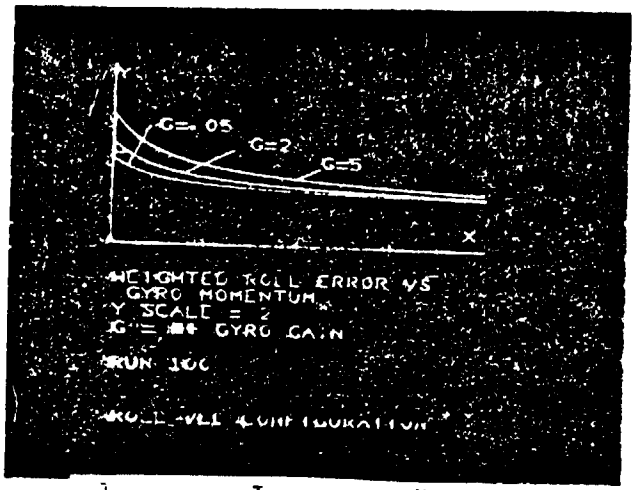

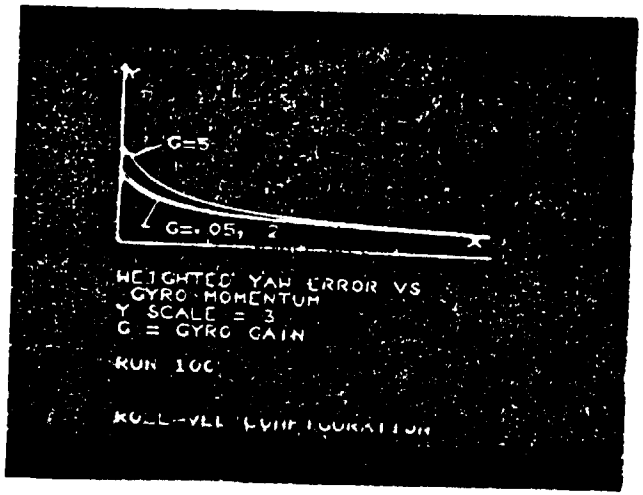

$\frac{I_x}{I_y} = 1.0$; $\frac{I_z}{I_y} = .05$; $\frac{H_m}{\omega_o I_y} = 0$; $\frac{K}{\omega_o D} = 0$; $\frac{H}{\omega_o I_y} = 1$ to 9 ; $\frac{H}{D} = .05,2.5$; $\mu = \alpha = 220°$

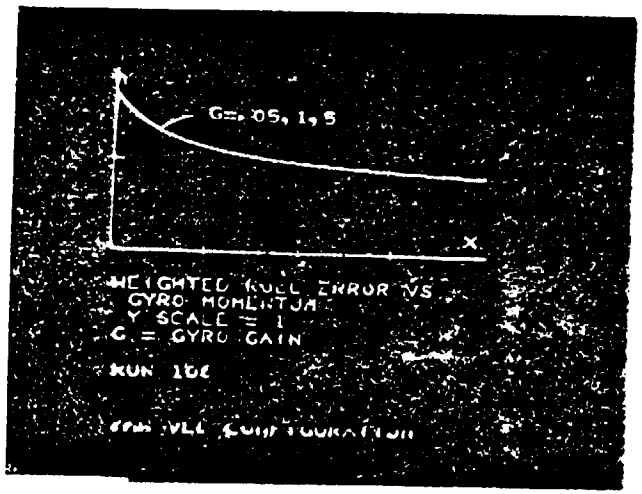

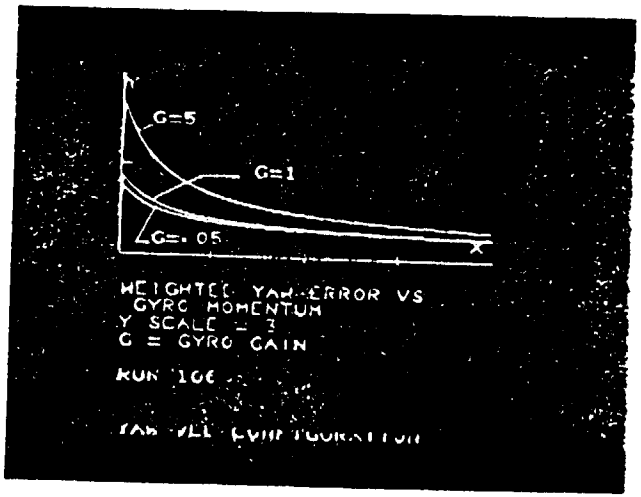

Figure B-16 $\frac{I_x}{I_y} = 1.0$; $\frac{I_z}{I_y} = .05$; $\frac{H_m}{\omega_o I_y} = 0$; $\frac{K}{\omega_o D} = 2$; $\frac{H}{\omega_o I_y} = 1$ to 9 ; $\frac{H}{D} = .05,1,5$; $\mu = \alpha = 220°$

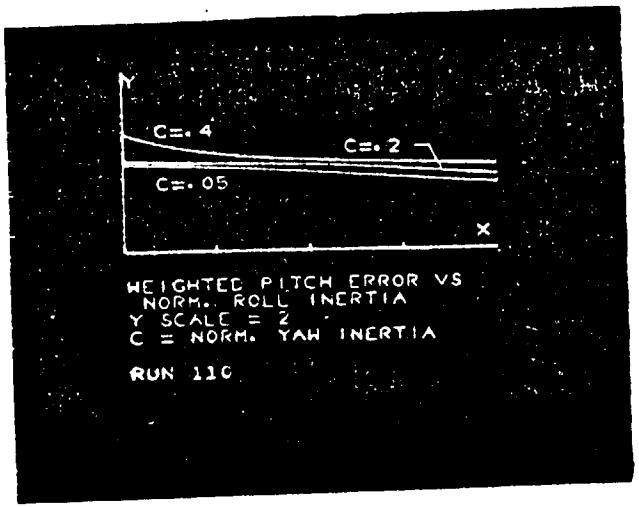

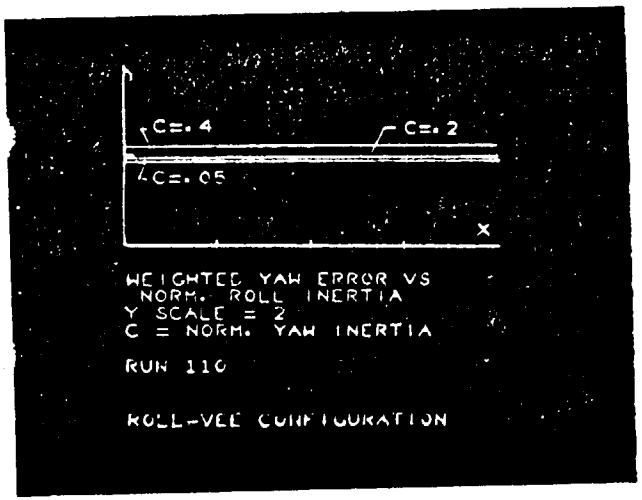

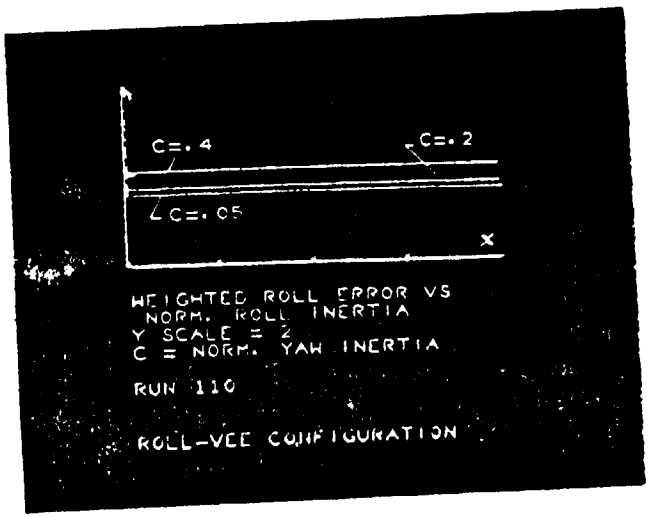

Figure B-17 $\frac{I_x}{I_y}$ = .6 to 1.0; $\frac{I_z}{I_y}$ = .05, .2, .4 $\frac{H_m}{\omega_o I_y} = 0$ $\frac{K}{\omega_o D} = 0$ $\frac{H}{\omega_o I_y} = 2$ $\frac{H}{D} = 1$ $\mu = \alpha = 220°$

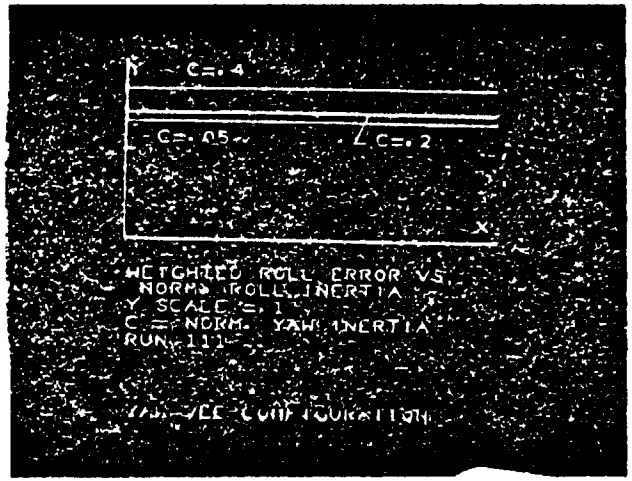

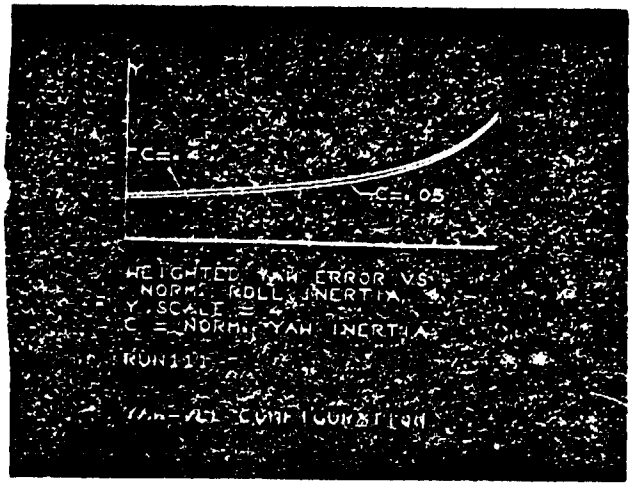

Figure B-18 $\frac{I_x}{I_y}$ = .5 to .9 $\frac{I_z}{I_y}$ = .05, .2, .4 $\frac{H_m}{\omega_o I_y}$ = 0 $\frac{K}{\omega_o D}$ = 0 $\frac{H}{\omega_o I_y}$ = 2 $\frac{H}{D}$ = 1 $\mu = \alpha = 220^\circ$

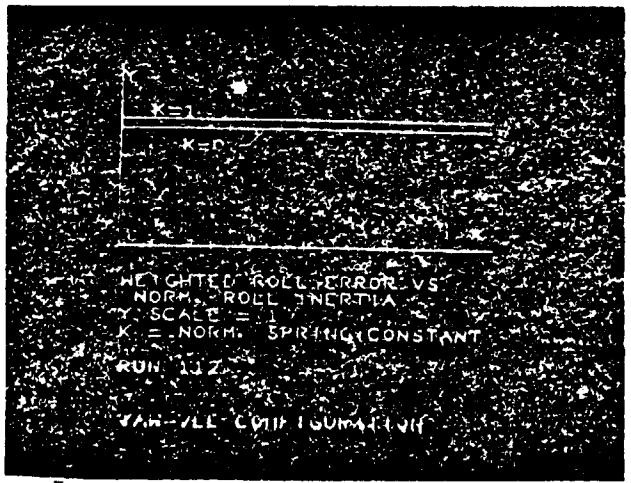

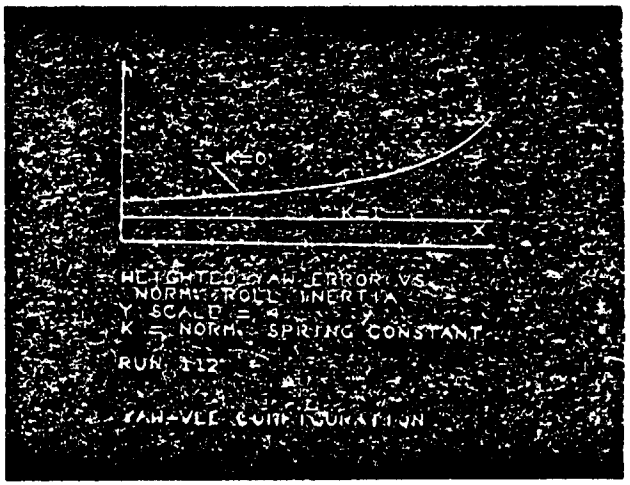

Figure B-19 $\frac{I_x}{I}$ = .5 to .9 $\frac{I_z}{I}$ = .05 $\frac{H_m}{\omega I}$ = 0 $\frac{K}{\omega D}$ = 0, 1 $\frac{H}{\omega I}$ = 2 $\frac{H}{D}$ = 1 $\mu = \alpha = 220^\circ$

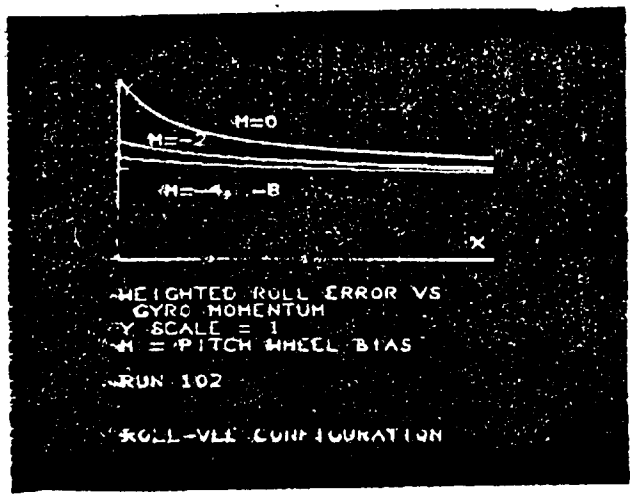

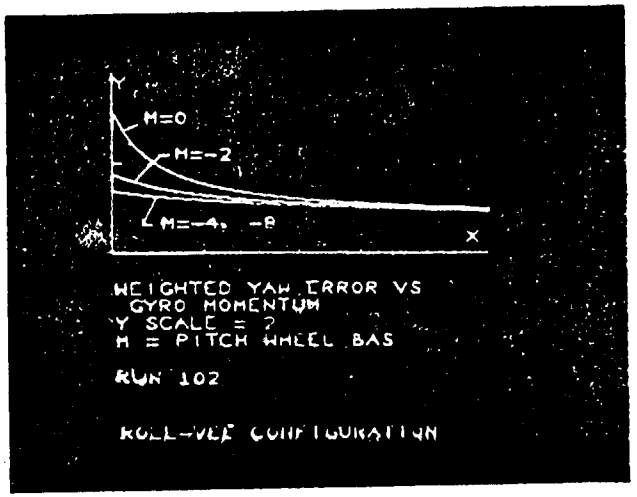

$\frac{I_x}{I_y} = 1.0$; $\frac{I_z}{I_y} = .05$, $\frac{H_m}{\omega_o I_y} = 0,-2,-4,-8$; $\frac{K}{\omega_o D} = 0$; $\frac{H}{\omega_o I_y} = 1$ to 9 ; $\frac{H}{D} = 1.0$; $\mu = \alpha = 220^o$

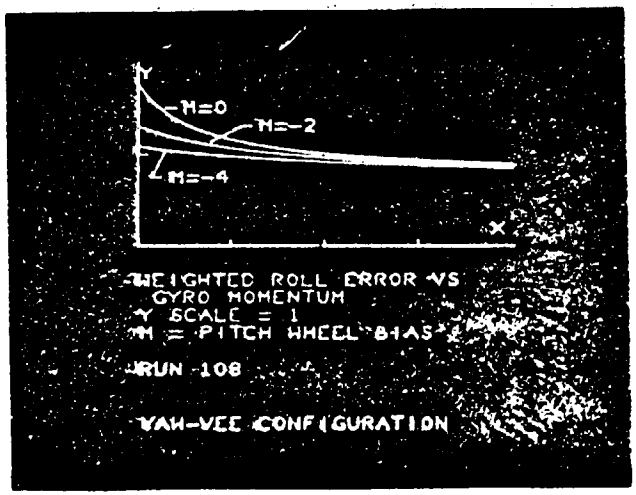

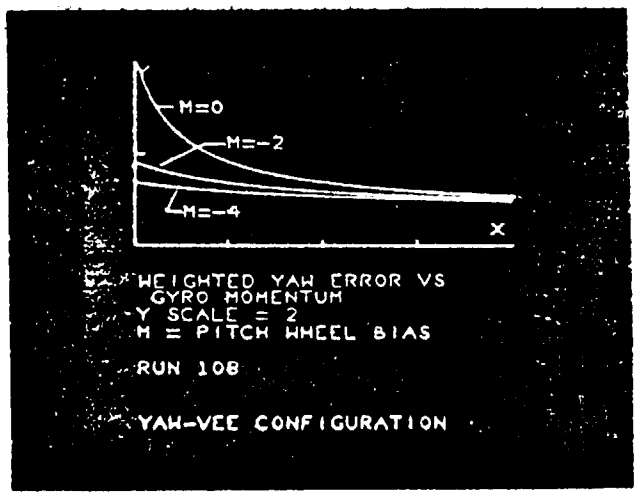

Figure B-20 $\frac{I_x}{I_y} = 1.0$; $\frac{I_z}{I_y} = .05$; $\frac{H_m}{\omega_o I_y} = 0,-2,-4$; $\frac{K}{\omega_o D} = 1.0$; $\frac{H}{\omega_o I_y} = 1$ to 9 ; $\frac{H}{D} = 1.0$; $\mu = \alpha = 220^o$

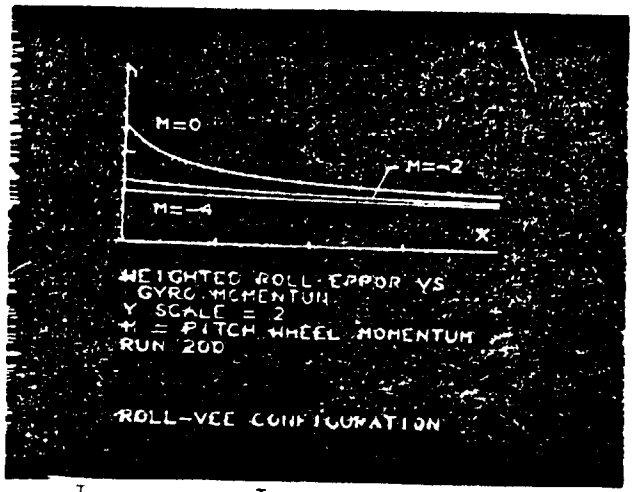

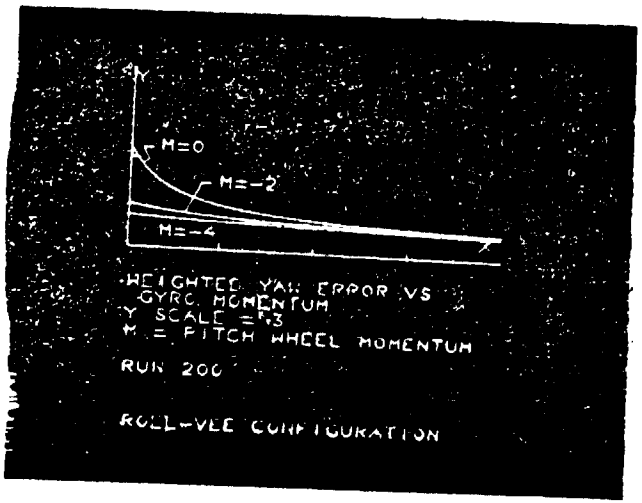

$\frac{I_x}{I_y} = 1.0$ $\frac{I_z}{I_y} = .05$ $\frac{H_m}{\omega_o I_y} = 0, -2, -4$ $\frac{K}{\omega_o D} = 0$ $\frac{H}{\omega_o I_y} = 1 \text{ to } 9$ $\frac{H}{D} = 1$

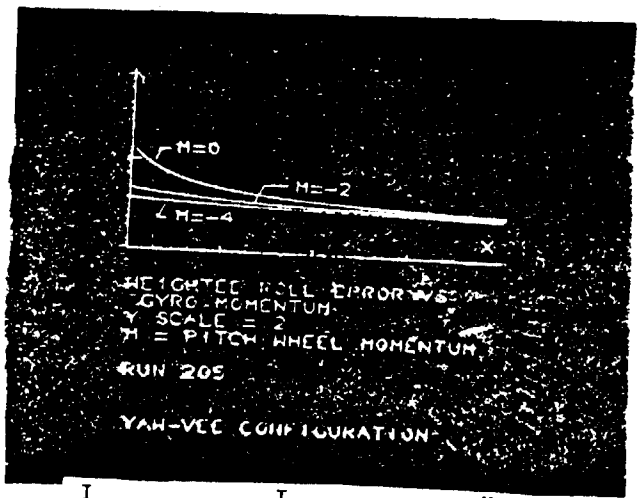

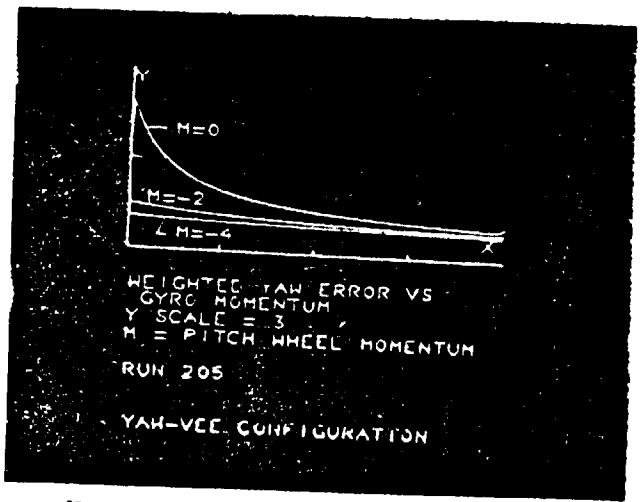

Figure B-21 $\frac{I_x}{I_y} = 1.0$ $\frac{I_z}{I_y} = .05$ $\frac{H_m}{\omega_o I_y} = 0, -2, -4$ $\frac{K}{\omega_o D} = 1.0$ $\frac{H}{\omega_o I_y} = 1 \text{ to } 9$ $\frac{H}{D} = 1$

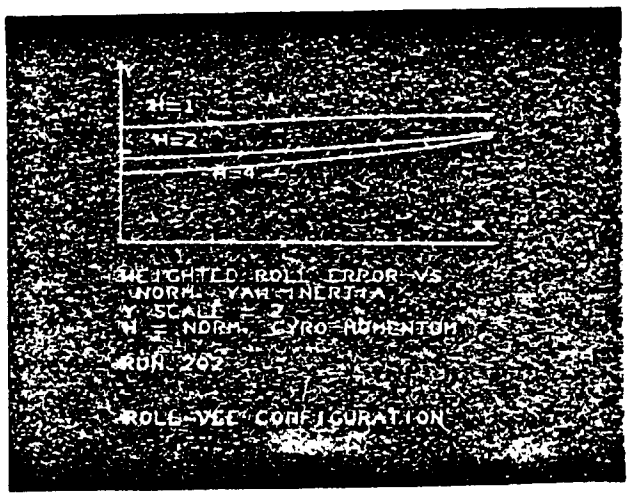

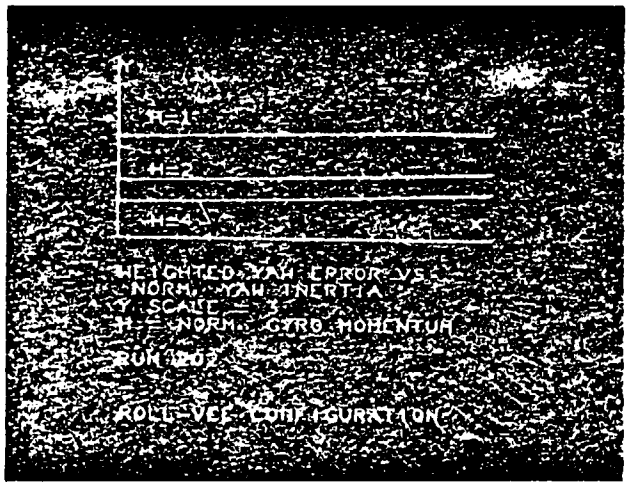

Figure B-22 $\frac{I_x}{I_y} = 1.0$ $\frac{I_z}{I_y} = .01$ to $.41$ $\frac{H_m}{\omega_o I_y} = 0$ $\frac{K}{\omega_o D} = 0$ $\frac{H}{\omega_o I_y} = 1, 2, 4$ $\frac{H}{D} = 1$

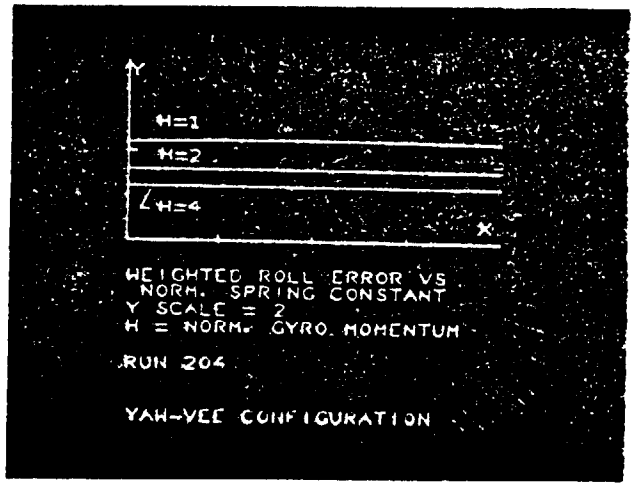

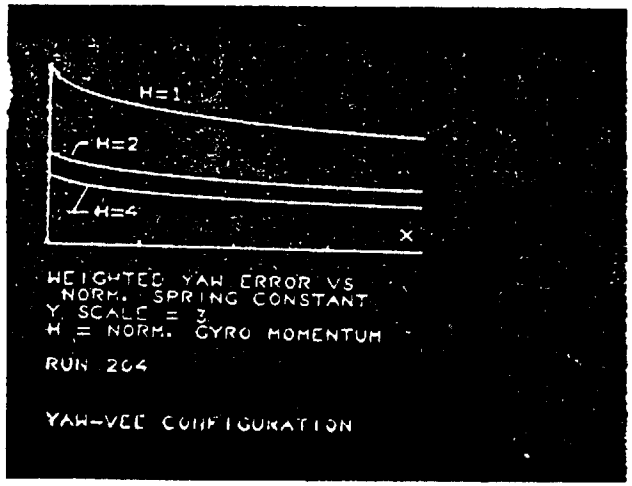

Figure B-23 $\frac{I_x}{I_y} = 1.0$ $\frac{I_z}{I_y} = .05$ $\frac{H_m}{\omega_o I_y} = 0$ $\frac{K}{\omega_o D} = .5$ to 4.5 $\frac{H}{\omega_o I_y} = 1, 2, 4$ $\frac{H}{D} = 1$

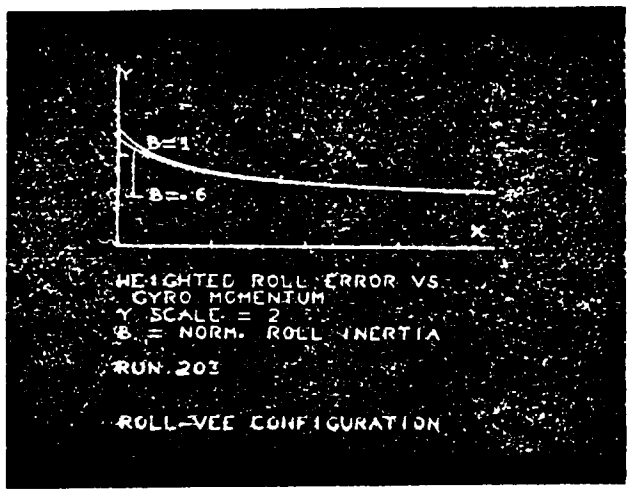

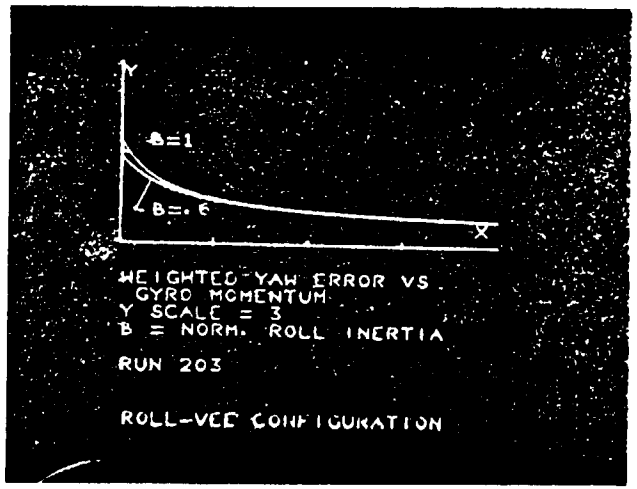

Figure B-24 $\frac{I_x}{I_y} = .6, 1.0$ $\frac{I_z}{I_y} = .05$ $\frac{H_m}{\omega_o I_y} = 0$ $\frac{K}{\omega_o D} = 0$ $\frac{H}{\omega_o I_y} = 1$ to 9 $\frac{H}{D} = 1$

APPENDIX C

Parameters for a Reaction Wheel Damped Gravity Gradient Stabilized Satellite

This Appendix presents the equations for a reaction wheel damped gravity gradient stabilized satellite. The parameters which minimize the weighted attitude errors defined in Section 3.3 are summarized. These weighted attitude errors are used for comparisons with gyro damped system in Section 4.3.

Two reaction wheel configurations are considered. The first uses three reaction wheels; one located about each control axis pitch, yaw and roll. The pitch and roll reaction wheel momentum is controlled proportional to the pitch and roll attitude error. These signals are assumed to be derived from an attitude sensor. The wheel control torque then is proportional to the pitch and roll attitude rates. For the frequencies of interest in this analysis, lags in the reaction wheel, sensors, etc. are negligible. Yaw attitude information is assumed to be derived from a gyro compass. This consists of a rate gyro located with its input axis nearly along the roll axis. The input axis is tilted upward slightly in the x-z plane to obtain yaw rate information as well. This is done for high frequency stability purposes and is of little consequence here. The output of the gyro for small angles is given in Equation (C.1).

$$\omega_{ia} = - S\epsilon (\dot{\psi} + \omega_o \phi) + C\epsilon (\dot{\phi} - \omega_o \psi) \qquad (C.1)$$

where ϵ is the gyro tilt angle with respect to the roll axis.

The second system consists of only two reaction wheels along the pitch and roll axes. The same attitude error signals are used as inputs. Yaw control is achieved through the use of pitch momentum bias.

Equations (C.2) and (C.3) below describe the small angle behavior of the reaction wheel systems and are taken from Reference 6. They have been suitably normalized to be consistent with the gyro equations derived in Appendix A.

Pitch

$$[p^2 + k_y p + 3 (b - c)] \theta = \frac{T_{dy}}{I_y \omega_o^2} \qquad (C.2)$$

where $k_y = \frac{K_y}{I_y \omega_o}$ the normalized pitch reaction wheel gain

K_y = pitch reaction wheel gain (ft-lb-sec/rad)

Roll-Yaw

$$[b p^2 + (k_x + C\epsilon k_z) p + 4 (1 - c) - m - S\epsilon k_z] \phi$$

$$- [(b + c + m + S\epsilon k_z - 1) p + C\epsilon k_z] \psi = \frac{T_{dx}}{I_y \omega_o^2} \qquad (C.3)$$

$$[- C\epsilon k_z p^2 + (b + c + m + S\epsilon k_z - 1) p + k_x] \phi$$

$$+ [(c + S\epsilon k_z) p^2 + C\epsilon k_z p + 1 - b - m] \psi = \frac{T_{dz}}{I_y \omega_o^2}$$

where $k_x = \frac{K_x}{I_y \omega_o}$ the normalized roll reaction wheel gain

K_x = roll reaction wheel gain (ft-lb-sec/rad)

$k_z = \frac{K_z}{I_y \omega_o^2}$ the normalized yaw reaction wheel gain

K_z = yaw reaction wheel gain (ft-lb-sec/rad/sec)

The pitch equation is easily optimized for best performance. Best zero frequency gain is obtained when the inertia ratios are b = 1 and c = 0. Attitude errors for disturbance torques at multiples of orbit rate are minimized for large reaction wheel gains. The studies of Reference 6 indicated a practical limit on k_y was about 50. Figure C-1 shows the weighted attitude errors as a function of the normalized pitch reaction wheel gain. Since for the systems under consideration some yaw inertia exists, ratios of b = 1 and c = .05 were used.

The roll-yaw equations (C.2) and (C.3) were analyzed in a manner similar to the gyro study. A short digital program was written for the PB 250 computer to determine frequency response at multiples of orbit rate. Figures C-2 and C-3 are plots of the weighted attitude errors for the three reaction wheel and two reaction wheel systems. The gyro tilt angle was assumed to be zero for the purposes of this analysis. Again, it was assumed a practical upper limit on normalized momentum and reaction wheel gains was 50.

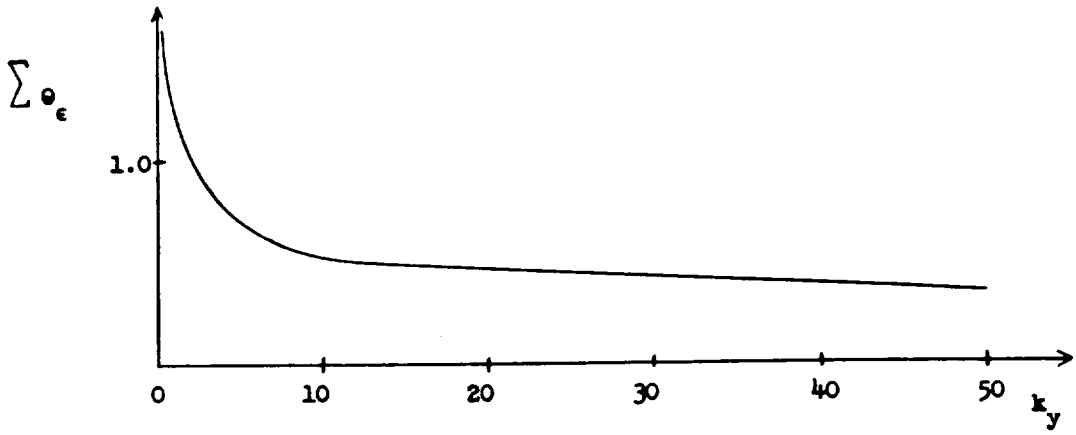

Figure C1 - Weighted Pitch Error vs. Normalized Pitch Wheel Gain

b = 1, c = .05

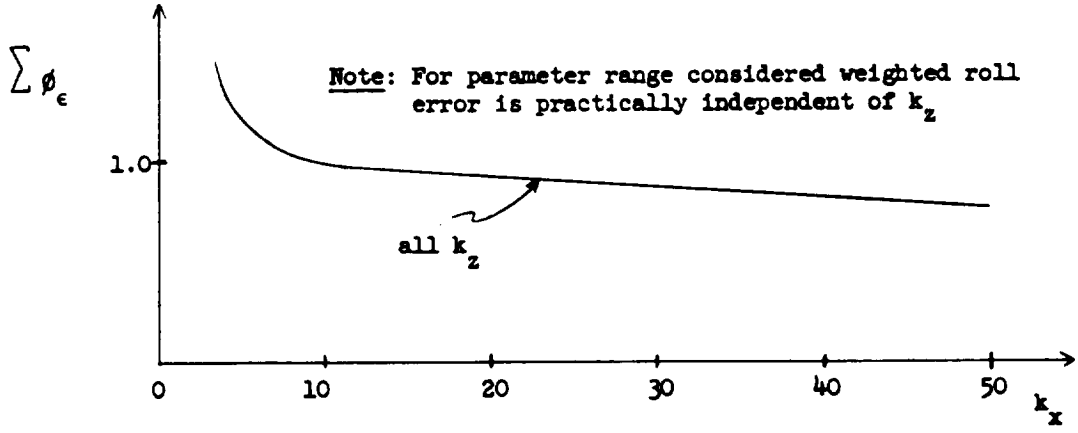

Figure C2a

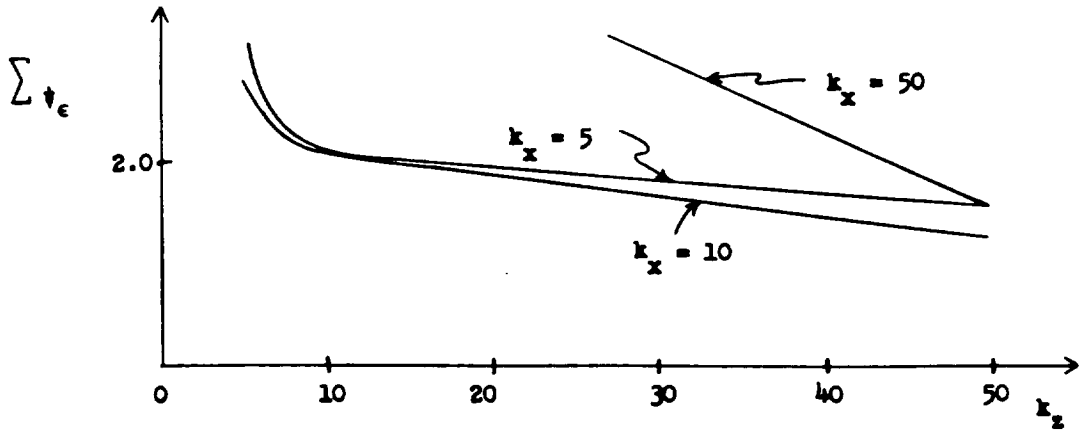

Figure C2b

Weighted Roll and Yaw Errors vs. Normalized Roll Wheel Gain
Three Reaction Wheels

b = 1, c = .05

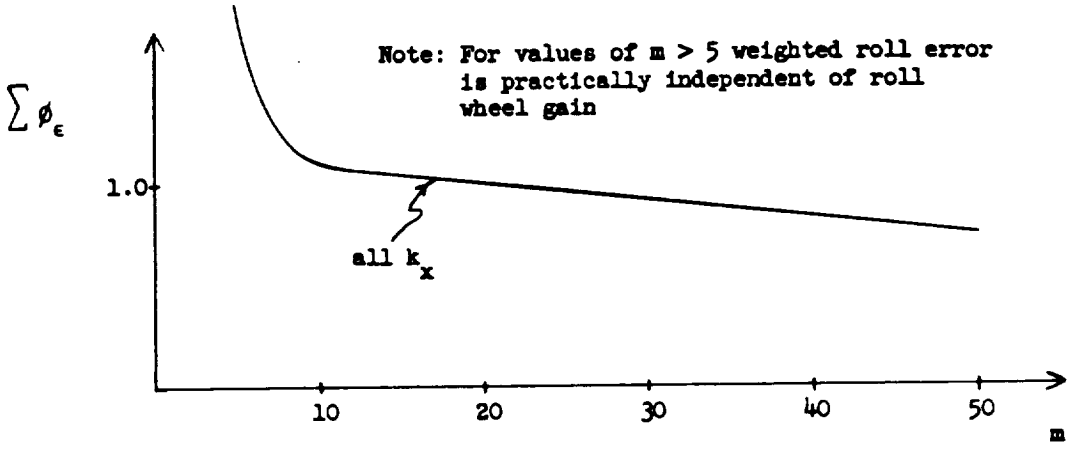

Figure C3a

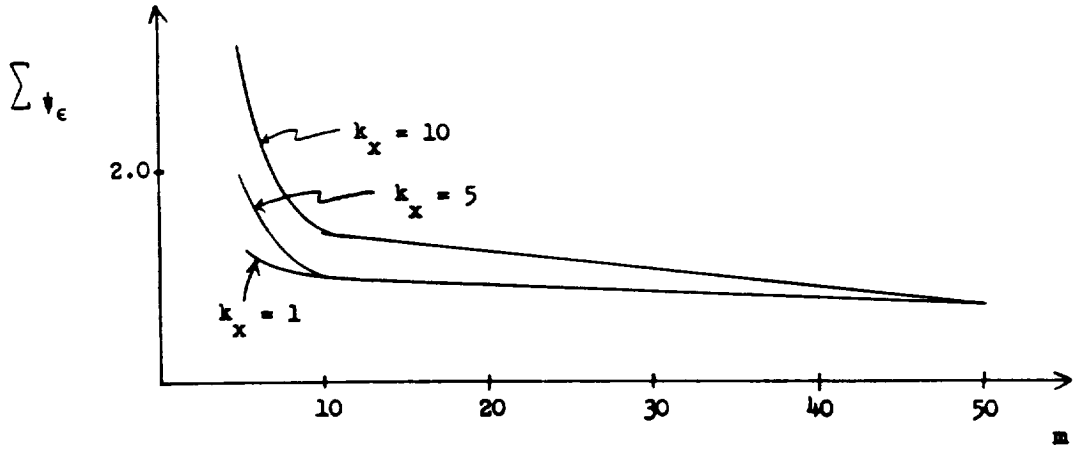

Figure C3b

Weighted Roll-Yaw Errors vs. Normalized Roll Wheel Gain

Two Reaction Wheels

b = 1, c = .05